INFORMATION TO USERS

This material was produced from a microfilm copy of the original document. While the most advanced technological means to photograph and reproduce this document have been used, the quality is heavily dependent upon the quality of the original submitted.

The following explanation of techniques is provided to help you understand markings or patterns which may appear on this reproduction.

1. The sign or "target" for pages apparently lacking from the document photographed is "Missing Page(s)". If it was possible to obtain the missing page(s) or section, they are spliced into the film along with adjacent pages. This may have necessitated cutting thru an image and duplicating adjacent pages to insure you complete continuity.

2. When an image on the film is obliterated with a large round black mark, it is an indication that the photographer suspected that the copy may have moved during exposure and thus cause a blurred image. You will find a good image of the page in the adjacent frame.

3. When a map, drawing or chart, etc., was part of the material being photographed the photographer followed a definite method in "sectioning" the material. It is customary to begin photoing at the upper left hand corner of a large sheet and to continue photoing from left to right in equal sections with a small overlap. If necessary, sectioning is continued again — beginning below the first row and continuing on until complete.

4. The majority of users indicate that the textual content is of greatest value, however, a somewhat higher quality reproduction could be made from "photographs" if essential to the understanding of the dissertation. Silver prints of "photographs" may be ordered at additional charge by writing the Order Department, giving the catalog number, title, author and specific pages you wish reproduced.

5. PLEASE NOTE: Some pages may have indistinct print. Filmed as received.

74-21,280

HIRATA, Theodore Tetsuo, 1945-
    A COMPARTMENTAL LUNG MODEL TO SIMULATE
    OPEN-CIRCUIT NITROGEN WASHOUT.

    Rice University, Ph.D., 1974
    Engineering, biomedical

University Microfilms, A XEROX Company , Ann Arbor, Michigan

RICE UNIVERSITY

A COMPARTMENTAL LUNG MODEL TO SIMULATE
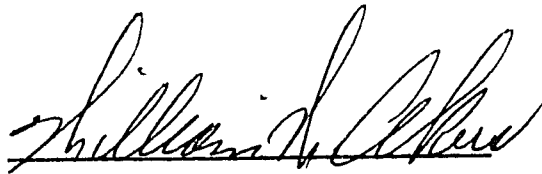
OPEN-CIRCUIT NITROGEN WASHOUT

by

Theodore Tetsuo Hirata

A THESIS SUBMITTED
IN PARTIAL FULFILLMENT OF THE
REQUIREMENTS FOR THE DEGREE OF

DOCTOR OF PHILOSOPHY

Thesis Director's Signature:

Houston, Texas

May, 1974

TABLE OF CONTENTS

ACKNOWLEDGMENTS

NOMENCLATURE

a, b	=	coefficients of model parameters
a_i, b_i	=	coefficients of model parameters
A_i, B_i, C_i	=	coefficients in solutions for concentration in model compartments
CETV	=	cumulative expired tidal volume
$\underset{\sim}{e}$	=	error vector for vector function $\underset{\sim}{f}$
$\underset{\sim}{\hat{e}}$	=	error vector for linearized vector function $\underset{\sim}{\hat{f}}$
E	=	vector norm of error vector $\underset{\sim}{e}$
$\hat{E}$	=	vector norm of error vector $\underset{\sim}{\hat{e}}$
f	=	volumetric concentration difference = $F - F_I$
F	=	volumetric concentration* in saturated gas phase
$\underset{\sim}{f}$	=	vector function of parameter set $\underset{\sim}{\alpha}$
$\underset{\sim}{\hat{f}}$	=	linearized vector function
FRC	=	functional residual capacity
$\underset{\sim}{J}$	=	transform of the Jacobian matrix, $\dfrac{\partial \underset{\sim}{f}}{\partial \underset{\sim}{\alpha}}$
l_i	=	alveolar compartment volume fraction $= \dfrac{V_{Li}}{V_L}$
M_i	=	roots of characteristic equation, $\Phi(E^P)M=0$
n	=	breath number
r	=	breathing rate
t_i	=	tidal volume fraction $= \dfrac{V_{Ti}}{V_T}$
V	=	volume (body temperature and pressure, saturated)

---

* Volumetric concentration is the pure-component volume divided by total volume, where pure-component volume is the volume of a gas component at total pressure and temperature conditions.

$\dot{V}$ = volume flow rate

$\underset{\sim}{y}$ = vector of data points

$\propto$ = separated dead-space volume fraction = $\dfrac{V_{DS}}{V_D}$

$\underset{\sim}{\propto}$ = vector of model parameters

$\in$ = concentration difference between discretely-ventilated and continuously-ventilated model

λ = Levenberg adjustment

ϕ = dilution factor = $\dfrac{V_T}{FRC}$

Subscripts and Superscripts

(n) = breath number n

A, L = alveolar compartment

c = continuously ventilated

d = discretely ventilated

D = total dead space

DC = common dead space

DS = separate dead space

(E) = end-expiration

i = branch number

I = inspired

(I) = end-inspiration

T = tidal

0 = initial condition

v

LIST OF TABLES

LIST OF FIGURES

FIGURES PAGE

I. INTRODUCTION

GENERAL INTRODUCTION

Transport of physiologic gases, O_2 and CO_2, between the environment and internal tissue cells requires an efficient gas-exchange organ and a distributing medium. In man the lungs and blood occupy these roles. The lungs are a highly-branched airway system terminating in tiny air sacs called alveoli whose primary functions are to provide low diffusional resistance by having a large surface area and thin membrane, and to provide stable concentrations of physiologic gases. Blood has a large capacity through chemical composition for transporting oxygen and carbon dioxide.

The three limitations to transport of gases to and from pulmonary blood are diffusion impairments, ventilation maldistribution and perfusion maldistribution. Methods of assessing ventilation maldistribution include radiologic scanning techniques, single-breath tests and open- and closed-circuit inert gas washout tests. Radiologic scanning techniques consist of an inspiration of a radioactive gas and detection of emissions in different parts of the lung by external counters. The peak emission is a measure of the ventilation of the tissue between the counters. Single-breath tests involve a single inspiration of oxygen and analysis of the nitrogen concentration and volume expired in the subsequent expiration. Maldistribution

of ventilation is indicated by the degree of rising concentration. Washout techniques consist of inducing a step change in concentration of an inert gas such as helium of nitrogen and monitoring the breath-by-breath decay of this initial step size.

Cournand, et al. [9] in 1941 were the first to devise the open-circuit washout procedure using pure oxygen to wash out atmospheric concentrations of nitrogen. Due to the lack of a rapid nitrogen analyzer at the time, the gas samples only at the beginning and at the end of a seven-minute period were used to assess maldistribution. Normal subjects washed out to less than 2.5 percent at the end of seven minutes. Clinically at present the same basic procedure is used, although a rapid nitrogen analyzer has long been available.

This study investigates the breath-by-breath course of nitrogen decay from an open-circuit washout system by simulation of subject data with a compartmental lung model which consists of a common dead space in series with two branches, each having a separate dead space leading to an alveolar compartment. The governing equations for this model are derived and a closed-form solution for end-expired common dead-space concentration is obtained. Parameter values for this model along with two simpler models are found which describe the relative sizes of the compartments as well as ventilation of the two branches. Uniqueness of the parameter set is examined and application to clinical use is discussed.

Previous studies concerning breath-by-breath analyses [28,40] have included compartmental models with common dead space, but correlation between these models and experimental data was usually not attempted. Where experimental correlations were made, only the simplest

model consisting of separate dead spaces was used and only for single washout curves [4,14,20,21]. The inclusion of mixing of expired gases in a common dead space complicates the analysis of the model considerably. Wise and Defares [40] obtained a closed-form solution for a similar model with common and separate dead spaces, but for a closed-circuit washout system. This differs from the present open-circuit system in that expired gases are mixed in a large bellows and re-breathed. Equilibration is arrived at when the bellows and lungs are at the same concentration of test gas. Inspired concentrations thus change with each breath, whereas for an open-circuit system the inspired concentration remains the same throughout the test. Functional residual capacity is determined by final concentrations in the bellows-lung system and Tissot spirometer for the closed-circuit and open-circuit procedures respectively (see Appendix A for apparatus and procedure for open-circuit washout test).

The following sections provide background on pulmonary anatomy and literature.

PULMONARY ANATOMY AND PHYSIOLOGY

Pulmonary Anatomy [17,35]

The lungs are the specialized organ responsible for most of the gas exchange that occurs between the environment and the body. They bring environmental gases in contact with blood through a large surface area, the alveolocapillary membrane, across which the respira-

tory gases, O_2 and CO_2, diffuse.

The lungs consist of a highly-branched airway system terminating in the respiratory surfaces of the respiratory bronchioles, alveolar ducts, alveolar sacs and the alveoli (see Figure [1]). Starting with the upper respiratory passages of the nose, mouth, pharynx and naso-pharynx, the inspired air is progressively warmed, humidified and filtered. It flows next through the larynx and the trachea before entering the right and left lungs through the two main bronchi, which in turn divide into the three right lobar bronchi leading to the three lobes of the right lung and into the two left lobar bronchi which lead to the two lobes of the left lung (see Figure [2]). Considering the trachea as the zeroth generation, there are 16 generations of bifurcations in the conducting airways. The total cross-sectional area varies from about 2.54 cm^2 in the trachea to 2.0 cm^2 in the third generation to about 180 cm^2 in the 16th generation. Up to and including the 16th generation, the airways do not participate in any appreciable gas exchange role. Rings of cartilege keep the bronchi open and plates of cartilege are contained in the bronchioles which have dimensions down to about 1 mm, so the airways become progressively more distensible as the generation increases. Smooth muscle is also contained in all airways to the alveolar ducts and these passages are subject to contraction due to physiologic influences. The columnar epithelial cells which line the airways down to and including the terminal bronchioles are cilia bearing and mucus secreting, and serve the purposes of filtering the air and cleaning the lungs of foreign particles and aerosols. They give rise to flattened cuboidal epithelial cells in the respiratory bronchioles
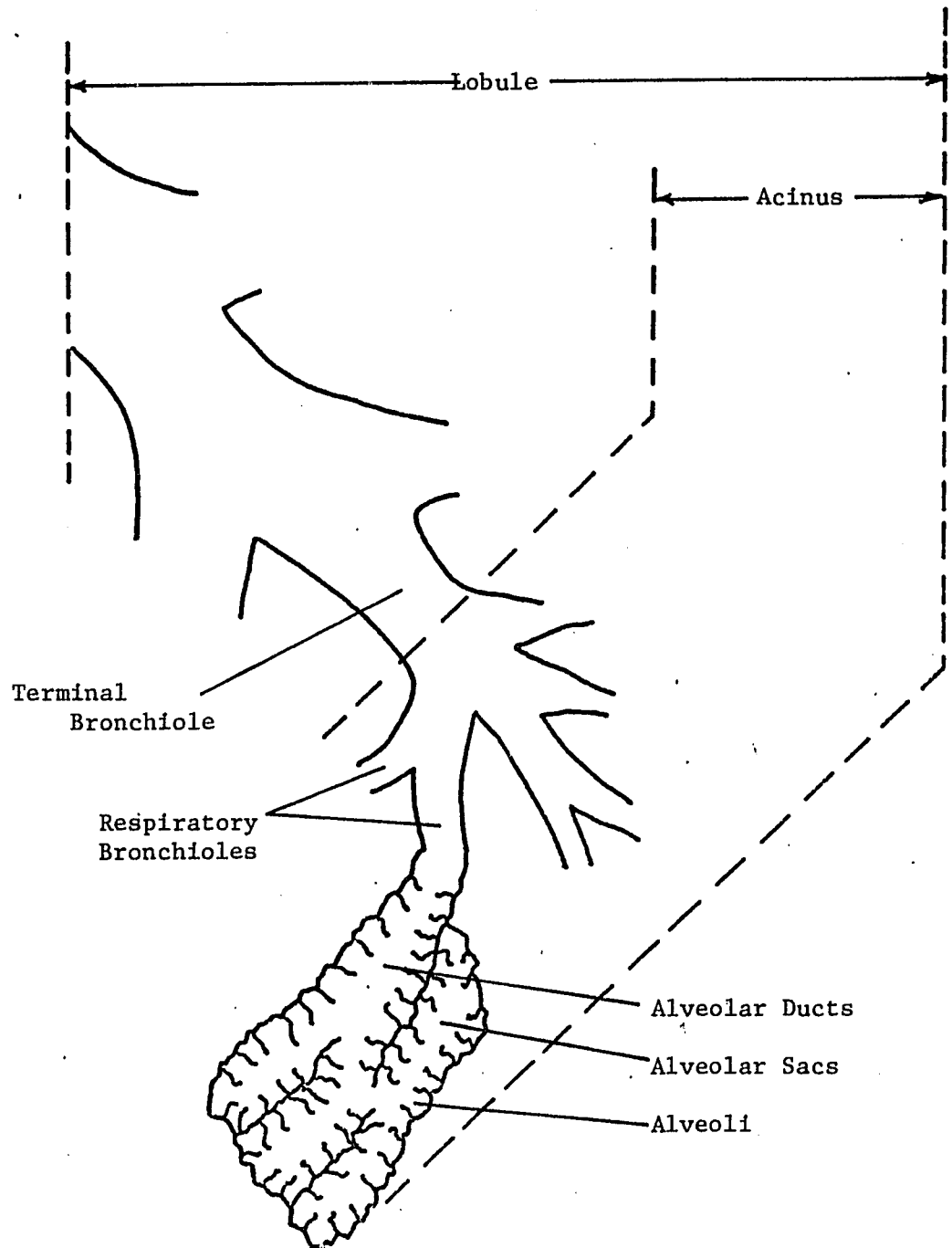
Figure 1. Distal Airways and Respiratory Units [35]
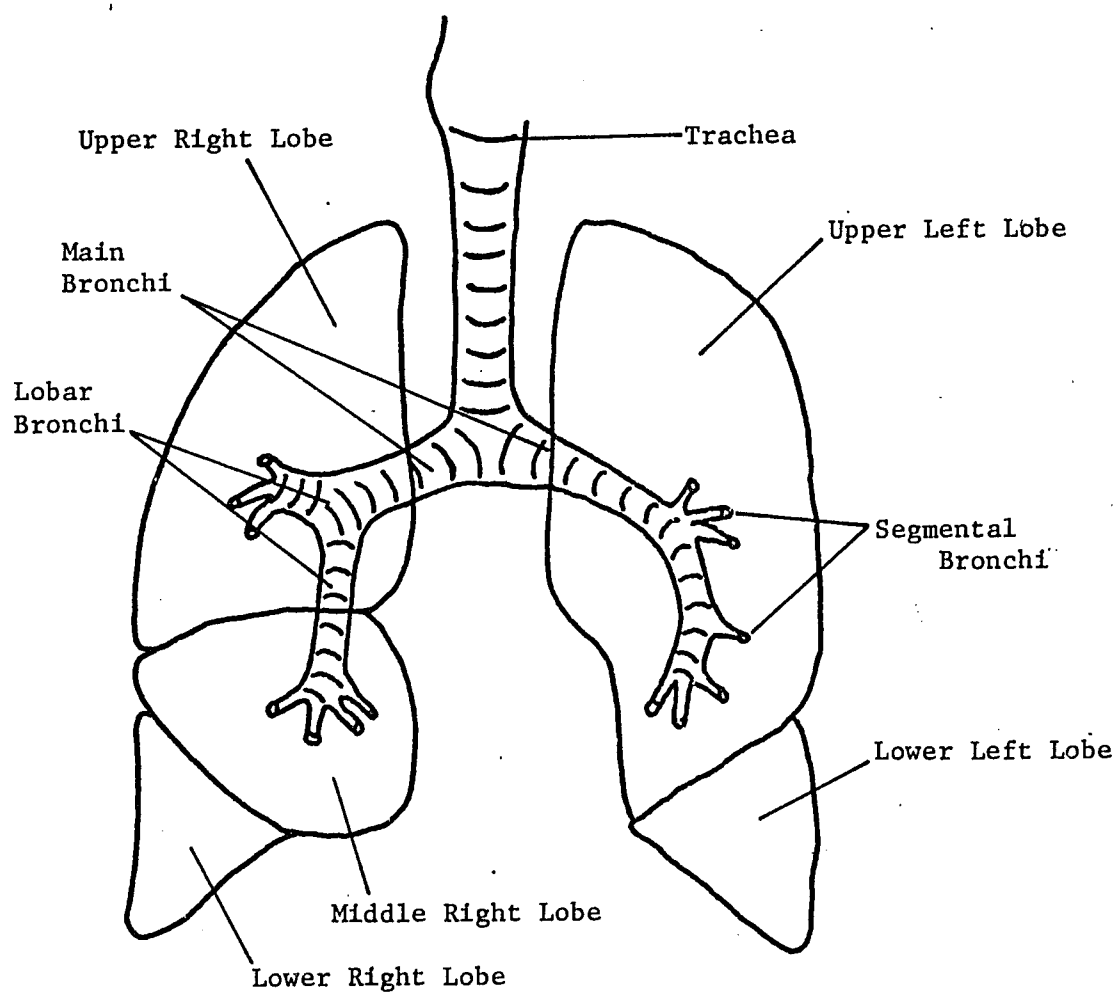
Figure 2. Upper Airway Branching Patterns [35]

which are about 0.5 mm in diameter or less and line the main gas ex-
change surfaces of the alveolar ducts, alveolar sacs and alveoli. In
the human lungs, there are about 300 million alveoli ranging in diame-
ter from 150-300 μ . Gas transport by convection occurs up to the
openings of the alveoli after which gaseous diffusion reduces concen-
tration differences in a fraction of a second [22,35].

There is an adjoining arterial tree which serves to collect
and transport physiologic gases to and from the rest of the body. About
280 billion capillaries with nominal diameters of 8 μ surround the
alveoli, and there is a common surface area between 50-80 m^2.

Mechanics of Respiration [35]

During resting inspiration, contraction of the diaphragm and
movement of the ribs, sternum and vertebrae cause an increase in thoracic
volume and distension of the lungs, which create a negative pressure
gradient for air to flow into the lungs. During expiration, cessation
of inspiratory muscle contraction causes the elastic recoil of the lungs
to force air out. Other muscles may be recruited during both inspira-
tion and expiration when more vigorous ventilation is required.

Physiologic Causes of Nonuniform Ventilation [17]

The causes of nonuniform ventilation can be divided into three
cases, the origin of which may or may not be assigned to a specific ana-
tomic area.

In Case 1, the cause is due to regional volume-expansion dif-
ferences. This can be due to local differences in lung tissue distensi-

bility or to nonuniform distribution of the forces of inspiration. Case II causes are due to differences in the time course of inspiration and expiration, physiologically due to differences in airway resistance and tissue compliance. Case III is attributed to nonuniform distribution of common dead space gas due to asynchronous filling or to regional differences in bronchial pathway length.

Nonuniform ventilation is present to some extent in even healthy individuals and can be detected by analysis of the nitrogen washout procedure.

Factors Affecting Nitrogen Washout [17,32]

The following factors are known to affect the course of nitrogen elimination from the lung:

1. Respiratory rate: Changes in breathing frequency or respiratory rate implicitly affect flow rates which may affect the distribution of inspired gas through altered airway resistances, increased convection and decreased diffusional equilibration times. Previous studies [3,33] have demonstrated that variations within physiological limits do not affect gas distribution significantly. Militano [25] has also experimentally verified that N_2 washouts can be treated as independent of breathing rates up to 20 breaths per minute in normal and diseased subjects. However in a more recent study [10] significant changes in washout results in abnormal subjects were observed when frequency increases of 50 percent or more than

resting values were made at the same tidal volume. The tendency was towards more unevenness at more rapid breathing rates.

2.   Tidal volume per breath (see Figure [3]): Due to possible asynchronous inflow and outflow patterns, certain lung regions may be affected in a nonlinear manner with respect to changes in tidal volume. It is generally believed [17] however that changes in tidal volume do not affect gas distribution greatly unless extreme values are encountered. It has been the experience of the author that although average tidal volume over the course of a washout test is significant, breath-by-breath variations about this average are not. This was arrived at after plotting N_2 concentration against a normalized cumulative tidal volume and comparing this curve with one plotted at equally-spaced intervals representing cumulative average tidal volume or breath number (see Figures [6,7]). Neither significant shifting of the curve nor large changes in curvature were found in tests of six subjects. This observation is substantiated by Robertson, et al. [33] who also noted that washout concentrations returned to almost normal values when hyperventilation ceased, as long as this period of deep and rapid breathing was not prolonged. Generally, increased average tidal volumes will hasten nitrogen elimination from the lungs.

3.   Volume of dead space: Maintaining the same tidal volume but increasing dead space decreases effective tidal volume (V_T-V_D) and decreases uneven distribution of inspired gas by coupling ventilation units through the portions of the dead space which
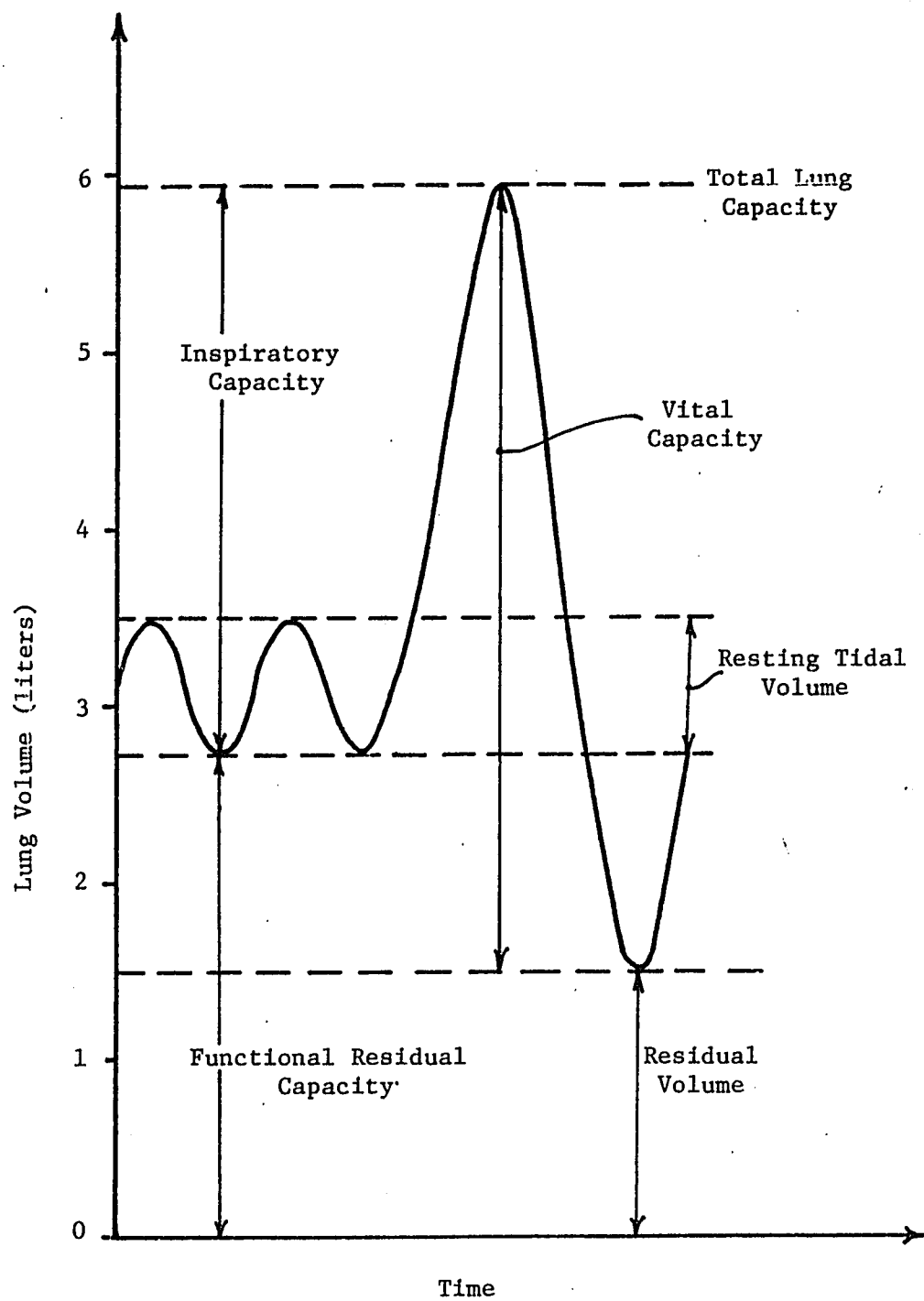
Figure 3. Lung Volume Divisions [35]

are common. Well-ventilated regions are delayed in their
nitrogen washout and poorly-ventilated regions are speeded
up. Multi-exponential curves can be made into single expo-
nentials by sufficient artificial enlargements of series dead
space [1].

4. Functional residual capacity (see Figure [3]): Generally the
larger the functional residual capacity for a given tidal vo-
lume and anatomic dead space, the slower the washout will be
due to the decrease in the effective dilution factor per
breath (V_T-V_D)/FRC.

5. Mixing of inspired gases with residual gases: Mixing in the
gas-exchange volumes is predominantly by diffusion and these
volumes are generally assumed to be well-mixed. Concentration
gradients quickly (relative to a breathing cycle) diminish due
to very short diffusion distances and high diffusivity of gases.

6. N_2 transfer from blood and tissues: This factor becomes sig-
nificant only at low alveolar N_2 concentrations on the order
of 5 percent or less [25], when the potential difference across
the alveolocapillary membrane becomes small enough for this
influx to become significant. The magnitude of this effect
is dependent on the solubility in blood and tissues, concen-
tration in the gas phase, tissue volume, perfusion rates and
distribution of blood in the lungs.

BACKGROUND LITERATURE REVIEW

The open-circuit nitrogen washout test was first devised by Cournand

and others [11] as an improved means of assessing functional residual capacity over the previously used closed-system equilibration technique. The main advantage was that the error in using an alveolar sample as a measure of the mean concentration of N_2 left in the lungs was reduced by washing out as much of the nitrogen as possible. Concentration in the Tissot spirometer, used to collect the expired gases, however requires more accurate measurement. In 1941 Cournand et al. published another paper [9] describing the open-circuit washout procedure as a means of assessing maldistribution of inspired gases in addition to determining functional residual capacity. This was based on the assumption that the course of nitrogen washout is determined to a large extent by the distribution of inspired oxygen. The period of the test was seven minutes to accommodate the functional residual capacity determination and the N_2 concentration at the end of this time or pulmonary emptying rate was less than 2.5 vol. percent in normal subjects. The advent of the continuous nitrogen analyzer was not until 1944, so alveolar samples were taken only at the beginning and at the end of the washout procedure, thus defining only two points.

Robertson, et al. [33] modified Cournand's experimental setup to include a mass spectrometer to continuously monitor N_2 concentration and were the first to analyze the resulting N_2 washout curve. They assumed a continuous-flow, multi-compartment model and looked at the effects of a series arrangement and a parallel arrangement for the specific case of two compartments. In the series arrangement there is recirculation of gases between the proximal and the deeper spaces, whereas in the parallel arrangement, the spaces are ventilated independently.

In both cases, their theory shows that the concentration of gas being washed out proceeds as the sum of two exponentials, so that distinction between series and parallel ventilation cannot be made by examination of the sum. However there are differences in minute ventilation and this can be used to confirm which arrangement was used to generate the washout curve. This paper showed that estimates of series dead space assuming no maldistribution in alveolar spaces would be erroneously large if maldistribution did actually exist. In order to find parameters to fit their data, Robertson et al. [33] assumed a continuous parallel-compartment model with no dead space. By graphical analysis, components of the washout curve were found, where the slopes corresponded to the turnover rates, k_i, and the volumes, v_i, were found by integrating the components from time zero to infinity. The turnover rate is defined as "the ratio of the number of new molecules which enter a space in unit time to the number present at the end of expiration" [33]. As a measure of the degree of maldistribution, they introduced an efficiency of ventilation, E, which is the ratio of the effective turnover rate for the model to a maximum turnover rate found by assuming no maldistribution. The effective turnover rate, k, is given by:

$$\frac{1}{k} = \sum_{i=1}^{N} \frac{f_i}{k_i} \tag{1.1}$$

where

$$f_i = \frac{V_i}{\sum\limits_{i=1}^{N} V_i} \quad ; \quad \sum_{i=1}^{N} f_i = 1$$

and   N   = number of compartments

           n   = respiratory rate

           T_i = tidal volume of compartment i

Maximum turnover rate, k_{max}, is defined by:

$$k_{max} = \frac{M}{FRA}$$ (1.2)

where   M   = minute ventilation

         FRA = functional residual air

so that:

$$E = \frac{k}{k_{max}} \times 100\%$$ (1.3)

As can be seen from equation (1.1), k is governed by the largest f_i/k_i, and will be small when there is a large lung volume fraction ventilated with a small turnover rate. Also E is a function of $f_i^2/(T_i/T)$ and is independent of FRA and n, so as long as f_i follows (T_i/T) closely, E will be high. Thus for large lung volumes, k may be small, but E may be large. This is because k reflects both overall ventilation and mal-distribution of ventilation.

An analysis using a cyclically-ventilated model was made by Fowler, et al. [14]. They separated the effects of respiratory dead space and uneven alveolar ventilation by assuming a separate dead-space model whose branches ventilated independently of each other. In other words there was no mixing of expired gases in a common dead space and reinspiration on the next breath, so that the washout became a function of effective tidal volumes $(V_{Ti}-V_{Di})$ instead of just V_{Ti}. This is implicit in the model and although values of $(V_{Ti}-V_{Di})$ can be found, individual values of V_{Ti} and V_{Di} are unknown. Fowler, et al. [14] used mean-expired N_2 concentration instead of the end-tidal concentration because of the continued rise of the alveolar slope in many cases, and

the subsequent need of an assumption of what is representative of mean alveolar concentration. This however requires a simultaneous volume-concentration measurement and an integration, which was done graphically in this case.

The describing equation for the model is:

$$\overline{F}_{En} = \sum_{i=1}^{M} F_{Ai_0} w_i^n r_i + F_b \tag{1.4}$$

where   M   = number of compartments

F_{Ai_0} = alveolar N_2 concentration for compartment i at the beginning of the test

w_i = alveolar dilution factor

$$= \frac{V_{Li}}{V_{Li} + (V_{Ti} - V_{Di})}$$

V_{Li} = volume of the alveolar space and the dead space for compartment i

V_{Ti} = tidal volume going to compartment i

r_i = dead-space dilution factor

$$= \frac{V_{Ti} - V_{Di}}{V_T}$$

n   = breath number

F_b = constant term to correct for N_2 from blood and tissues

An exponential stripping technique was used to decompose the washout curve, after which w_i and r_i were found knowing F_{Ai_0}. $(V_{Ti} - V_{Di})$ and V_{Li} were also found with a value of V_T, from which V_D and V_L were estimated.

To measure the degree of uneven ventilation, Fowler et al.

introduced an actual average breath number and an ideal average breath number, the average breath number corresponding to the average number of breaths that N_2 molecules remain in the system. These terms are defined by:

$$\text{Actual average breath number} = \sum_{i=1}^{M} \frac{f_i}{1 - w_i} \qquad (1.5)$$

$$\text{where} \quad f_i = \frac{v_{Li}}{V_L}$$

$$\text{Ideal average breath number} = \frac{1}{1 - w} \qquad (1.6)$$

$$\text{where} \quad \frac{1}{w} = \sum_{i=1}^{M} \frac{f_i}{w_i}$$

and $\quad w \quad$ = ideal alveolar dilution factor

The pulmonary N_2 clearance delay (percent) was then defined as:

$$N_2 \text{ clearance delay} = \frac{(\text{Actual average breath number} - \text{Ideal average breath number})}{(\text{Ideal average breath number})} \times 100 \; ;$$

$$(1.7)$$

Lundin [21] following basically Fowler's [14] model, studied the course of N_2 washout for end-tidal nitrogen concentration and for the volume of nitrogen given off per breath, in order to determine the differences and whether the more laborious second method was warranted. The volume of nitrogen expired per breath was found by mixing accumulated expirations in a large Tissot spirometer and measuring the nitrogen concentration and spirometer volume. Both the end-tidal concentration

and volume of nitrogen expired were corrected for N_2 in the inspired gases and for tissue and blood elimination. The equation describing the volume of expired N_2 is:

$$R_n = \sum_{i=1}^{M} R_{1i} w_i^{n-1} \qquad (1.8)$$

where   M   = number of compartments

         n   = breath number

         w_i = alveolar dilution factor

             $= \dfrac{V_{Li}}{V_{Li} + V_{Ti} - V_{Di}}$

         R_n = volume of nitrogen given off for breath n

         R_{1i} = volume of nitrogen given off for compartment i,

                breath number 1

Lundin found that at least in normals, both curves were pretty much parallel when plotted on semilogarithmic graph paper and led to the same values of fractional volumes and alveolar dilution factors.

Lillington [20] studied the differences between using end-tidal concentration and mean-expired concentration and determined that for unevenly ventilated lungs, end-tidal measurements led to end-inspired fractional volumes for the components, whereas mean-expired values led to end-expired fractional volumes, which are different. Studies with emphysematous patients [2] showed differences in washout curves, but pulmonary N_2 clearance delays calculated for each method were of the same order of magnitude.

As a means of developing ventilation-perfusion characteristics, Briscoe and Cournand [5] analyzed helium washins and washouts in terms

of Fowler's [14] model, but monitored mixed-expired alveolar concentration rather than mean-expired concentration, and used alveolar flow rates rather than tidal volume and respiratory rate. They neglected dead space completely in their definition of alveolar dilution ratio, w,

$$w = \frac{L}{L + t} \tag{1.9}$$

where   L   = alveolar volume

        t   = alveolar ventilation per breath

Semilogarithmic plots of washout curves were expressed as functions of time rather than breath number and the slopes of the exponential components were expressed in terms of M, the time required for concentrations to decrease one cycle or to 1/10th of any previous value. w and M are related by:

$$w^{Mf} = \frac{1}{10} \tag{1.10}$$

where   f   = respiratory rate.

An alveolar ventilation, $\dot{V}_A$, was defined as:

$$\dot{V}_A = ft \tag{1.11}$$

Then

$$\frac{\dot{V}_A}{L} = f \left[\frac{1 - 10^{-1/Mf}}{10^{-1/Mf}} \right] \tag{1.12}$$

and $\dot{V}_A/L$ is equivalent to the turnover rate, k, of Robertson, et al. [33]. Their model assumed continuous flow, whereas this study deals with a

discretely-ventilated model with an equivalent alveolar ventilation term, V_A/L, expressed in terms of time rather than breath number for compatibility with perfusion rates.

From curves of normals and emphysematous patients, Briscoe and Cournand found normals generally have lungs which behave as if half their alveolar volume is half as well ventilated as the other, whereas emphysematous subjects had curves which represented three-quarters of the alveolar volume ventilated from one-fifth to one-tenth as well as the other one-quarter.

Up to this point all the models considered did not have a common dead space, which physiologically is at least present in the upper respiratory tract down to the trachea. Weber and Bouhuys [39] made a theoretical study of a continuously-ventilated model with common dead space and two alveolar compartments. The significant gas flows were f_1 and f_2 representing the flow of inspired gases to compartments 1 and 2, and $_1$ and $_2$ representing recirculating flows from compartments 1 and 2 respectively through the common dead space volume, V_3. The differential equations describing the concentration changes in the three compartments were set up and the solutions took the form of the sum of three exponentials for each of the concentrations, C_1, C_2, and C_3. C_3 is of the form:

$$C_3(t) = \Gamma_1 e^{\lambda_1 t} + \Gamma_2 e^{\lambda_2 t} + \Gamma_3 e^{\lambda_3 t}$$

(1.13)

The authors noted that the three components should not be identified with the three compartments. There is however an error in the approximation required in a continuous-flow model, that the flow rate through the model is equal to the respiratory rate times the tidal volume, the

the error increasing with faster clearance rates (see Appendix D).

Nye [28] treated the case of a cyclically-ventilated model
with common dead space for open- and closed-circuit inert gas washout.
For the open circuit system, he did a breath-by-breath analysis which
led to an equation of linear difference that has a solution of the
form:

$$\frac{F_{A_n}}{F_{A_o}} = AB^n + CD^n \tag{1.14}$$

where F_{A_n} = fractional concentration of mixed alveolar expirate

for breath number n

He equated mixed dead-space concentration at end-expiration for the model
to mixed alveolar concentration for a subject.

Nye also stated that for a two-component curve, the number
of numerical constants that can be read from it is four, and therefore
a unique determination of parameters for the case of two-compartment
model with common dead space cannot be made. To show the differences
in volume and ventilation estimates in assuming a simple two-chambered
model in place of one with a common dead space, he generated curves from
given parameters for the common dead-space model and found parameter
values for the simple two-chambered model from them. The effect of
dead-space mixing is to decrease the apparent unevenness: the more even
the ventilation, the greater is this distortion.

In studying a slightly more complicated model, Wise and De-
fares [40] formulated an equation describing the difference in concen-
trations from breath-to-breath in a spirometer for the case of a closed-
circuit washout and for a model consisting of a common dead space and

separate dead spaces leading to two alveolar compartments. In a similar manner to Nye [28] they set up an equation of linear difference and found the solution to consist of the sum of two exponentials. The concentration in the spirometer also consists of two exponentials, but includes a term representing an equilibration value. The breath-by-breath difference in spirometer concentration is of the form:

$$U_r = A \alpha^r + B \beta^r \tag{1.15}$$

and the concentration:

$$u_r = u_\infty + \frac{A \alpha^r}{1-\alpha} + \frac{B \beta^r}{1-\beta} \tag{1.16}$$

Their's was a theoretical study and did not attempt to correlate this model with experimental studies nor investigate the inverse problem of obtaining model parameters given a closed-circuit washout curve.

In the early 1960's, Gomez [15] introduced the concept of an infinite number of functional lung units corresponding to a continuous distribution of a specific tidal volume whose image is the washout function of a tracer indicator. The specific transformation between the washout curve and the distribution of specific tidal volume is the inverse Laplace transform. For a single-compartment model, the rate of nitrogen elimination is given by:

$$V_{N_2}(t) = V_{N_2}(0) e^{-t/\tau} \tag{1.17}$$

where τ = clearance time constant

= $V/\dot{V}$

V_{N_2} = volume of N_2 in the compartment

For n-parallel compartments:

$$V_{N_2}(t) = \sum_{i=1}^{n} V_{N_2 i}(0) e^{-t/T_i} \qquad (1.18)$$

Dividing by the concentration of N_2 at t = 0 to give the lung volume washed out, and taking the limit as $n \rightarrow \infty$:

$$V(t) = \lim_{n \to \infty} \left[\sum_{i=1}^{n} V_i(0) e^{-t/T_i} \right] = \lim_{n \to \infty} \left[\sum G(T_i) \Delta T e^{-t/T_i} \right]$$

$$= \int_0^{\infty} G(T) e^{-t/T} dT \qquad (1.19)$$

where G(T) is the distribution function of lung volumes according to clearance time constant T, and is defined by:

$$V(0) = \int_0^{\infty} G(T) dT \qquad (1.20)$$

and T_i is some value in the interval ΔT such that:

$$G(T_i) \Delta T = V_i(0) \qquad (1.21)$$

Replacing T by 1/S in equation (1.19):

$$V(t) = \int_0^{\infty} F(s) e^{-st} dS \qquad (1.22)$$

which is the form of the Laplace transform of F(S). The inverse transform will yield F(S) and was done by Gomez [15], Okubo and Lenfant [29], and Nakamura, et al. [27] using different approximations.

The division into functional units was such that each venti-lated independently of the rest, implying that mixing in a common dead space was ignored.

Following thru on Militano's work [25], Saidel, et al. [36] described a five-compartment model consisting of a non-distensible common upper-airway compartment in series with two parallel branches, each consisting of a distensible conducting airway compartment followed by a distensible alveolar space. The five compartments are characterized by seven independent parameters, the remaining two resulting from two constraint equations. One of these equated the sum of the volumes to functional residual capacity and the other equated the distensibilities, normalized with respect to total ventilation, to unity. Breathing was assumed sinusoidal and differential equations for mass balances were set up and solved numerically in order to match the model output to experimentally obtained data for nitrogen washout and carbon-monoxide diffusion tests. A manual search technique was used to obtain the parameter set resulting in the closest data-model match. Intracyclic simulation was attempted with inconclusive results.

Since 1950, researchers have tried to analyze the N_2 washout test with models, most of which consisted of a small number of well-mixed compartments ventilated cyclically or continuously [14,28,33,36, 39,40]. Anatomic dead space was included as separated dead spaces which decreased effective tidal volume, or as a common dead space which coupled functional units and increased the complexity of the analysis considerably. The most elaborate models were by Wise and Defares [40] and Saidel, et al. [36]. Wise and Defares divided the anatomic dead space into a common and separate portion and derived describing equations for a closed-circuit washout procedure. They restricted their paper to a theoretical derivation and did not attempt to solve the inverse problem

of obtaining model parameters from given patient data. Saidel, et al. had a model with the flexibility to simulate mixed-expired nitrogen washouts as well as intra-breath variations in nitrogen concentration, though the latter proved inconclusive. The uniqueness of their model parameter set is questionable, there being seven independent parameters to search for, though the model-data match seemed fairly good.

The transform method of Gomez [15] was more realistic in the sense that individual alveoli as the functional units are actually distributed in a structural dimension which implies functional distribution, but consideration of the common airways where mixing and reinspiration take place was not included.

II. MODEL

MODEL STRUCTURE

The model to simulate nitrogen open-circuit washout consists of a common dead-space compartment is series with two branches, each consisting of a separate dead-space compartment followed by a respiratory volume (see Figure [4]). This is the simplest model that can incorporate regional and stratified inhomogeneity as well as coupling between parallel ventilation units. The functional unit or respiratory space in the model does not have a specific anatomic assignment. The designation is a functional one and as such it may be artificial, however it does prove useful in characterizing the system and providing quantitative answers to specific questions. The actual system which has in fact a distribution of individual respiratory spaces (alveoli), at least in terms of structural dimension may be more accurately represented by a large number of functional units. However studies up to now [15,27,29] show that this necessitates exclusion of other aspects of the physiologic system, including mixing in a common dead space, which has been shown to affect system characterization [28].

This model follows along classical lines. It is compartmental and the contents are assumed well-mixed. Most previous models have assumed either separate or common dead space leading to at least two alveolar spaces. This model incorporates both common and separate dead
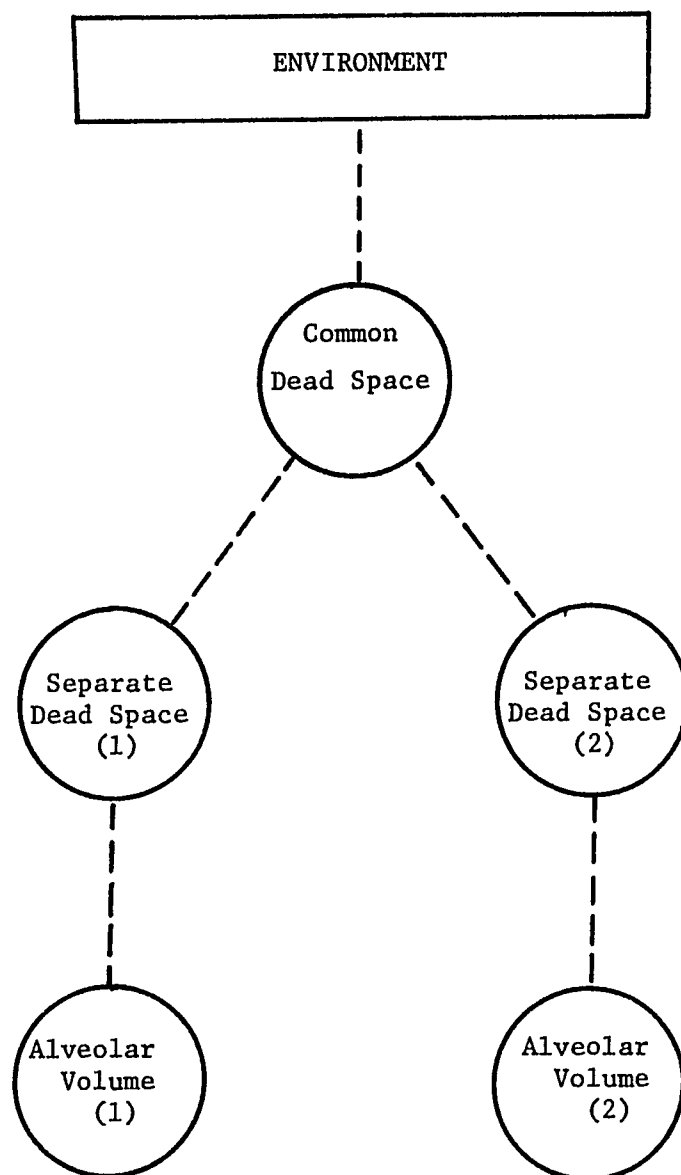
Figure 4. Schematic of Five-Compartment Ventilation Model.

spaces and can degenerate to include one or the other if desired.

The model development contains the following assumptions:

1. Perfect gas law is valid ($P_A V = n_A RT$), such that partial pressures and pure-component volumes are additive. Compressibility factors for respiratory gases at normal body temperature and atmospheric pressure varies from unity by less than 1 percent.

2. Alveolar compartments are well-mixed and are of variable volume.

3. Dead-space compartments are of constant volume.

4. Diffusional effects between compartments is not explicitly included in the model, but is implicit in the volume and ventilation estimates of the compartments.

5. Flow through the separate dead spaces is plug flow. Flow through the common dead space is plug flow on inspiration, and plug flow on expiration with the added condition that concentrations from both branches are mixed in proportion to their respective fractional tidal volumes at end-expiration. This assumes synchronous ventilation to the two branches. The mixed common dead-space gas is re-inspired prior to the new inspirate on the next breath.

6. Tidal volumes to the two branches are constant fractions of the total tidal volume and the same on inspiration and expiration. Under normal resting conditions, about 250 ml/min. of O_2 is consumed and about 200 ml/min. of CO_2 is given off into the lungs, resulting in a net efflux of 50 ml/min. of O_2.

For an average respiratory rate of 12 breaths/min. and tidal volume of 500 ml, this efflux amounts to 4 ml/breath or less than 1 percent of the total tidal volume.

7. Nitrogen concentration at the start of a washout procedure is assumed uniform throughout the alveolar spaces and from consideration of the constraint ($\sum_i t_i = 1$), this concentration is equal to the end-expired concentration in the common dead-space volume.

8. Nitrogen transport from blood and tissues is assumed negligible with reference to its effect in changing alveolar concentrations during the washout procedure. Nitrogen is an inert metabolic gas and has low solubility in blood and tissues. N_2 is assumed in equilibrium across the alveolocapillary membrane at the start of a washout, and this influx will become of increasing importance as the washout proceeds. However due to limitations of the nitrogen analyzer to monitor concentrations less than 2 vol. percent, the range of concentrations considered will for the most part exclude regions where N_2 from blood becomes significant [25].

9. End-tidal concentrations from washout tests is assumed to be end-expired concentrations from the model.

DEVELOPMENT OF MODEL EQUATIONS

The describing equations for this model consists of material balances for nitrogen. A breath-by-breath analysis was made to derive

an expression for end-expired concentration of nitrogen in the common dead-space compartment.

The following notation is used:

$F_{Ai(I)}^{(n)}$ = volumetric concentration[1] in alveolar compartment i at the end of inspiration (I) for breath number n.

$F_{Ai(E)}^{(n)}$ = volumetric concentration in alveolar compartment i at the end of expiration (E) for breath number n.

F_I = volumetric concentration in inspired gas.

F_0 = initial volumetric concentration in the model.

f = volumetric concentration difference

= $F - F_I$

FRC = functional residual capacity[2]

= $V_L + V_D$

V_{Ti} = tidal volume of alveolar compartment i.

V_T = total tidal volume

= $\sum_i V_{Ti}$

V_{DC} = volume of common dead-space compartment.

V_{DSi} = volume of separate dead space in branch i.

V_{DS} = total volume of separate dead-space compartments

= $\sum_i V_{DSi}$

V_D = total volume of dead space = $V_{DC} + V_{DS}$.

---

[1] Volumetric concentration refers to saturated gas phase and is equal to pure component volume divided by total volume (vol. percent).

[2] All volumes refer to body temperature and pressure, saturated conditions (liters or cc).

V_{Li} = volume of alveolar compartment i at end-expiration.

V_L = total alveolar compartment volume at end-expiration.

= $\sum_{i} V_{Li}$

t_i = fraction of tidal volume going to branch i.

= V_{Ti}/V_T

l_i = fraction of total alveolar volume at end-expiration that is in alveolar compartment i

= V_{Li}/V_L

α = fraction of total dead space that is separate.

= V_{DS}/V_D

The following relationships are true by conservation of mass:

$$\sum_{i} l_i = 1 \tag{2.1}$$

$$\sum_{i} t_i = 1 \tag{2.2}$$

Assuming that washout of nitrogen begins with the inspiration of oxygen at breath number 1, then at the end of inspiration:

$$(V_{L1} + V_{T1}) F_{A1(I)}^{(1)} = F_{A1(E)}^{(o)} V_{L1} + F_{DS1(E)}^{(o)} V_{DS1} + \frac{V_{T1}}{V_T} F_{DC(E)}^{(o)} V_{DC}$$

$$+ \left[\frac{V_{T1}}{V_T} (V_T - V_{DC}) - V_{DS1} \right] F_I \tag{2.3a}$$

$$(V_{L2} + V_{T2}) F_{A2(I)}^{(1)} = F_{A2(E)}^{(o)} V_{L1} + F_{DS2(E)}^{(o)} V_{DS2} + \frac{V_{T2}}{V_T} F_{DC(E)}^{(o)} V_{DC}$$

$$+ \left[\frac{V_{T2}}{V_T} (V_T - V_{DC}) - V_{DS2} \right] F_I \tag{2.3b}$$

Assuming: $\quad V_{Ti} > V_{DSi} + \dfrac{V_{Ti}}{V_T} V_{DC}$

then: $\quad F_{DS1(I)}^{(1)} = F_{DS2(I)}^{(1)} = F_{DC(I)}^{(1)} = F_I$ (2.3c)

Rearranging equations (2.3) and introducing the concentration difference f :

$$f = F - F_I \qquad (2.4)$$

$$(V_{L_1} + V_{T_1}) f_{A1(I)}^{(1)} = V_{L_1} f_{A1(E)}^{(o)} + V_{DS1} f_{DS1(E)}^{(o)} + t_1 V_{DC} f_{DC(E)}^{(o)}$$
(2.4a)

$$(V_{L_2} + V_{T_2}) f_{A2(I)}^{(1)} = V_{L_2} f_{A2(E)}^{(o)} + V_{DS2(E)}^{(o)} + t_2 V_{DC} f_{DC(E)}^{(o)}$$
(2.4b)

$$f_{DS1(I)}^{(1)} = f_{DS2(I)}^{(1)} = f_{DC(I)}^{(1)} = 0 \qquad (2.4c)$$

At the end of expiration for breath number 1:

$$f_{A1(E)}^{(1)} = f_{DS1(E)}^{(1)} = f_{A1(I)}^{(1)} \qquad (2.5a)$$

$$f_{A2(E)}^{(1)} = f_{DS2(E)}^{(1)} = f_{A2(I)}^{(1)} \qquad (2.5b)$$

$$f_{DC(E)}^{(1)} = t_1 f_{A1(E)}^{(1)} + t_2 f_{A2(E)}^{(1)} \qquad (2.5c)$$

Similarly at the end of inspiration for breath number 2:

$$(V_{L_1}+V_{T_1})\, f_{A1(I)}^{(2)} = V_{L_1} f_{A1(E)}^{(1)} + V_{DS1}\, f_{DS1(E)}^{(1)} + t_1 V_{DC} f_{DC(E)}^{(1)}$$

$$(2.6a)$$

$$(V_{L_2}+V_{T_2})\, f_{A2(I)}^{(2)} = V_{L_2} f_{A2(E)}^{(1)} + V_{DS2}\, f_{DS2(E)}^{(1)} + t_2 V_{DC} f_{DC(E)}^{(1)}$$

$$(2.6b)$$

$$f_{DS1(I)}^{(2)} = f_{DS2(I)}^{(2)} = f_{DC(I)}^{(2)} = 0$$

$$(2.6c)$$

And at the end of expiration for breath number 2:

$$f_{A1(E)}^{(2)} = f_{DS1(E)}^{(2)} = f_{A1(I)}^{(2)}$$

$$(2.7a)$$

$$f_{A2(E)}^{(2)} = f_{DS2(E)}^{(2)} = f_{A2(I)}^{(2)}$$

$$(2.7b)$$

$$f_{DC(E)}^{(2)} = t_1\, f_{A1(E)}^{(2)} + t_2\, f_{A2(E)}^{(2)}$$

$$(2.7c)$$

or in general for breath number n:

$$(V_{L_1}+V_{T_1})\, f_{A1(I)}^{(n+1)} = V_{L_1} f_{A1(E)}^{(n)} + V_{DS1}\, f_{DS1(E)}^{(n)} + t_1 V_{DC} f_{DC(E)}^{(n)}$$

$$(2.8a)$$

$$(V_{L_2}+V_{T_2})\, f_{A2(I)}^{(n+1)} = V_{L_2} f_{A2(E)}^{(n)} + V_{DS2}\, f_{DS2(E)}^{(n)} + t_2 V_{DC} f_{DC(E)}^{(n)}$$

$$(2.8b)$$

$$f_{DS1(I)}^{(n+1)} = f_{DS2(I)}^{(n+1)} = f_{DC(I)}^{(n+1)} = 0$$

$$(2.8c)$$

$$f_{A1(E)}^{(n+1)} = f_{DS1(E)}^{(n+1)} = f_{A1(I)}^{(n+1)}$$

$$(2.8d)$$

$$f_{A2(E)}^{(n+1)} = f_{DS2(E)}^{(n+1)} = f_{A2(I)}^{(n+1)}$$

$$(2.8e)$$

$$f_{DC}^{(n+1)} = t_1\, f_{A1(E)}^{(n+1)} + t_2\, f_{A2(E)}^{(n+1)}$$

$$(2.8f)$$

The equations of interest are (2.8a), (2.8b), (2.8f) and after using equations (2.8c), (2.8d), and (2.8e) to simplify:

$$f_{DC(E)}^{(n)} = t_1 f_{A1(E)}^{(n)} + t_2 f_{A2(E)}^{(n)} \qquad (2.9a)$$

$$f_{A1(E)}^{(n+1)} = \left(\frac{1}{V_{L1}+V_{T1}}\right)\left[(V_{L1}+V_{DS1})f_{A1(E)}^{(n)} + t_1 V_{DC} f_{DC(E)}^{(n)}\right] \qquad (2.9b)$$

$$f_{A2(E)}^{(n+1)} = \left(\frac{1}{V_{L2}+V_{T2}}\right)\left[(V_{L2}+V_{DS2})f_{A2(E)}^{(n)} + t_2 V_{DC} f_{DC(E)}^{(n)}\right] \qquad (2.9c)$$

for $n = 0,1, \ldots$

The subscript (E) will henceforth be dropped, and end-expired concentration will be assumed.

Equation (2.9c) describes the end-expired concentration in the common dead space and will be used to simulate the end-tidal concentration from N_2 washout tests. Looking at equations (2.9a) and (2.9c), the concentration in alveolar compartment 1 at breath (n+1) is formed by a fraction, $f_{A1}^{(n)}(V_{L1}+V_{DS1})/(V_{L1}+V_{T1})$, representing the previous concentration, another fraction, $t_1 f_{A1}^{(n)}(t_1 V_{DC})/(V_{L1}+V_{T1})$, representing recirculation of the previous concentration through mixing in the common dead space, and a third fraction, $t_2 f_{A2}^{(n)}(t_1 V_{DC})/(V_{L1}+V_{T1})$, representing the contribution from alveolar compartment 2. This last term shows the coupling between the two alveolar compartments.

For K-parallel branches, the (K+1) describing equations are:

$$f_{Ai}^{(n+1)} = \left(\frac{1}{V_{Li}+V_{Ti}}\right)\left[(V_{Li}+V_{DSi})f_{Ai}^{(n)} + t_i V_{DC} f_{DC}^{(n)}\right] \qquad (2.10a)$$

$$f_{DC}^{(n)} = \sum_{i=1}^{K} t_i f_{Ai}^{(n)} \qquad (2.\ 10b)$$

For i = 1,2,...,K

n = 0,1,2,...

DISCUSSION

It is shown in Appendix C that the system of linear difference equations (2.9) reduces to a second-order linear homogeneous difference equation with constant coefficients in $f_{DC}^{(n)}$ which has a solution consisting of the sum of two exponentials:

$$f_{DC}^{(n)} = C_1 M_1^n + C_2 M_2^n \qquad (2.11)$$

where M_1, M_2 are functions of the model parameters, and C_1, C_2 are functions of the model parameters and initial conditions.

The inverse problem however consists of obtaining a unique set of parameters given estimates of C_1, C_2, M_1, and M_2. According to Nye [28], assuming a washout curve is representable by the sum of two exponentials, the number of unknown parameters that can be found is four. This is the same as the number of equations available from the two intercepts, C_1 and C_2, and the two slopes, M_1 and M_2, of the components when the curve is decomposed and plotted on semilogarithmic graph paper. The number of independent parameters that can be uniquely solved for however, is three, since the model incorporates a constraint equation at n = 0, namely:

$$C_1 + C_2 = f_{DC}^{(o)} \tag{2.12}$$

Once C_1 or C_2 is specified, the other is constrained by the above relation and does not provide an independent relationship for the model parameters. The number of parameters that characterizes the common dead-space model is five, say V_{T1}, V_{T2}, V_{L1}, V_{L2}, and V_D. Assuming average tidal volume, V_T, and functional residual capacity, FRC, are input quantities, the number of independent parameters is three, the required number for unique determination. The following relations were used:

$$V_T = V_{T1} + V_{T2} \tag{2.13}$$

$$FRC = V_{L1} + V_{L2} + V_D \tag{2.14}$$

For the case of separated dead space only, there are six parameters that describe the model, say V_{T1}, V_{T2}, V_{L1}, V_{L2}, V_{DS1}, and V_{DS2}. The above two constraints can be used, but that reduces the number to four independent parameters. Another relation which will be assumed is that the separate dead spaces are divided in the same proportion as the respective alveolar volumes at end-expiration:

$$\frac{V_{DS1}}{V_{DS2}} = \frac{V_{L1}}{V_{L2}} \tag{2.15}$$

which implies that:

$$\frac{V_{DSi}}{V_{DS}} = \frac{V_{Li}}{V_L} = \lambda_i \tag{2.16}$$

for $i = 1,2$.

Thus three independent parameters describe the separate dead-space model.

The general model incorporating both common and separate dead spaces has seven parameters, V_{T1}, V_{T2}, V_{L1}, V_{L2}, V_{DS1}, V_{DS2}, and V_{DC}. The three constraint equations are used to give four independent parameters. Since a single washout will uniquely determine only three parameters, another washout at a sufficiently different dilution factor will be used in conjunction to define the fourth parameter. The parameter set for a particular subject will be assumed to be constant from one run to the next in this procedure.

In general for K-parallel branches, the number of parameters which can uniquely be solved for is (2K-1).

Equations (2.9) can be nondimensionalized with respect to the characteristic dimensions of the model, FRC and f_0, where f_0 = $F_0 - F_I$:

$$\frac{f_{A1}^{(n+1)}}{f_o} = \left(\frac{1}{\ell_1 \frac{V_L}{FRC} + t_1 \frac{V_T}{FRC}}\right)\left\{\ell_1\left(\frac{V_L}{FRC} + \alpha\frac{V_D}{FRC}\right)\frac{f_{A1}^{(n)}}{f_o} + \left[t_1(1-\alpha)\frac{V_D}{FRC}\right]\frac{f_{DC}^{(n)}}{f_o}\right\}$$

(2.17a)

$$\frac{f_{A2}^{(n+1)}}{f_o} = \left(\frac{1}{\ell_2 \frac{V_L}{FRC} + t_2 \frac{V_T}{FRC}}\right)\left\{\ell_2\left(\frac{V_L}{FRC} + \alpha\frac{V_D}{FRC}\right)\frac{f_{A2}^{(n)}}{f_o} + \left[t_2(1-\alpha)\frac{V_D}{FRC}\right]\frac{f_{DC}^{(n)}}{f_o}\right\}$$

(2.17b)

$$\frac{f_{DC}^{(n)}}{f_o} = t_1\frac{f_{A1}^{(n)}}{f_o} + t_2\frac{f_{A2}^{(n)}}{f_o}$$

(2.17c)

where $f^{(n)}/f_0$ = normalized volumetric concentration.

V_D/FRC   = fractional dead space volume

V_L/FRC   = fractional alveolar volume

V_T/FRC   = dilution factor

These equations will be used as the working equations for the simulation. The parameters of interest are t_1, t_2, l_1, l_2, α, V_L/FRC, V_D/FRC, and V_T/FRC. The constraint equations are:

$$\frac{V_L}{FRC} + \frac{V_D}{FRC} = 1 \qquad (2.18a)$$

$$l_1 + l_2 = 1 \qquad (2.18b)$$

$$t_1 + t_2 = 1 \qquad (2.18c)$$

The dilution factor, V_T/FRC, will be considered an input quantity.

For the case of $\alpha = 0$, equations (2.17) reduce to those describing washout for common dead space only, and for $\alpha = 1$, the equations for the alveolar concentrations become uncoupled and describe the model with separate dead spaces only.

The next chapter deals with the method of simulation required to obtain the parameter set.

III. SIMULATION

The method of simulation is a system identification problem where computer solutions to the model equations are matched to test data and corrections to the describing parameter set are made in order to minimize a chosen error criteria. The structure of the model is developed as relevant to the physiological system and from known input and output a parameter set is found which characterizes the system. If the model is a true representation of the physiological system, the error criteria is zero at all times in the simulation. However in almost all cases, there appears a residual error, so the validity of the model rests in the determination of a sufficiently close data-model match. In this study, the feasibility to characterize the present model as well as the models incorporating either separate dead space or common dead space will be ascertained and the application to clinical usage will be investigated.

DATA CHARACTERISTICS

The data consists of end-tidal nitrogen concentrations measured in volumetric percent with a rapid nitrogen analyzer. Details of the washout procedure and equipment may be found in Appendix A. The subject is breathing room air consisting of approximately 80 vol. percent nitrogen. The washout test begins at the end of a normal expira-

tion at which time the subject is connected to an oxygen source. The subject breathes normally for a period of usually seven minutes during which time continuous flow at the mouth is monitored with a pneumotachograph (bi-directional pitot tubes) and nitrogen concentration is measured with the nitrogen meter. The expirate is collected in a large Tissot spirometer whose total volume and mixed-concentration are measured at the end of the test for determination of average tidal volume and FRC.

When nitrogen concentration is plotted against breath number on semilogarithmic graph paper, clinically diagnosed normal subjects wash out very fast, typically down to 2.5 vol. percent in 40 breaths or less, whereas chronically diseased subjects may not wash out their nitrogen to 2.5 vol. percent within 100 breaths. Usually washout curves can be fitted by the sum of two exponentials and sometimes by three [28]. This does not necessarily imply that the lungs consist of only two or three distinct divisions of alveoli, but it does lend support to the compartmental structure as representative of functional aspects of the lungs as a whole. In fact it has been shown that within limits of accuracy of the nitrogen analyzer, the same curves can be represented by the sum of five to twenty exponentials [17,38]. The inverse problem of exponential decomposition however precludes extending the number of exponentials to more than three. The accuracy required is heavily dependent on the number of exponentials comprising the sum and the ratios of the exponential time constants [37]. The closer the ratios, the more accurate the concentrations must be in order that a relatively consistent parameter set be obtained, thus even for two exponentials difficulties arise when the time constants are fairly close. This is

typically the case for normals, but decomposition generally becomes
more consistent for abnormal patients where the time constants are
separated much more.

The flow signal was integrated electronically to generate
volume signals. This was monitored to determine whether breath-by-
breath variations in tidal volume significantly affected the course
of nitrogen washout and whether the course of these variations were
in any way systematic. Absolute values were not obtained due to mal-
functioning of the calibration system in the pneumotach converter, but
relative values were determined to be valid after linearity of the
converter was checked.

PARAMETER ADJUSTMENT ALGORITHM

The error criteria used was of a least squares form, the sum
of the squares of the differences between selected data points and mo-
del output. Minimization of this term led to the parameter set which
"best fit" the data points.

No transformation is available to convert a sum of exponen-
tials into a linear equation in the parameters, therefore a nonlinear
least squares approximation method had to be used. This consists of
expanding the function in a Taylor series about an initial parameter
set and linearizing the series with respect to an increment in the
parameter set. The linearized function is now used to minimize the
error criteria, hopefully leading to a parameter set which at least

decreases the sum of squares of the deviations. The method can be repeated using the new parameter set and linearizing the function about it.

The specific algorithm that was used to perform a least-squares curve fit to the data is from Marquadt [23]. The previously discussed method fails when the increment in the parameters is too large for the error criteria to decrease. Marquadt's algorithm introduces a Lagrange multiplier, λ , to increase or decrease the step size for faster convergence and convergence respectively. This method incorporates the best features of the Gauss-Newton procedure which converges very fast when the function can be linearized, and the method of steepest descent which assures convergence, but may do so very slowly. Appendix B contains more details on the algorithm.

The program began with initial values for the parameter set. Using these values, deviations from the data points were calculated and a change in the parameter set was made to minimize the largest deviation. The process was repeated using the new parameter set until all deviations were within a prescribed interval or until the number of iterations exceeded a specified limit. These were the two stopping criteria. It was found that a limit of 50 iterations was sufficient for convergence to within the prescribed interval if convergence did occur. The bounds for the deviations were determined from the accuracy of the nitrogen analyzer and readability of the oscillograph recording. The bounds were adjusted to accommodate convergence within 50 iterations.

The data points that were used were selected from a smooth curve which was drawn through all the data points. The number of points

varied from five to ten and were usually selected at equal intervals or closer where curvature was greater.

The measure of closeness of fit was selected to be the root mean square relative error (RMSRE) given by:

$$\text{RMSRE} = \left[\frac{\sum\limits_{i=1}^{n} \left(\frac{y_i - f_i(\underset{\sim}{\alpha})}{y_i} \right)^2}{n-1} \right]^{1/2}$$

where y_i = i^{th} data point.

$f_i(\underset{\sim}{\alpha})$ = model output at parameter set $\underset{\sim}{\alpha}$ corresponding to the ith data point.

n   = number of data points used.

This index measures deviations relative to the magnitude of the data point, which would be indicative of the size of deviations on semilogarithmic graph paper.

IV. RESULTS AND DISCUSSION

The data used in this study is from two sources. One was clinically obtained from Baylor College of Medicine's Pulmonary Disease Laboratory and typically from physiologically abnormal subjects, and the other source is patient data from Militano [25] taken at different dilution factors.

The data recorded from the Baylor laboratory was nitrogen concentration and tidal volume as functions of time. Typical recordings are shown in Figure [5]. The decay is not smooth but fluctuates about a mean curve which is due at least in part to variations in the tidal breathing. An attempt was made to isolate this effect by plotting nitrogen concentration against cumulative expired tidal volume and comparing the resulting curve with one plotted against cumulative average tidal volume which represents breath number also. Figures [6,7] show some of the results. There is some smoothing but the basic shapes were not significantly changed. It was therefore concluded that an average tidal volume would suffice to describe a washout curve and the much more laborious breath-by-breath monitoring of tidal breathing was not necessary except to verify that the subject was breathing normally. Average tidal volume was obtained from measuring the accumulated expirations in the Tissot spirometer and dividing by the total number of breaths.

In conjunction with the above results, an investigation was made to see whether the effects of the ventilation parameters such as tidal volume and functional residual capacity could be displayed apart from the effects of the distribution parameters such as t_i and l_i. The purpose was that if such a separation was possible, specific causes of nitrogen decay could be clinically evaluated easier.

Looking at the case of two alveolar compartments with no dead space ventilated by tidal volume, V_T, the governing equation for nitrogen decay is:

$$f^{(n)} = t_1 \left(1 + \frac{V_{T_1}}{FRC_1}\right)^{-n} + t_2 \left(1 + \frac{V_{T_2}}{FRC_2}\right)^{-n} \qquad (4.1)$$

where
$$V_{Ti} = t_i V_T$$
$$FRC_i = l_i FRC$$
$$f^{(n)} = \text{end-expired concentration at breath number } n.$$

Equation (4.1) can also be written:

$$f^{(n)} = t_1 e^{-\ln\left(1 + \frac{t_1}{l_1}\frac{V_T}{FRC}\right)} + t_2 e^{-\ln\left(1 + \frac{t_2}{l_2}\frac{V_T}{FRC}\right)} \qquad (4.2)$$

Expanding $e^{(t_i/l_i)(V_T/FRC)}$ in a series form and neglecting second-order and higher terms:

$$e^{\frac{t_i}{l_i}\frac{V_T}{FRC}} = 1 + \frac{t_i}{l_i}\frac{V_T}{FRC} + \frac{1}{2!}\left(\frac{t_i}{l_i}\frac{V_T}{FRC}\right)^2 + \cdots,$$

$$\sim 1 + \frac{t_i}{l_i}\frac{V_T}{FRC} \qquad (4.3)$$

Then equation (4.2) becomes:

$$f^{(n)} = t_1 e^{-\frac{t_1}{l_1}\left(\frac{V_T}{FRC}n\right)} + t_2 e^{-\frac{t_2}{l_2}\left(\frac{V_T}{FRC}n\right)} \qquad (4.4)$$

which could then be plotted with an abscissa scale of $(V_T n)/FRC$ making the curvature of $f^{(n)}$ a function of the distribution parameters t_1, t_2, t_1/l_1, and t_2/l_2 only.

In general however the second order terms cannot be neglected without incurring a significant error of the order,

$$\left[n\left(\frac{t_i}{l_i}\frac{V_T}{FRC}\right)^2 \left(1+\frac{t_i}{l_i}\frac{V_T}{FRC}\right)^{n-1} \right]$$

and relative error of the order,

$$\left[\frac{n\left(\frac{t_i}{l_i}\frac{V_T}{FRC}\right)^2}{\left(1+\frac{t_i}{l_i}\frac{V_T}{FRC}\right)} \right]$$

both of which increase with n. Any correction terms which may be included would be functions of the distribution parameters and so it does not seem possible to separate distribution effects from cumulative ventilation effects.

Initial parameter identification was restricted to the common dead-space model and the separate dead-space model to ascertain the feasibility of the curve-fit method. Ten washout runs at different dilution factors from four subjects were initially looked at. Two were normals, subjects KA and TM, one was asthmatic, subject MS, and the fourth had chronic obstructive lung disease, subject LD. Subject KA's data was from Baylor's Pulmonary Laboratory and the others were from Militano [25].

In this first group of washout data, the curve fit was very good when single washout simulations were performed. The curve fit criteria, RMSRE, was always less than 0.04 (see Table 1). Figures [8-11] show the simulated curves and the data points used in the curve fit. The RMSRE values for both models were the same since both solutions are the sum of two exponentials and the algorithm essentially adjusts the coefficients and the exponential time constants to best fit the data points. The parameter values for each washout curve were different however, as would be expected. It can also be seen that the parameter set, t_1, l_1, and V_D/V_L, is highly dependent on the dilution factor, V_T/FRC. Values of V_D/V_L are generally greater in the common dead-space model and there is greater separation in the dilution factors for the individual compartments. Table 2 shows the individual dilution factors and tidal volumes. Comparison of subjects show that the ratio of dilution factors is of the range of 4-6 for normals and 8-9 for abnormals for the common dead-space model. The separate dead-space model has ratios of 1-3 for normals and 4-8 for abnormals. The difference in ratios between normals and abnormals is attributed to a significant decrease in dilution factor in the section of lung with poorer ventilation for the case of abnormal subjects. The better ventilated compartments in all four subjects have comparable dilution factors. Inspection of the individual tidal volumes for each subject shows that the better ventilated compartment reflects the system tidal breathing more than the poorer ventilated compartment. This is one indication that the fractional tidal volume is not a constant of the system, but varies with overall tidal volume. This change in fractional tidal

volume can be attributed to two causes, either the better ventilated section is increasing its tidal volume relatively more than the poorer ventilated section for the same fractional lung volume, or a larger section of the lung is being better ventilated, thereby increasing the fractional tidal volume of that section. Both causes seem to be operating, since the volume fraction generally increased with system dilution factor, but the respective increase in tidal volume was even greater indicating that the section as a whole was being better ventilated.

Another indication that parameters were not remaining constant at different dilution factors was found by generating curves using a given parameter set (t_2 = constant) but with dilution factors for other washouts and comparing these with the original curves (see Figures [12-19]). RMSRE values for both models ranged from 0.083 to 1.438 with most greater than 0.200, indicating that parameters were changing as functions of overall dilution factor. Curves were also generated assuming the tidal volume of the poorer ventilated compartment remained constant (see Figures [20-25]). Except for a few cases, RMSRE for these curves were greater than for the curves generated assuming constant tidal volume fractions (see Table 3).

Parameters for the more general model with common and separate dead spaces were obtained using pairs of washout runs. Results are shown in Table 4 and Figures [26-29]. For comparison, both the common dead-space model and the separate dead-space mode were also used. The Marquadt algorithm adjusted parameter values to best fit the data points in both runs. Values of RMSRE for all three models were about the same for each pair of runs. This suggests that α , the fraction of the

dead space which is separate, is a very insensitive if not an unstable parameter. Convergence was studied by increasing the number of iterations and varying the Levenberg adjustment weighting factor. It was found that for some cases, α was outside the physically realistic range [$0 \leq \alpha \leq 1$], although the curve fit was optimized.

The simpler models consisting of a common dead space or separate dead spaces neglect important aspects of the physical system, though their parameter values appear to be unique. The general model is more realistic, but the problem of defining the additional parameter by curve fitting two washout runs concurrently is not tractable. One reason is that the assumption that the parameter set remains constant between is probably not true as was shown by the simulation of single runs by the two simpler models. But the main reason is that curve fitting two runs instead of just one leads to a single parameter set which best fits both curves, but the number of independent parameters which can be uniquely defined is still three, the number that defines the solution of the general model.

As a result, one of the four independent parameters needs to be specified for the general model to be used. Characterization of the two simpler models will put bounds on the more general model. If the parameter sets for both simple models are close enough to each other, a good approximation to the general model can be made, exclusive of .

Aspects of clinical diagnosis were investigated using data from eight patients who were tested at Baylor's Pulmonary Laboratory. There were two runs made per patient, but usually the curves were nearly coincidental, so a single average curve was used for the data points

(see Figures [30,31]). Two sets of parameter values were found corresponding to the two models, and certain selected factors were calculated (see Tables 5 and 6). Simulation was good with RMSRE values less than 0.05. Inspection of the tabulated results show that functional residual capacities were usually abnormal, both larger and smaller than predicted for normals of similar physical size, age and sex. The ventilation factors of significance are the effective dilution factor, $(V_T - V_D)/V_L$, and the distribution factor, $(V_{T1}/V_{L1})/(V_{T2}/V_{L2})$, both of which showed a large degree of spread. No conclusions were drawn concerning diagnostic correlations other than to say that low effective dilution factors and high distribution factors contribute to decreased ventilation effectiveness and slower washouts. Since both models neglect important aspects of lung structure and fit the data equally well, there is little basis for choice as to which is more representative of the physical system.

Table 1. Best Fit Parameters Using Single Runs[+]

Subject	Model Code	V_T/FRC	t_1	l_1	V_D/V_L	RMSRE
TM	COM2[*]	0.55	0.73	0.41	0.12	0.022
		0.33	0.47	0.19	0.01	0.005
		0.20	0.57	0.23	0.08	0.008
LD	COM2	0.20	0.75	0.24	0.08	0.014
		0.14	0.62	0.15	0.04	0.037
		0.08	0.41	0.07	0.01	0.008
MS	COM2	0.267	0.83	0.34	0.09	0.013
		0.14	0.66	0.18	0.02	0.015
KA	COM2	0.41	0.84	0.46	0.18	0.010
		0.331	0.88	0.61	0.19	0.009
TM	SEP2[**]	0.55	0.61	0.37	0.09	0.022
		0.33	0.44	0.18	0.01	0.005
		0.20	0.37	0.16	0.06	0.008
LD	SEP2	0.20	0.62	0.27	0.05	0.014
		0.14	0.50	0.15	0.03	0.037
		0.08	0.39	0.07	0.00	0.008
MS	SEP2	0.267	0.74	0.40	0.05	0.013
		0.14	0.63	0.19	0.01	0.015
KA	SEP2	0.41	0.69	0.47	0.13	0.010
		0.331	0.61	0.48	0.17	0.009

[*]   COM2:   common dead-space model

[**]   SEP2:   separate dead-space model

[+]   Subjects TM, LD, MS from Militano [25]
    Subject KA from Baylor College of Medicine's Pulmonary Lab

Table 2. Alveolar Compartment Dilution Factors and Tidal Volumes

(from Table 1)

Subject	Model Code	V_T/FRC	V_T/V_L [+]	V_{T_1}/V_{L_1} [++]	V_{T_2}/V_{L_2}	$\dfrac{V_{T_1}/V_{L_1}}{V_{T_2}/V_{L_2}}$	V_{T_1}/FRC [+++]	V_{T_2}/FRC
TM	COM2*	0.55	0.616	1.098	0.282	3.89	0.402	0.148
		0.33	0.333	0.824	0.218	3.78	0.175	0.155
		0.20	0.216	0.535	0.121	4.44	0.114	0.086
LD	COM2	0.20	0.216	0.675	0.071	9.50	0.150	0.050
		0.14	0.146	0.602	0.065	9.25	0.087	0.053
		0.08	0.081	0.473	0.051	9.23	0.033	0.047
MS	COM2	0.267	0.291	0.711	0.075	9.48	0.222	0.045
		0.14	0.143	0.524	0.059	8.84	0.092	0.048

*   COM2:   common dead-space model

**   SEP2:   separate dead-space model

\+ $V_T/V_L = (V_T/FRC)(1 + V_D/V_L)$

\+\+ $V_{T_i}/V_{L_i} = (t_i/l_i)(V_T/V_L)$

\+\+\+ $V_{T_i}/FRC = t_i(V_T/FRC)$

Table 2 continued

Subject	Model Code	V_T/FRC	V_T/V_L	V_{T_1}/V_{L_1}	V_{T_2}/V_{L_2}	$\dfrac{V_{T_1}/V_{L_1}}{V_{T_2}/V_{L_2}}$	V_{T_1}/FRC	V_{T_2}/FRC
KA	COM2	0.41	0.484	0.884	0.143	6.16	0.344	0.066
		0.331	0.394	0.568	0.121	4.69	0.291	0.040
TM	SEP2**	0.55	0.600	0.988	0.371	2.66	0.336	0.214
		0.33	0.333	0.815	0.228	3.58	0.145	0.185
		0.20	0.212	0.490	0.159	3.08	0.074	0.126
LD	SEP2	0.20	0.210	0.482	0.109	4.41	0.124	0.076
		0.14	0.144	0.481	0.085	5.67	0.070	0.070
		0.08	0.08	0.446	0.052	8.49	0.031	0.049
MS	SEP2	0.267	0.280	0.519	0.122	4.27	0.198	0.069
		0.14	0.141	0.469	0.065	7.26	0.088	0.052
KA	SEP2	0.41	0.463	0.680	0.271	2.51	0.283	0.127
		0.331	0.387	0.492	0.291	1.69	0.202	0.129

Table 3. RMSRE Values for Generated Curves (Common Dead-Space Model and Separate Dead-Space Model)

Subject	Parameter Set used (V_T/FRC)	V_T/FRC used	Common RMSRE (t_2=const.)	Common RMSRE (V_{T_2}=const.)	Separate RMSRE (t_2=const.)	Separate RMSRE (V_{T_2}=const.)
TM	0.55	0.33	0.684	0.584	0.741	0.337
		0.20	0.375	0.419	0.341	4.723
	0.33	0.55	0.307	0.197	0.313	0.205
		0.20	0.379	0.442	0.367	0.435
	0.20	0.55	0.096	0.469	0.205	1.036
		0.33	0.431	0.659	0.339	1.143
LD	0.20	0.14	0.296	0.425	0.214	0.287
		0.08	1.438	1.559	0.559	0.530
	0.14	0.20	0.149	0.217	0.117	0.151
		0.08	0.319	0.567	0.277	0.467
	0.08	0.20	0.271	0.392	0.312	0.411
		0.14	0.157	0.286	0.209	0.319
MS	0.267	0.14	0.774	1.056	0.457	0.562
	0.14	0.267	0.169	0.324	0.171	0.312
KA	0.41	0.331	0.083	0.054	0.217	0.274
	0.331	0.41	0.107	0.053	0.182	0.386

Table 4. Best Fit Parameter Set Using Pairs of Runs

Subject	Model Code	$(V_T/FRC)_1$, $(V_T/FRC)_2$	t_1	l_1	α	V_D/V_L	RMSRE1[+]	RMSRE2	RMSRE[++]
TM	MOD2*	0.55, 0.33	0.503	0.875	0.368	0.004	0.199	0.154	0.172
		0.55, 0.20	0.358	0.679	0.448	0.071	0.064	0.050	0.055
		0.33, 0.20	0.480	0.641	0.776	0.056	0.184	0.163	0.166
LD	MOD2	0.20, 0.14	0.321	0.722	0.762	0.041	0.075	0.069	0.070
		0.14, 0.08	0.443	0.853	0.860	0.018	0.110	0.075	0.091
MS	MOD2	0.267, 0.14	0.346	0.794	0.626	0.017	0.153	0.053	0.102
KA	MOD2	0.41, 0.331	0.247	0.549	0.230	0.166	0.061	0.060	0.058
TM	COM1**	0.55, 0.33	0.595	0.234	0.0	0.017	0.199	0.151	0.171
		0.55, 0.20	0.319	0.687	0.0	0.086	0.061	0.044	0.051
		0.33, 0.20	0.380	0.578	0.0	0.061	0.184	0.169	0.168

+ RMSRE1: RMSRE for curve with $(V_T/FRC)_1$

++ RMSRE: RMSRE for both curves

* MOD2: common and separate dead-space model

** COM1: common dead-space model

Table 4 continued

Subject	Model Code	$(V_T/FRC)_1$, $(V_T/FRC)_2$	t_1	l_1	α	V_D/V_L	RMSRE1	RMSRE2	RMSRE
LD	COM1	0.20, 0.14	0.334	0.834	0.0	0.053	0.099	0.069	0.083
		0.20, 0.08	0.396	0.897	0.0	0.025	0.208	0.083	0.153
		0.14, 0.08	0.496	0.915	0.0	0.018	0.130	0.072	0.101
MS	COM1	0.267, 0.14	0.644	0.170	0.0	0.021	0.162	0.049	0.107
KA	COM1	0.41, 0.331	0.148	0.482	0.0	0.186	0.047	0.048	0.045
TM	SEP1***	0.55, 0.33	0.402	0.757	1.0	0.007	0.206	0.150	0.175
		0.55, 0.20	0.441	0.738	1.0	0.057	0.070	0.080	0.072
		0.33, 0.20	0.533	0.380	1.0	0.055	0.183	0.160	0.164
LD	SEP1	0.20, 0.14	0.674	0.294	1.0	0.038	0.073	0.069	0.069
		0.20, 0.08	0.678	0.217	1.0	0.026	0.158	0.092	0.125
		0.14, 0.08	0.562	0.155	1.0	0.018	0.108	0.075	0.090
MS	SEP1	0.267, 0.14	0.652	0.217	1.0	0.015	0.150	0.054	0.101
KA.	SEP1.	0.41, 0.331	0.508	0.749	1.0	0.127	0.090	0.014	0.082

*** SEP1: separate dead-space model

Table 5. Best Fit Parameters Using Single Runs[+]

Subject	Model Code	V_T/FRC	t_1	l_1	V_D/V_L	RMSRE
JG	COM2[*]	0.130	0.72	0.04	0.10	0.014
AS	"	0.134	0.74	0.30	0.08	0.015
OS	"	0.172	0.78	0.35	0.13	0.030
KF	"	0.211	0.69	0.21	0.11	0.021
MN	"	0.222	0.82	0.19	0.17	0.046
EM	"	0.246	0.92	0.57	0.22	0.017
DB	"	0.288	0.87	0.35	0.25	0.042
LB	"	0.368	0.76	0.39	0.30	0.006
KA(1)	"	0.41	0.84	0.46	0.18	0.010
KA(2)	"	0.331	0.88	0.61	0.19	0.009
JG	SEP2[**]	0.130	0.40	0.08	0.06	0.014
AS	"	0.134	0.46	0.24	0.06	0.015
OS	"	0.172	0.38	0.23	0.11	0.030
KF	"	0.211	0.47	0.19	0.07	0.021
MN	"	0.222	0.53	0.27	0.11	0.046
EM	"	0.246	0.55	0.46	0.19	0.017
DB	"	0.288	0.52	0.36	0.19	0.042
LB	"	0.368	0.30	0.20	0.26	0.006
KA(1)	"	0.41	0.69	0.47	0.13	0.010
KA(2)	"	0.331	0.61	0.48	0.17	0.009

[+] From Baylor College of Medicine's Pulmonary Lab

[*] COM2: common dead-space model

[**] SEP2: separate dead-space model

Table 6.   Alveolar Compartment Dilution Factors and Tidal Volumes

(from Table 5)

Subject	Model Code	FRC (% of Predicted)	r [breaths/min]	V_T/V_L +	$\dfrac{V_T - V_D}{V_L}$	V_{T_1}/V_{L_1} ++	V_{T_2}/V_{L_2}	$\dfrac{V_{T_1}/V_{L_1}}{V_{T_2}/V_{L_2}}$	V_D +++ [cc]
JG	COM2*	3.90 (135)	14.4	0.143	0.04	2.57	0.042	61.71	355
AS	"	5.18 (182)	20.0	0.145	0.06	0.357	0.054	6.64	448
OS	"	3.72 (145)	19.8	0.194	0.06	0.433	0.066	6.58	428
KF	"	4.29 (141)	11.6	0.234	0.12	0.770	0.092	8.37	425
MN	"	2.97 (97)	16.0	0.260	0.09	1.12	0.058	19.42	432
EM	"	2.19 (93)	16.4	0.300	0.08	0.484	0.056	8.68	395
DB	"	2.05 (74)	19.7	0.360	0.11	0.895	0.072	12.43	410
LB	"	1.82 (71)	26.3	0.478	0.17	0.932	0.188	4.95	420
KA(1)	"	2.59 (95)	12.9	0.484	0.30	0.883	0.143	6.16	395
KA(2)	"	2.59 (95)	14.0	0.394	0.20	0.568	0.121	4.69	413

+ $V_T/V_L = (V_T/FRC)(1 + V_D/V_L)$

++ $V_{T_i}/V_{L_i} = (t_i/l_i)(V_T/V_L)$

+++ $V_D = FRC(V_D/V_L)/(1 + V_D/V_L)$

*   COM2:   common dead-space model

57

Table 6 continued

Subject	Model Code	FRC (% of Predicted)	r [breaths/min]	V_T/V_L	$\dfrac{V_T - V_D}{V_L}$	V_{T_1}/V_{L_1}	V_{T_2}/V_{L_2}	$\dfrac{V_{T_1}/V_{L_1}}{V_{T_2}/V_{L_2}}$	V_D [cc]
JG	SEP2**	3.90 (135)	14.4	0.138	0.07	0.689	0.090	7.67	221
AS	"	5.18 (182)	20.0	0.142	0.08	0.272	0.101	2.70	293
OS	"	3.72 (145)	19.8	0.191	0.08	0.315	0.154	2.05	369
KF	"	4.29 (141)	11.6	0.226	0.15	0.559	0.148	3.78	281
MN	"	2.97 (97)	16.0	0.246	0.13	0.484	0.159	3.05	294
KM	"	2.19 (93)	16.4	0.293	0.10	0.350	0.244	1.43	350
DB	"	2.05 (74)	19.7	0.343	0.15	0.495	0.257	1.93	327
LB	"	1.82 (71)	26.3	0.464	0.20	0.670	0.406	1.72	375
KA(1)	"	2.59 (95)	12.9	0.463	0.33	0.680	0.271	2.51	298
KA(2)	"	2.59 (95)	14.0	0.387	0.22	0.492	0.290	1.70	376

** SEP2: separate dead-space model

Figure 5. Nitrogen Concentration and Tidal Volume Recordings.
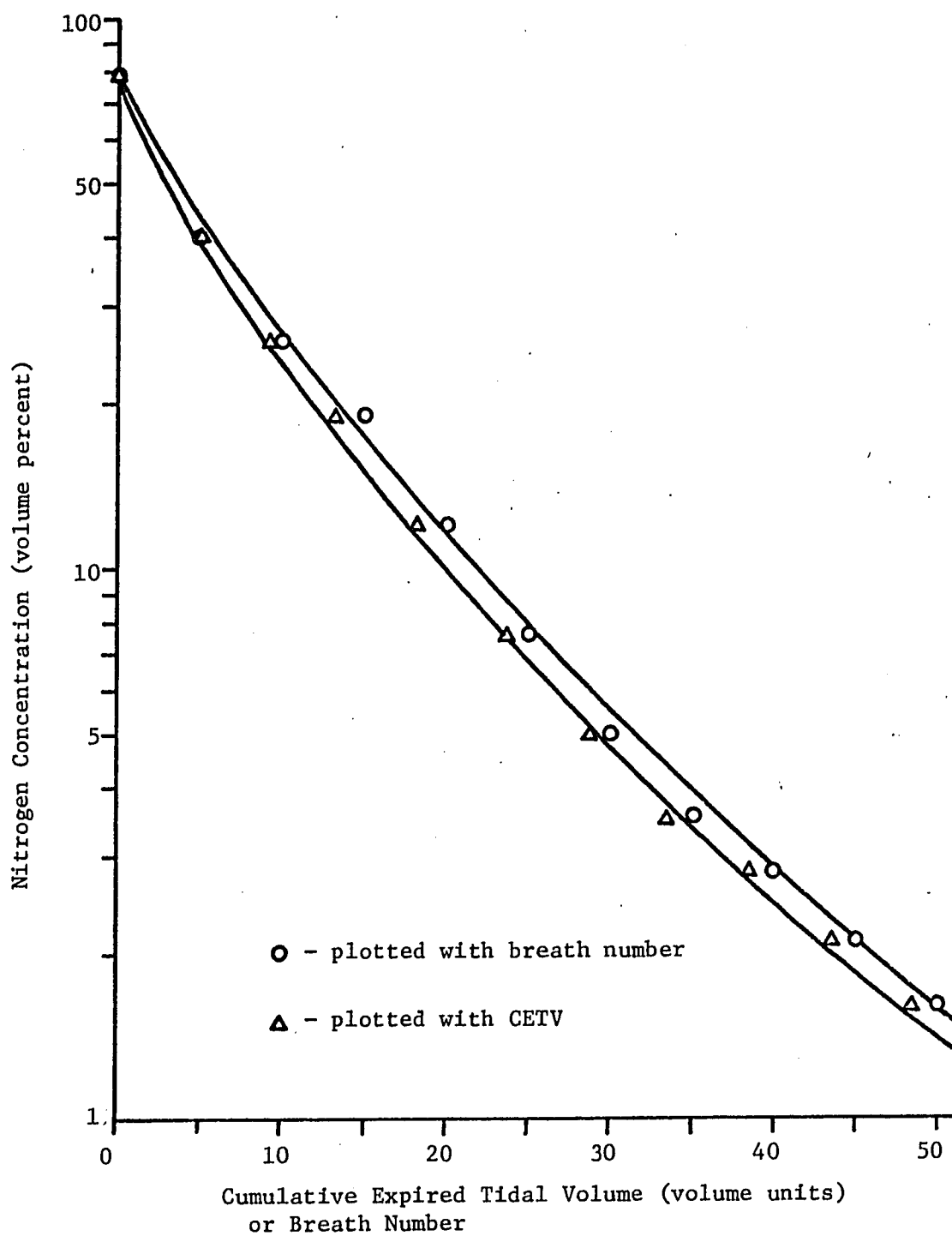
Figure 6. Typical Washout Curve (subject KF). N_2 Concentration Plotted as a Function of Cumulative Expired Tidal Volume (CETV) and as a Function of Breath Number.
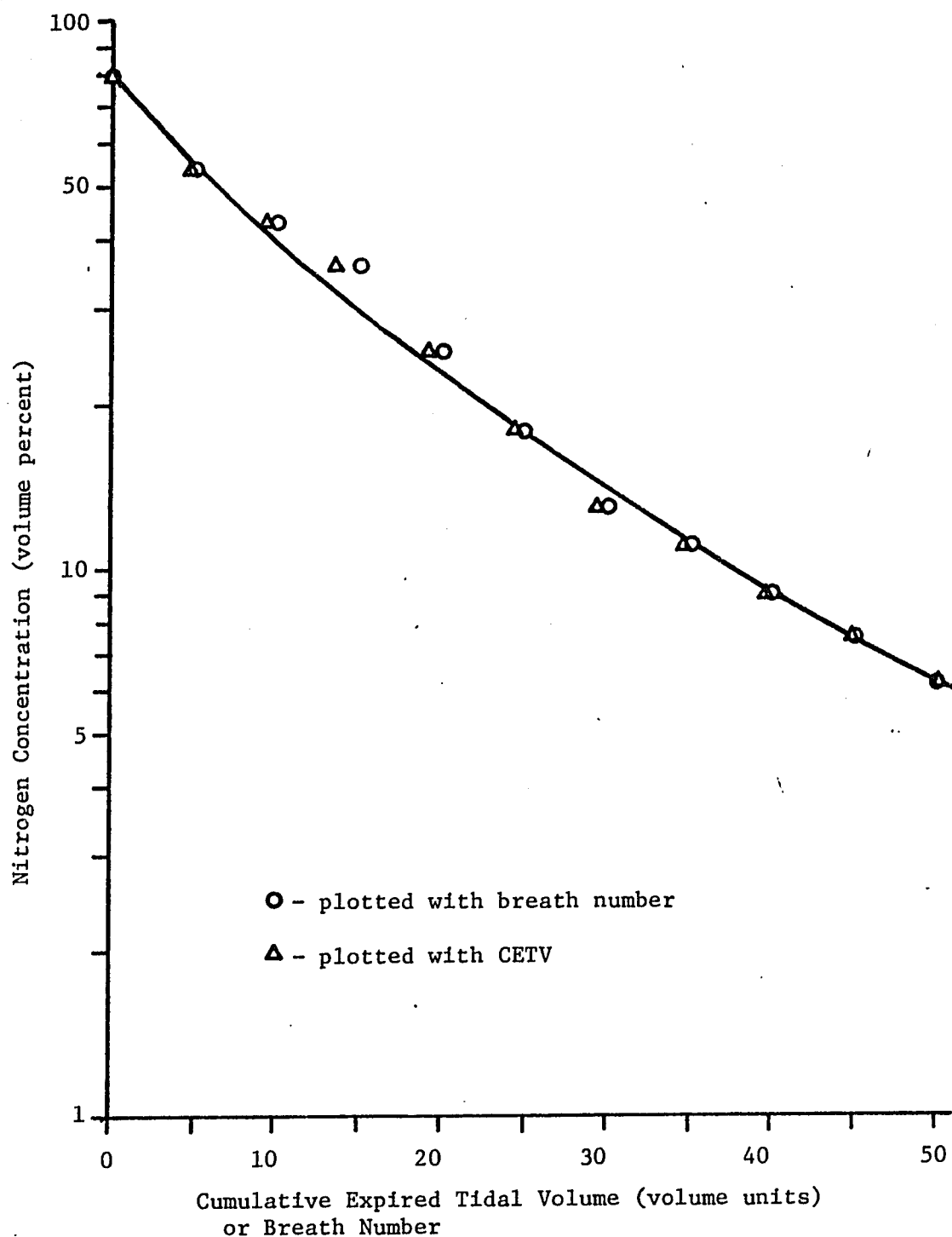
Figure 7. Typical Washout Curve (subject EM). N_2 Concentration Plotted as a Function of Cumulative Expired Tidal Volume (CETV) and as a Function of Breath Number.
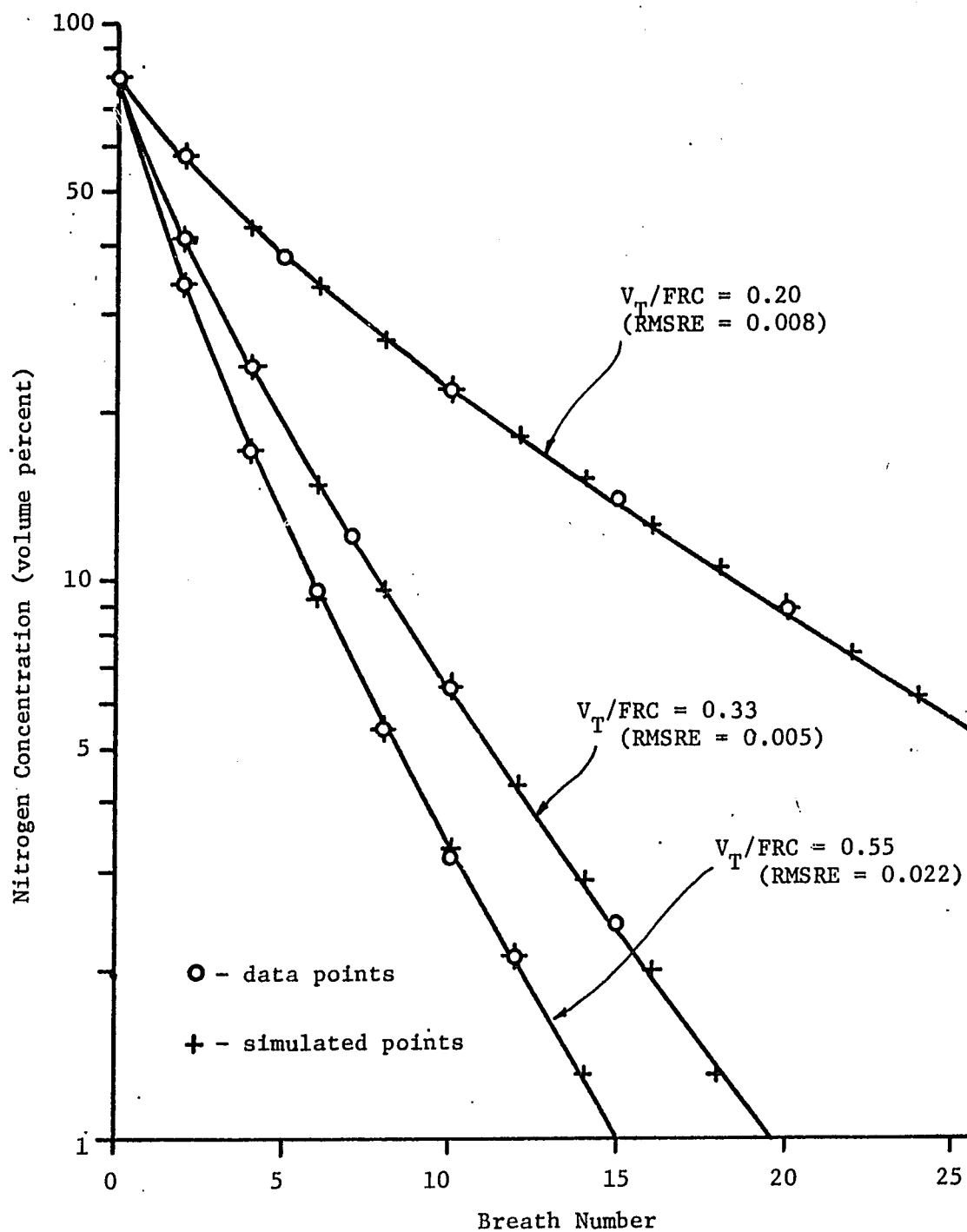
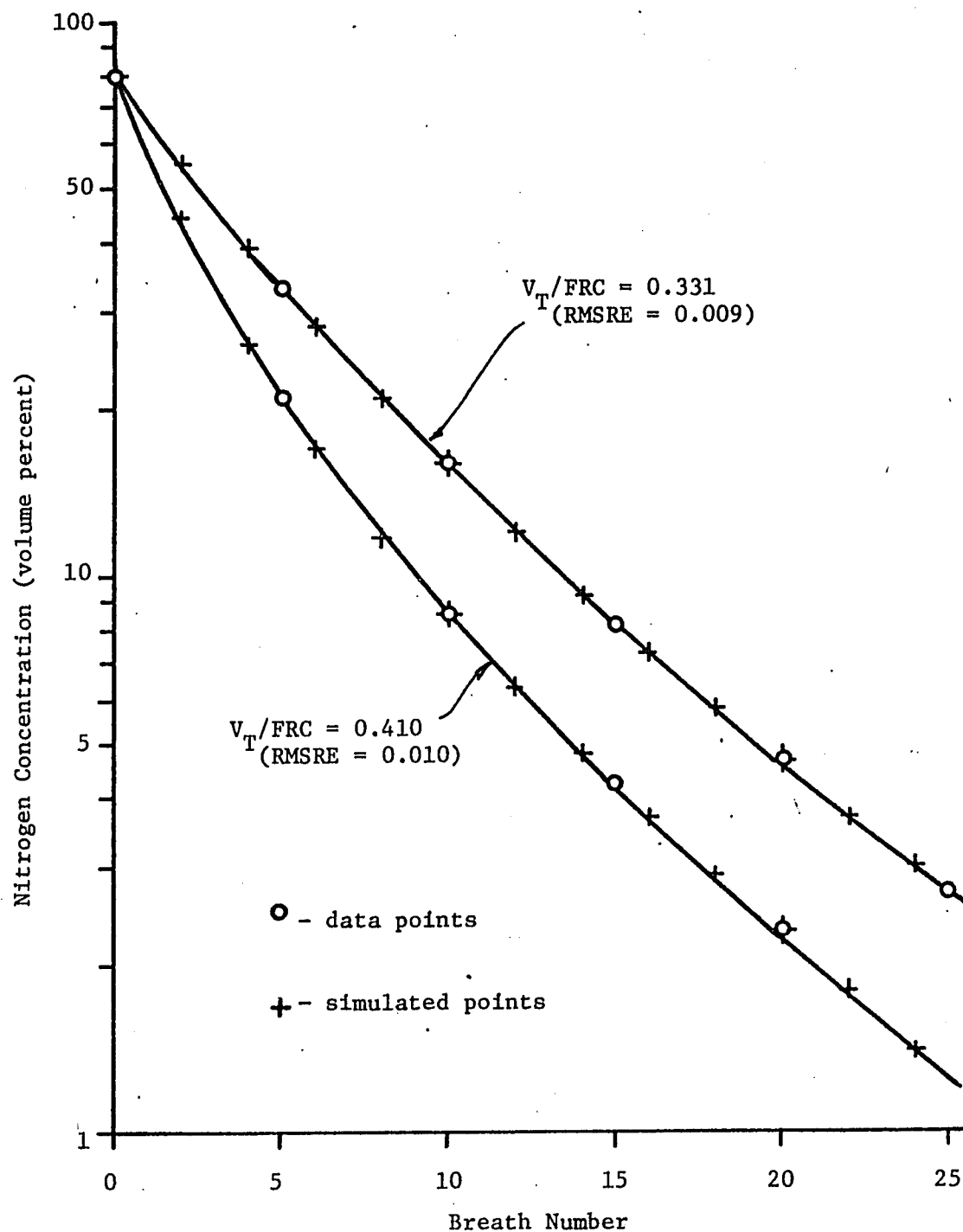Figure 8. Simulation with Common Dead-Space Model and
Separate Dead-Space Model for Individual Runs (subject TM).
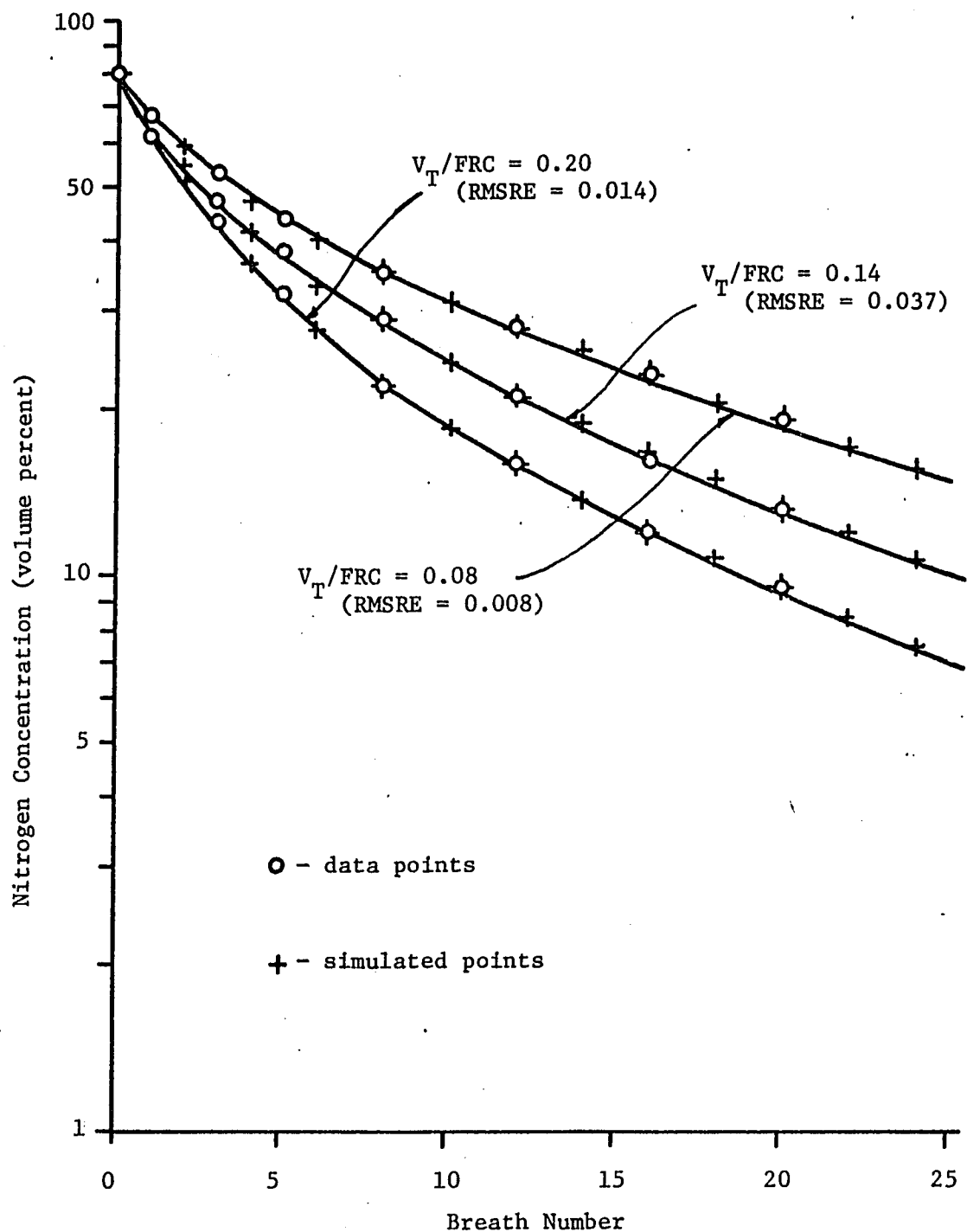
Figure 9. Simulation with Common Dead-Space Model and
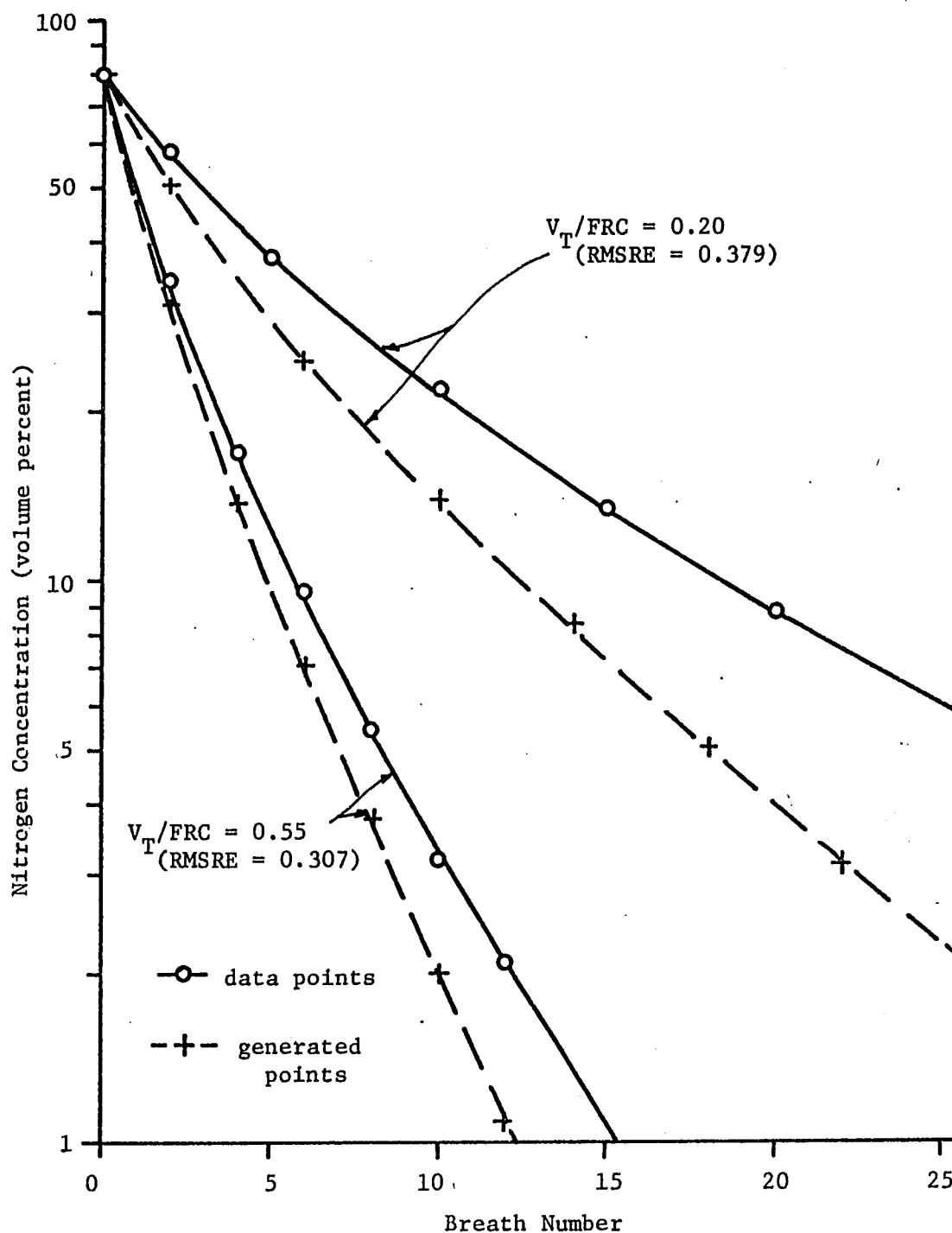Separate Dead-Space Model for Individual Runs (subject LD).
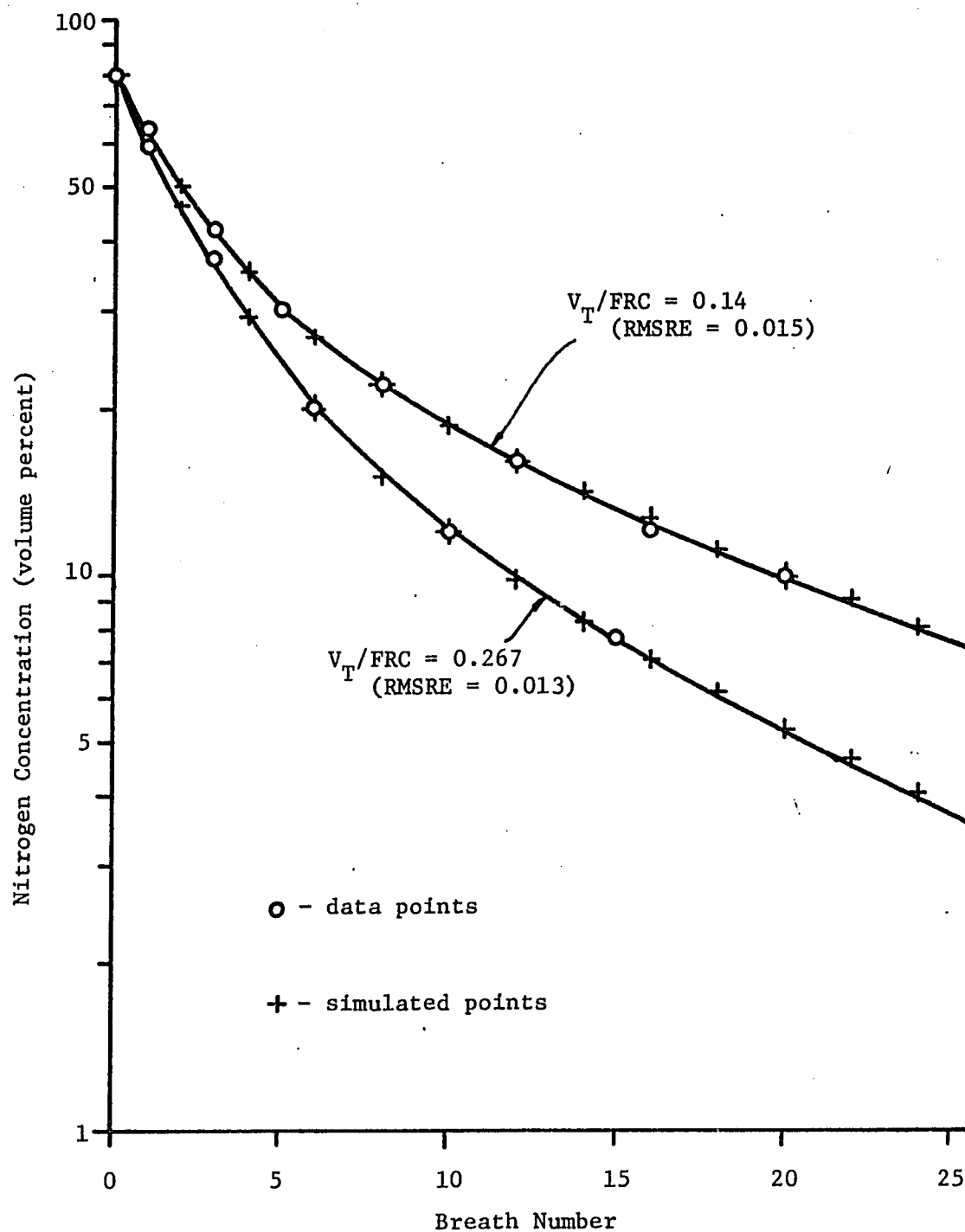
Figure 10. Simulation with Common Dead-Space Model and
Separate Dead-Space Model for Individual Runs (subject MS).

Figure 11. Simulation with Common Dead-Space Model ·and
Separate Dead-Space Model for Individual Runs (subject KA).

Figure 12. Generated Curves From Common Dead-Space Model
(subject TM) Using Parameter Set (V_T/FRC = 0.33) and
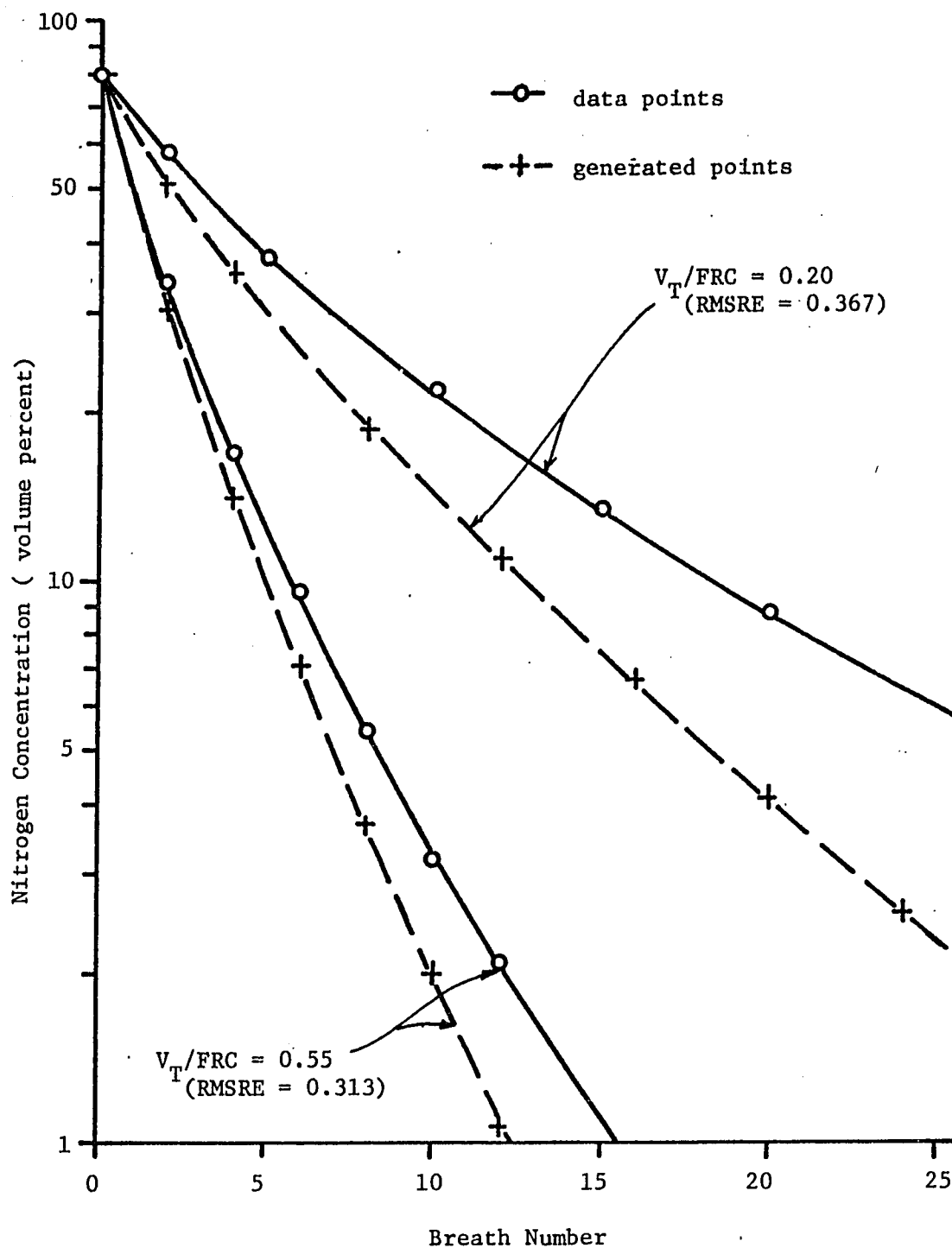V_T/FRC = 0.55,0.20; t_2 = constant.

Figure 13. Generated Curves From Separate Dead-Space Model
(subject TM) Using Parameter Set (V_T/FRC = 0.33) and
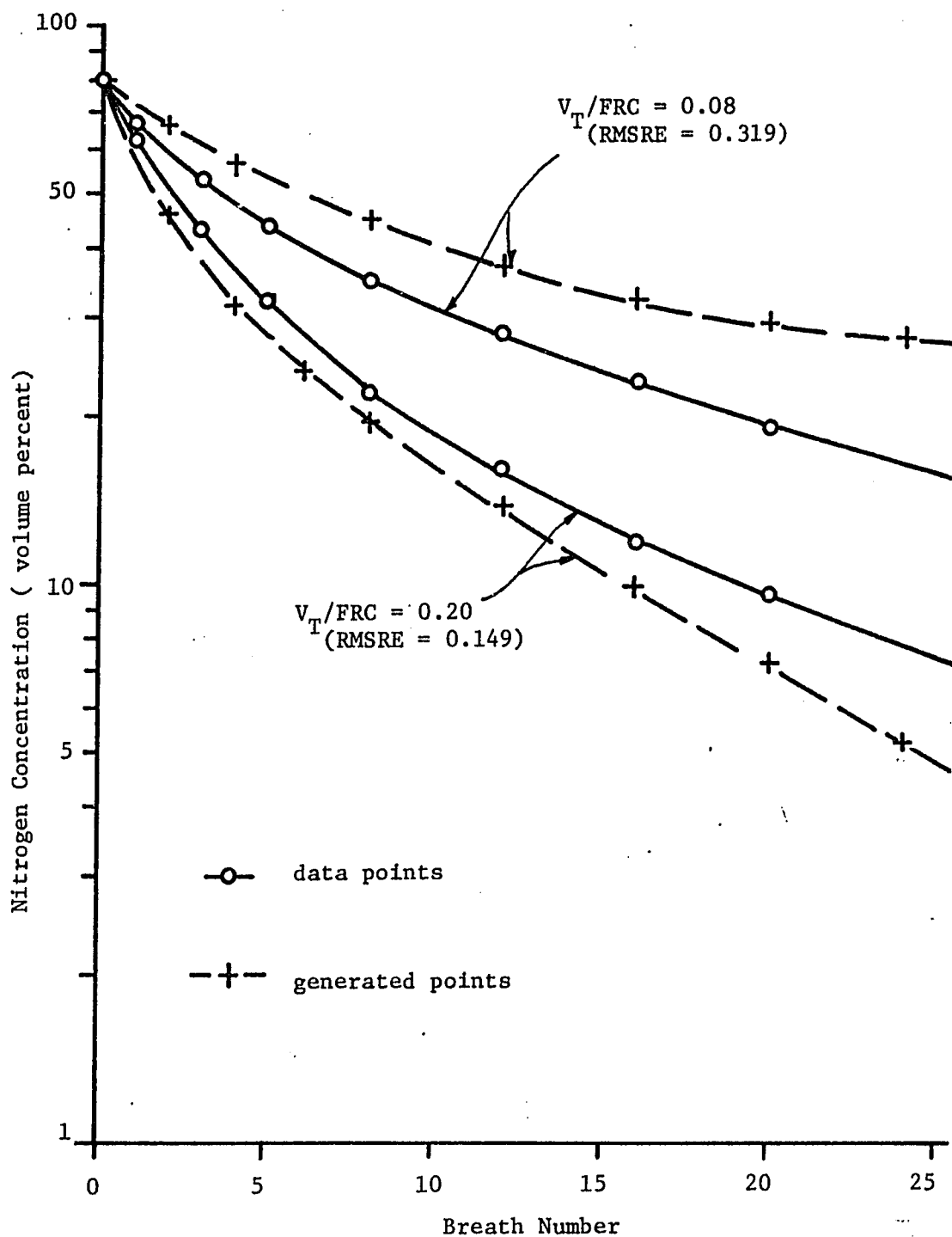V_T/FRC = 0.55,0.20; t_2 = constant.

Figure 14. Generated Curves From Common Dead-Space Model
(subject LD) Using Parameter Set (V_T/FRC = 0.14) and
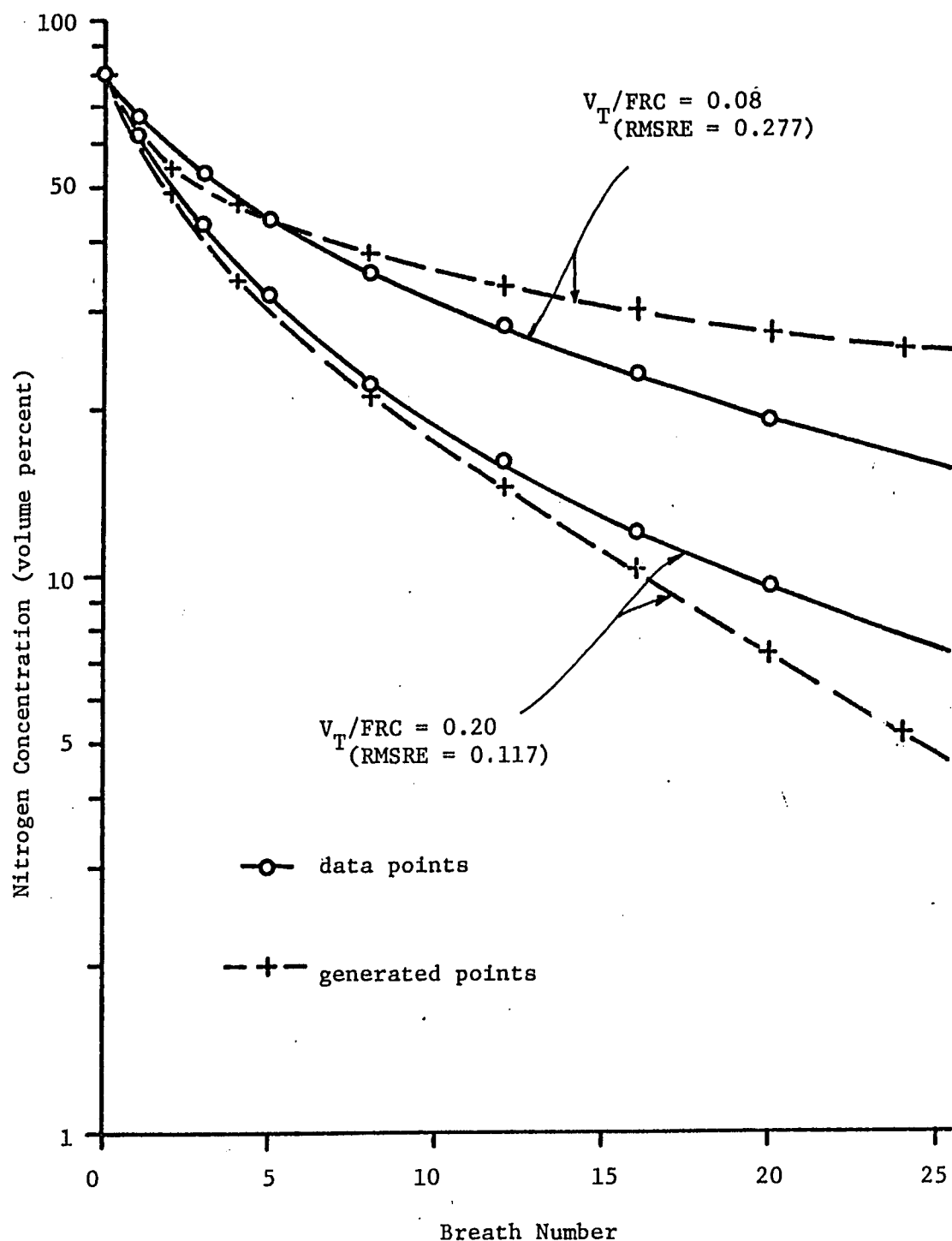V_T/FRC = 0.20,0.08; t_2 = constant.

Figure 15. Generated Curves From Separate Dead-Space Model
(subject LD) Using Parameter Set (V_T/FRC = 0.14) and
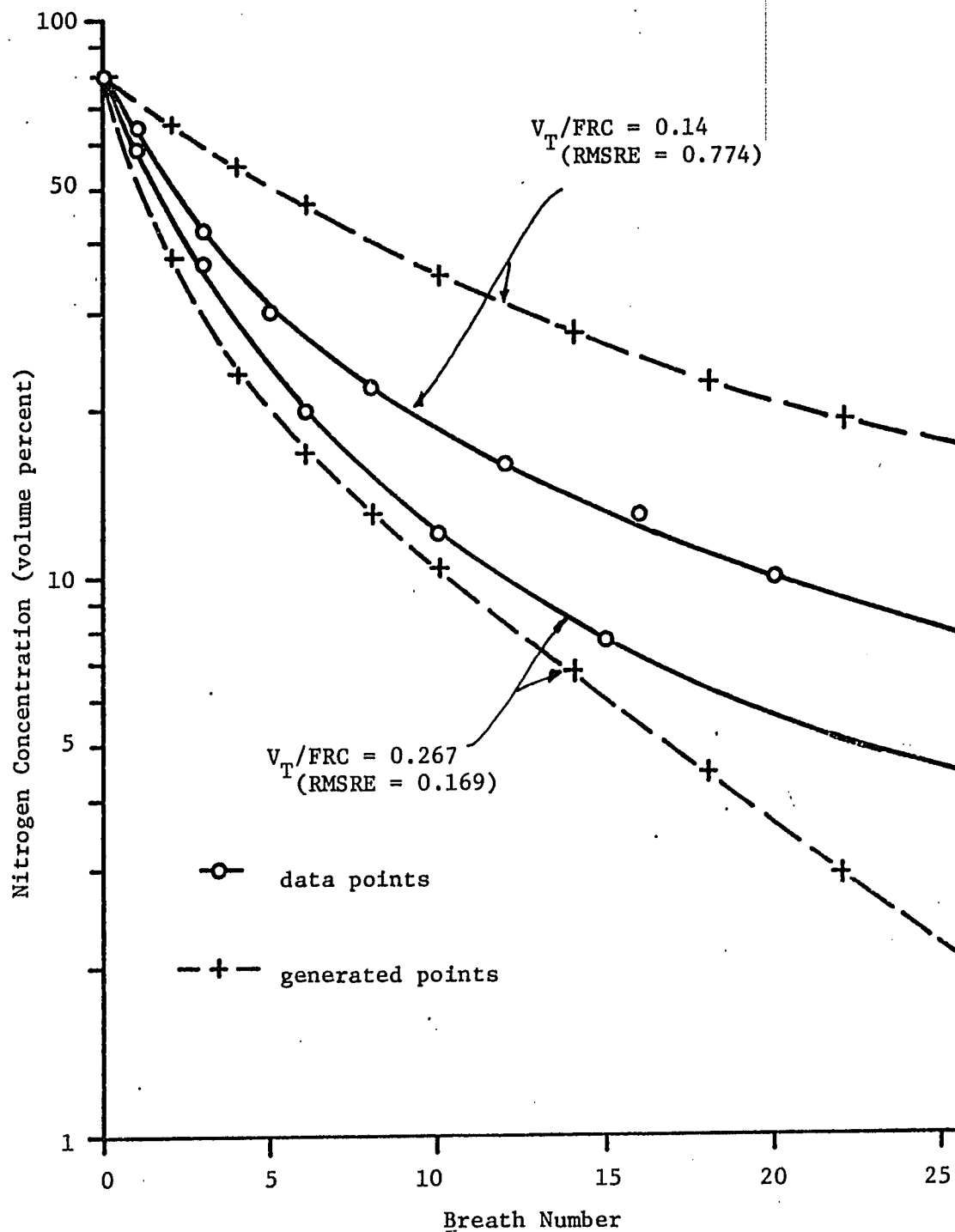V_T/FRC = 0.20, 0.08; t_2 = constant.

Figure 16. Generated Curves From Common Dead-Space Model
(subject MS) Using Parameter Sets (V_T/FRC = 0.267, 0.14)
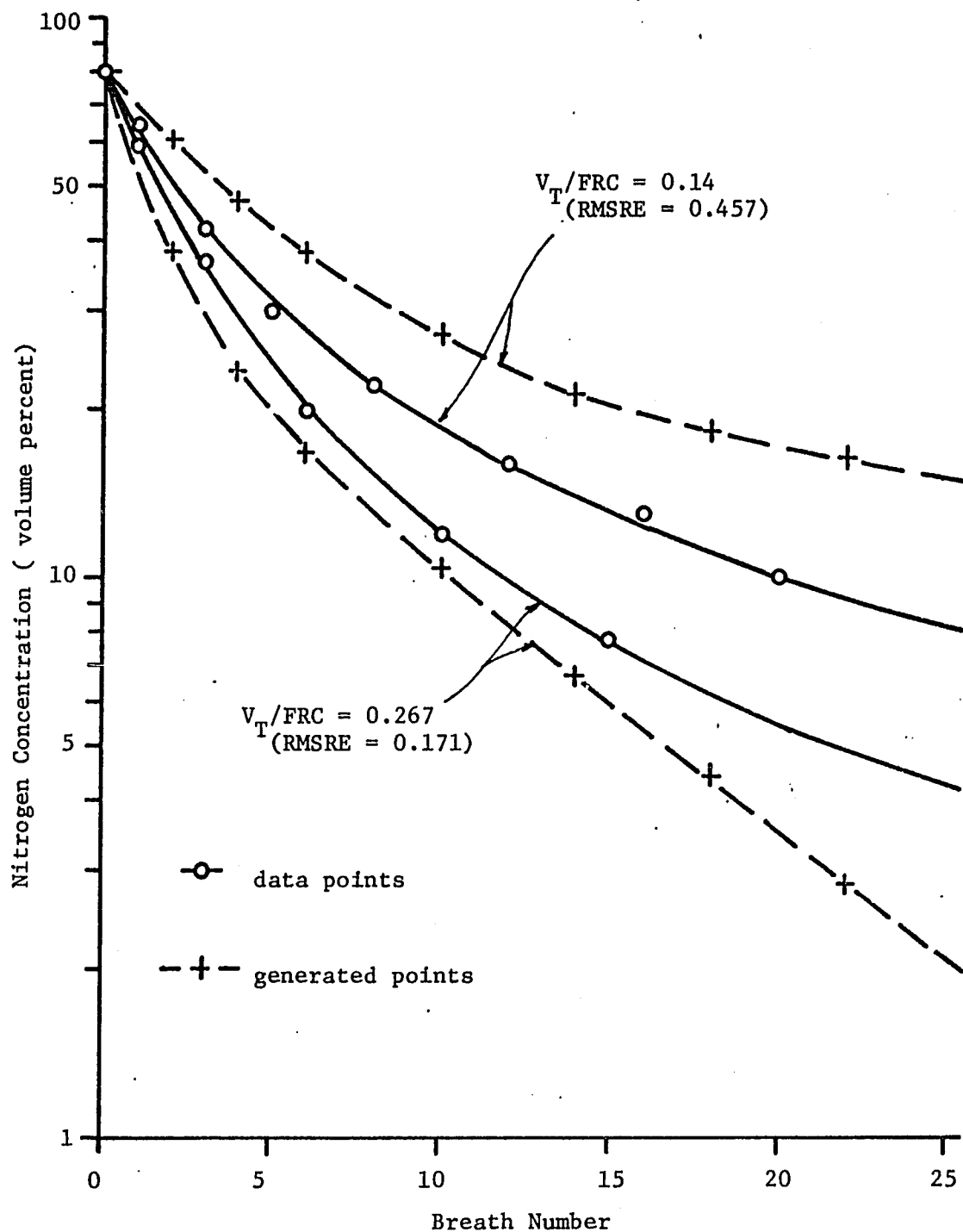and V_T/FRC = 0.14, 0.267 respectively; t_2 = constant.

Figure 17. Generated Curves From Separate Dead-Space Model
(subject MS) Using Parameter Sets (V_T/FRC = 0.267, 0.14)
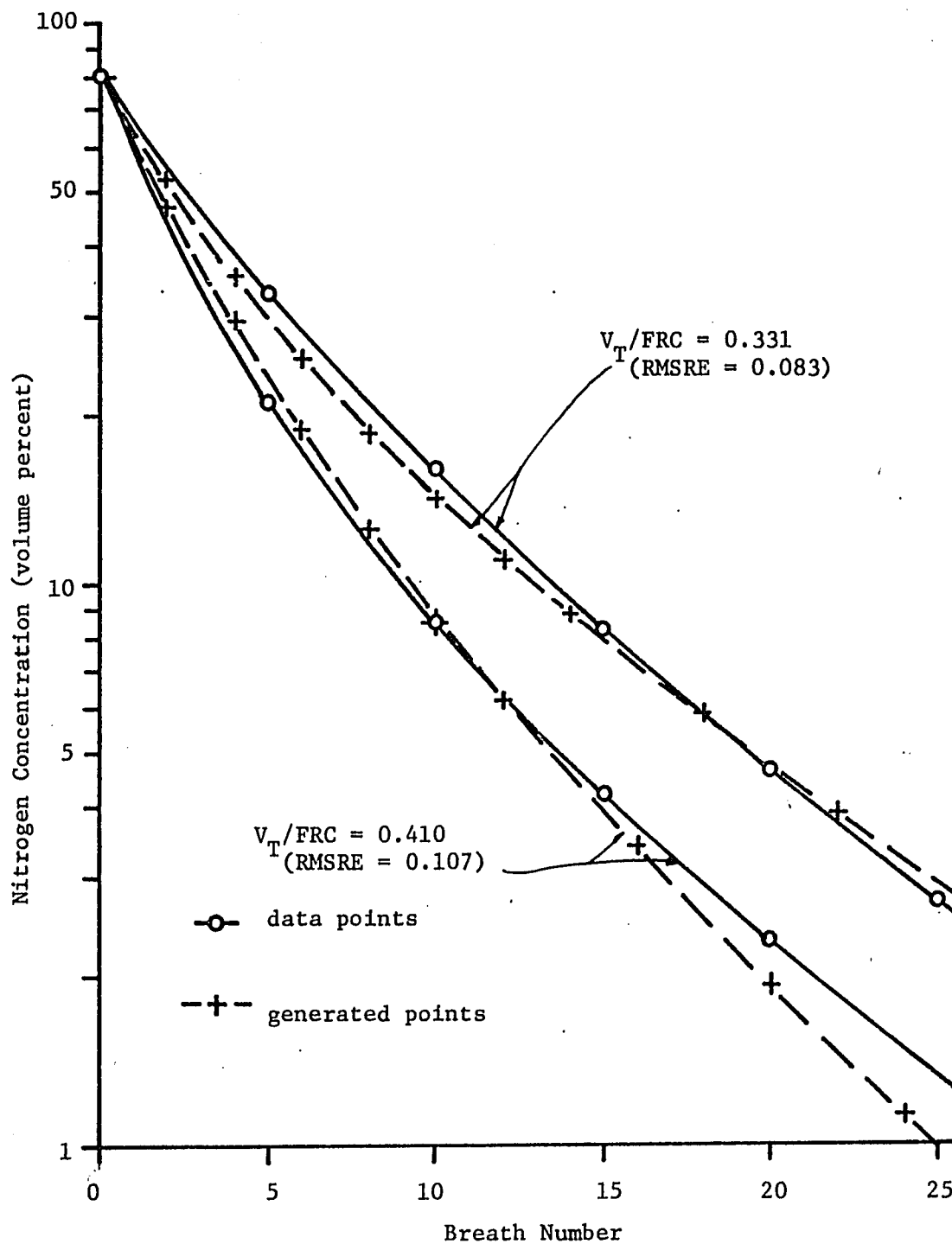and V_T/FRC = 0.14, 0.267 respectively; t_2 = constant.

Figure 18. Generated Curves From Common Dead-Space Model
(subject KA) Using Parameter Sets (V_T/FRC = 0.41, 0.331)
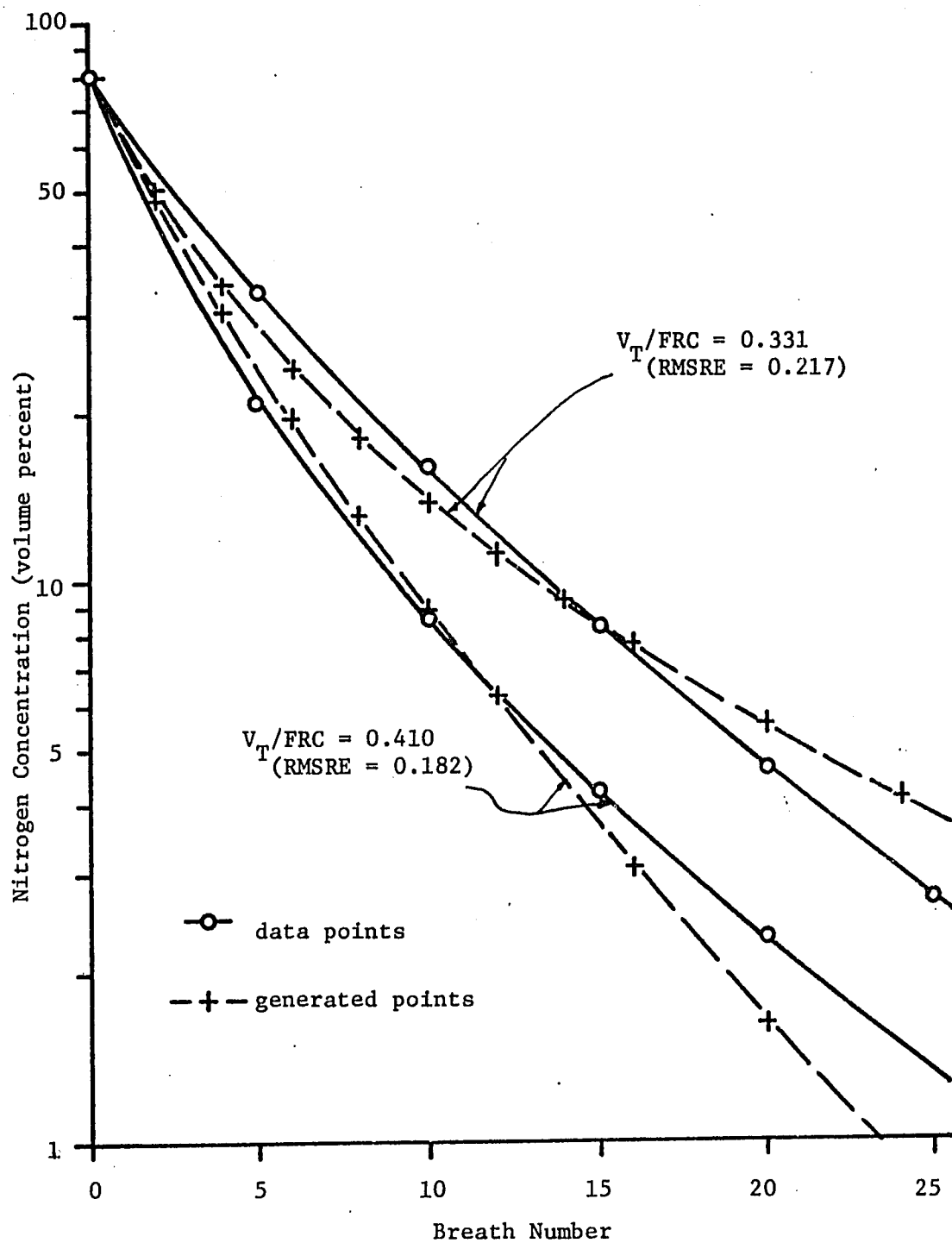and V_T/FRC = 0.331, 0.41 respectively; t_2 = constant.

Figure 19. Generated Curves From Separate Dead-Space Model (subject KA) Using Parameter Sets (V_T/FRC = 0.331, 0.41) and V_T/FRC = 0.41, 0.331 respectively; t_2 = constant.

Figure 20. Generated Curves From Common Dead-Space Model
(subject LD) Using Parameter Set (V_T/FRC = 0.08) and
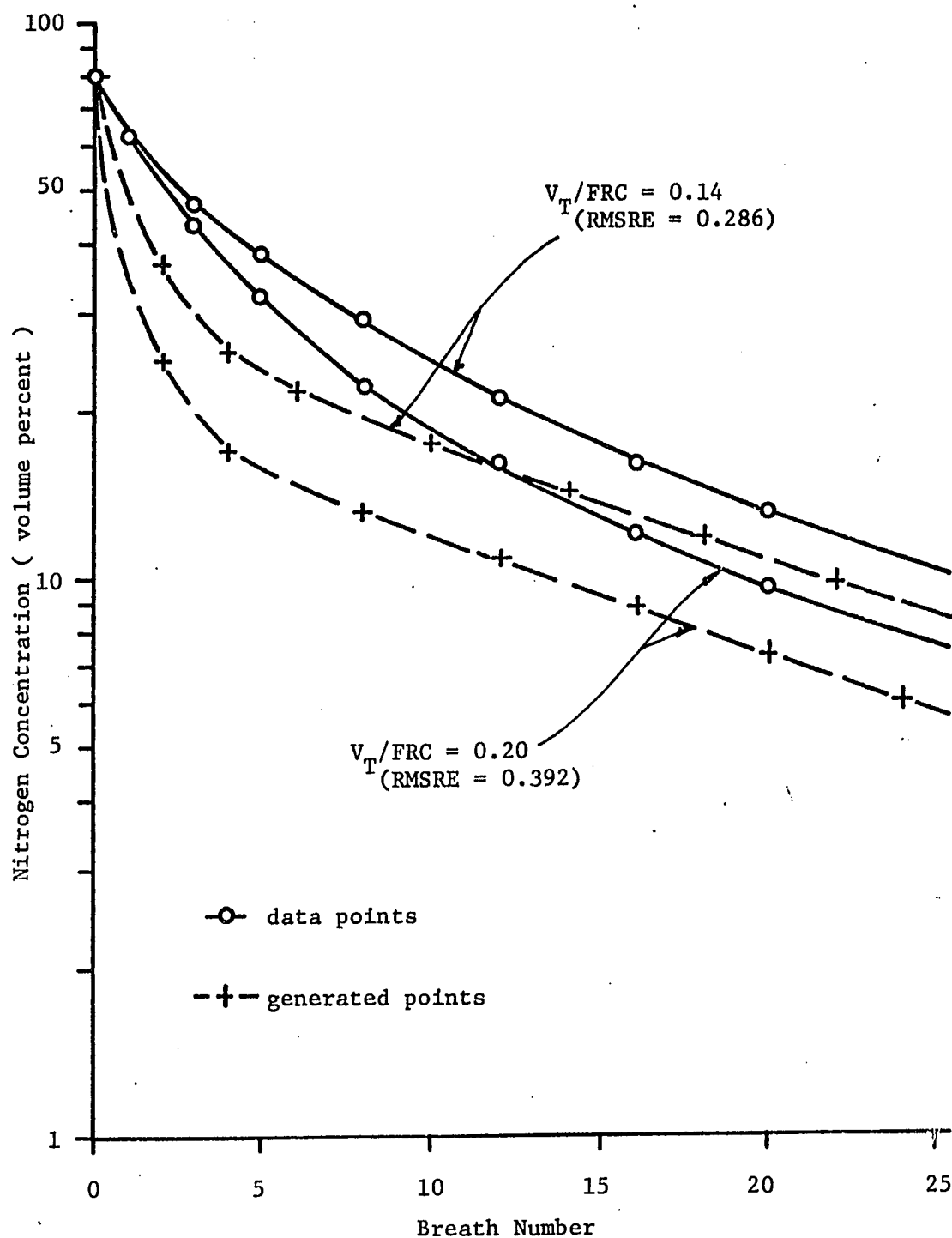V_T/FRC = 0.20, 0.14; V_{T2} = constant.

Figure 21.   Generated Curves From Separate Dead—Space Model
(subject LD) Using Parameter Set (V_T/FRC = 0.08) and
V_T/FRC = 0.20, 0.14; V_{T2} = constant.

Figure 22. Generated Curves From Common Dead-Space Model (subject MS) Using Parameter Sets(V_T/FRC = 0.267, 0.14) and V_T/FRC = 0.14, 0.267 respectively; V_{T2} = constant.

Figure 23. Generated Curves From Separate Dead-Space Model (subject MS) Using Parameter Sets (V_T/FRC = 0.267, 0.14) and V_T/FRC = 0.14, 0.267 respectively; V_{T2} = constant.

Figure 24. Generated Curves From Common Dead-Space Model
(subject KA) Using Parameter Sets (V_T/FRC = 0.41, 0.331)
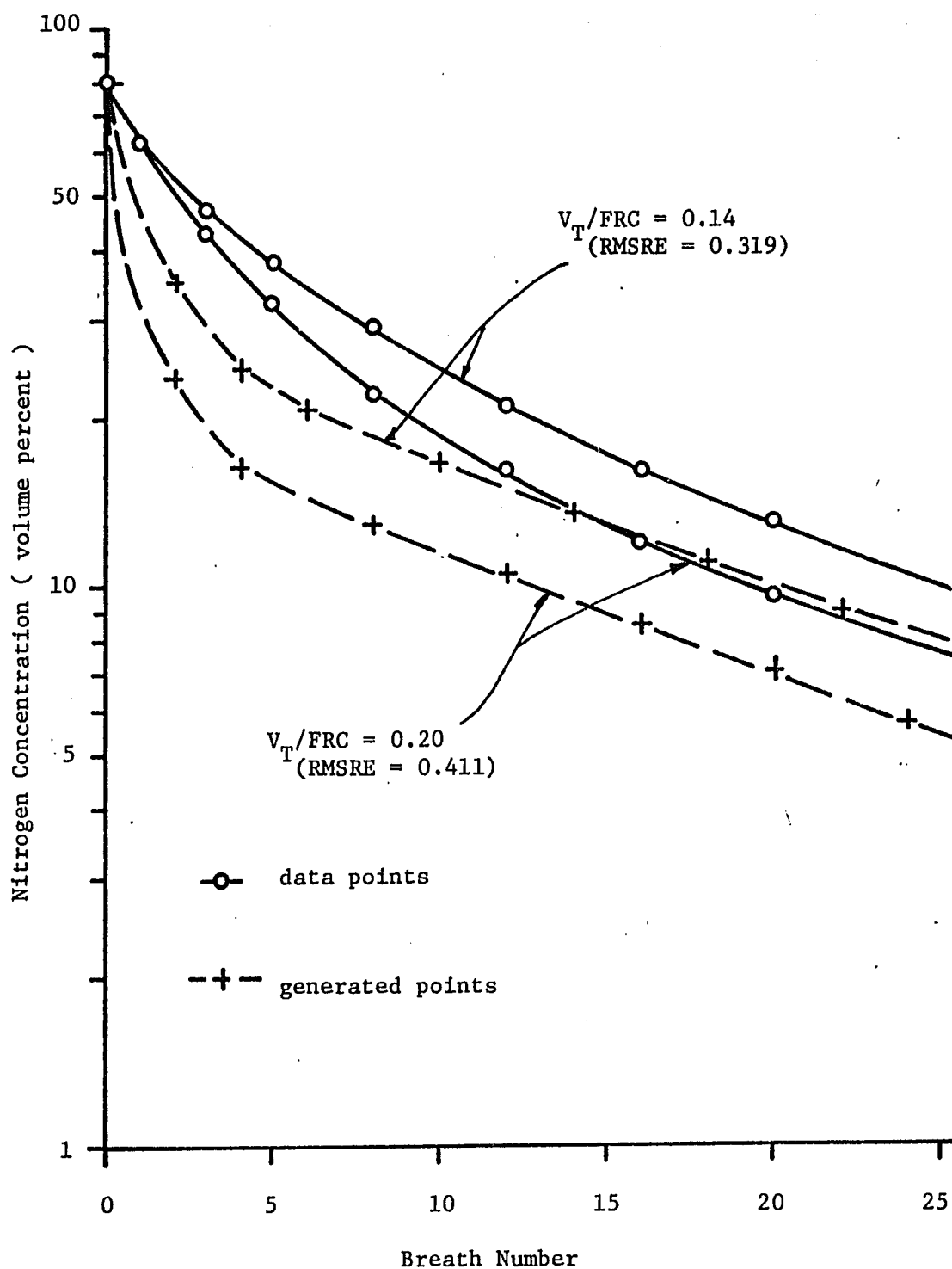and V_T/FRC = 0.331, 0.41 respectively; V_{T2} = constant.

Figure 25. Generated Curves From Separate Dead-Space Model (subject KA) Using Parameter Sets (V_T/FRC = 0.41, 0.331) and V_T/FRC = 0.331, 0.41 respectively; V_{T2} = constant.

Figure 26. Generated Curves From Common Dead-Space Model
(subject TM) Using Parameter Set (V_T/FRC = 0.55 <u>and</u> 0.20)
and V_T/FRC = 0.55, 0.20.

Figure 27. Generated Curves From Common Dead-Space Model
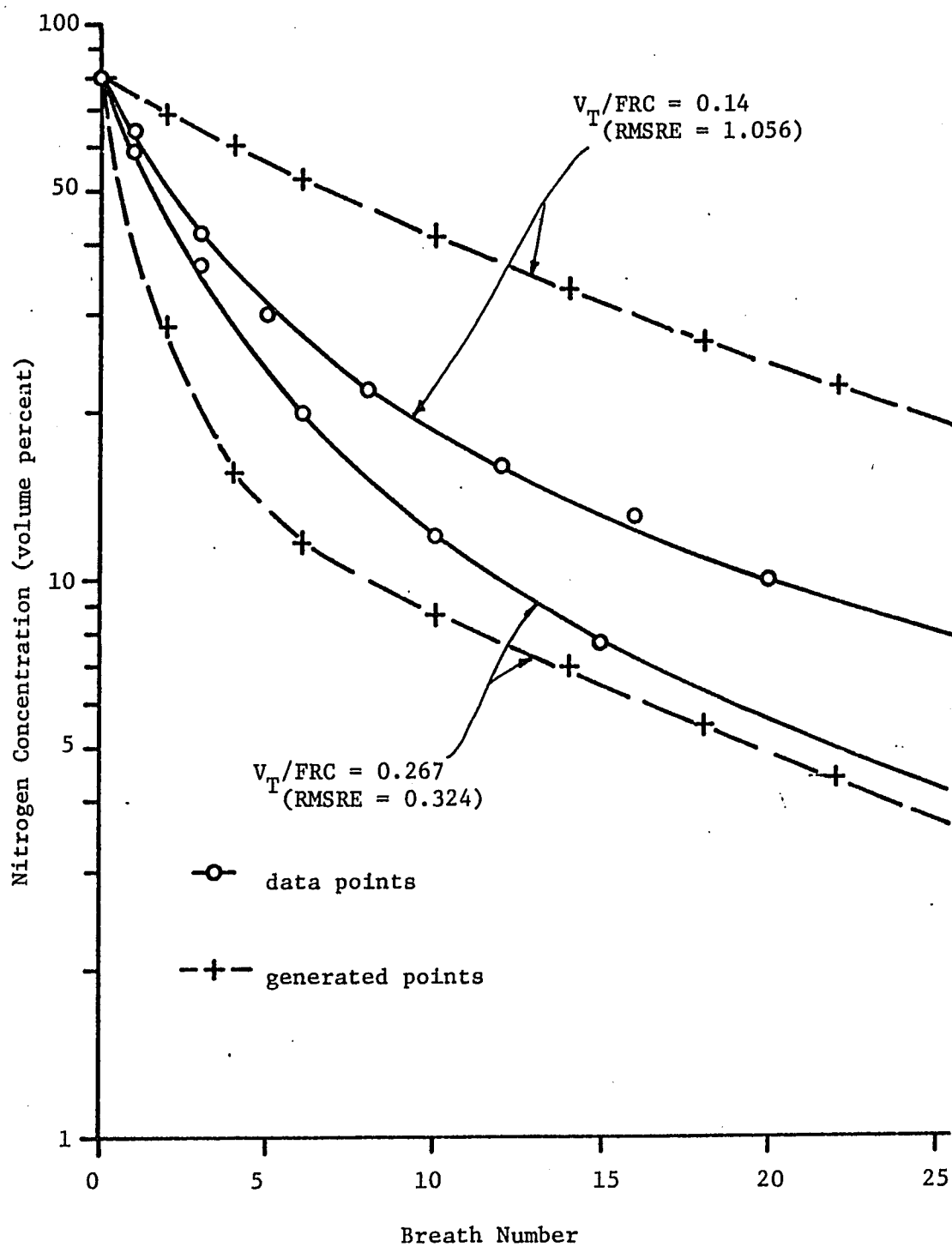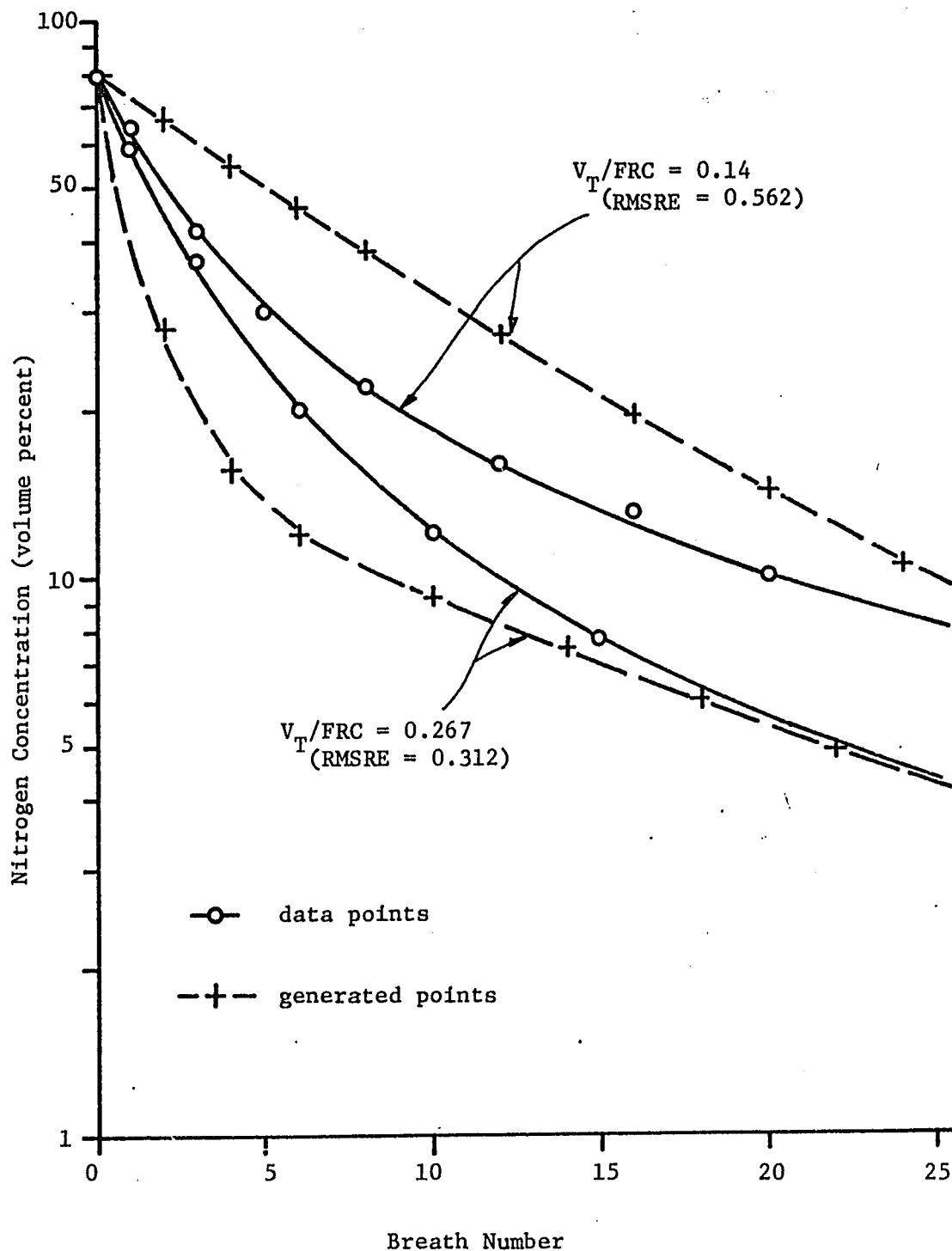(subject LD) Using Parameter Set (V_T/FRC = 0.14 and 0.08)
and V_T/FRC = 0.14, 0.08.

Figure 28. Generated Curves From Common Dead-Space Model
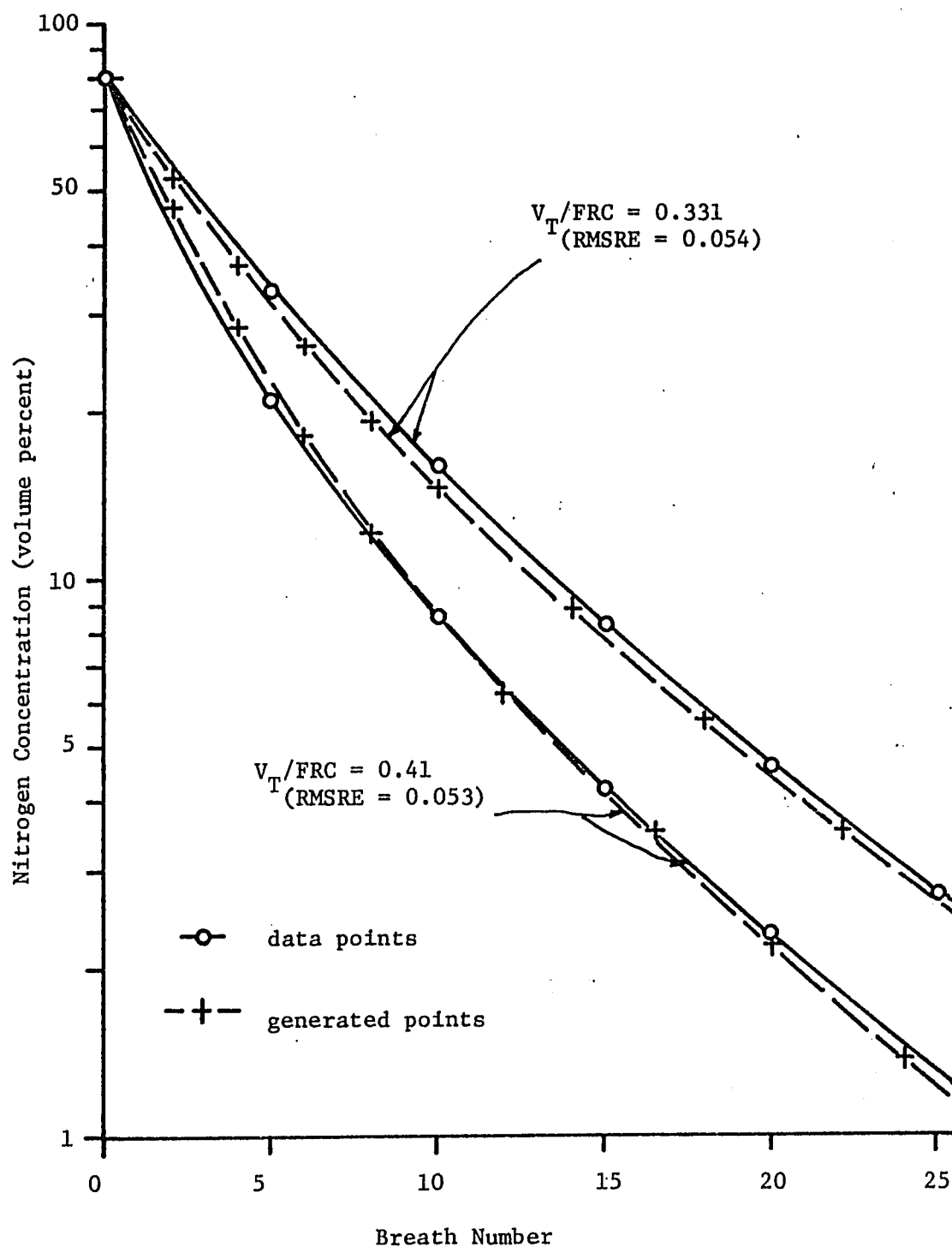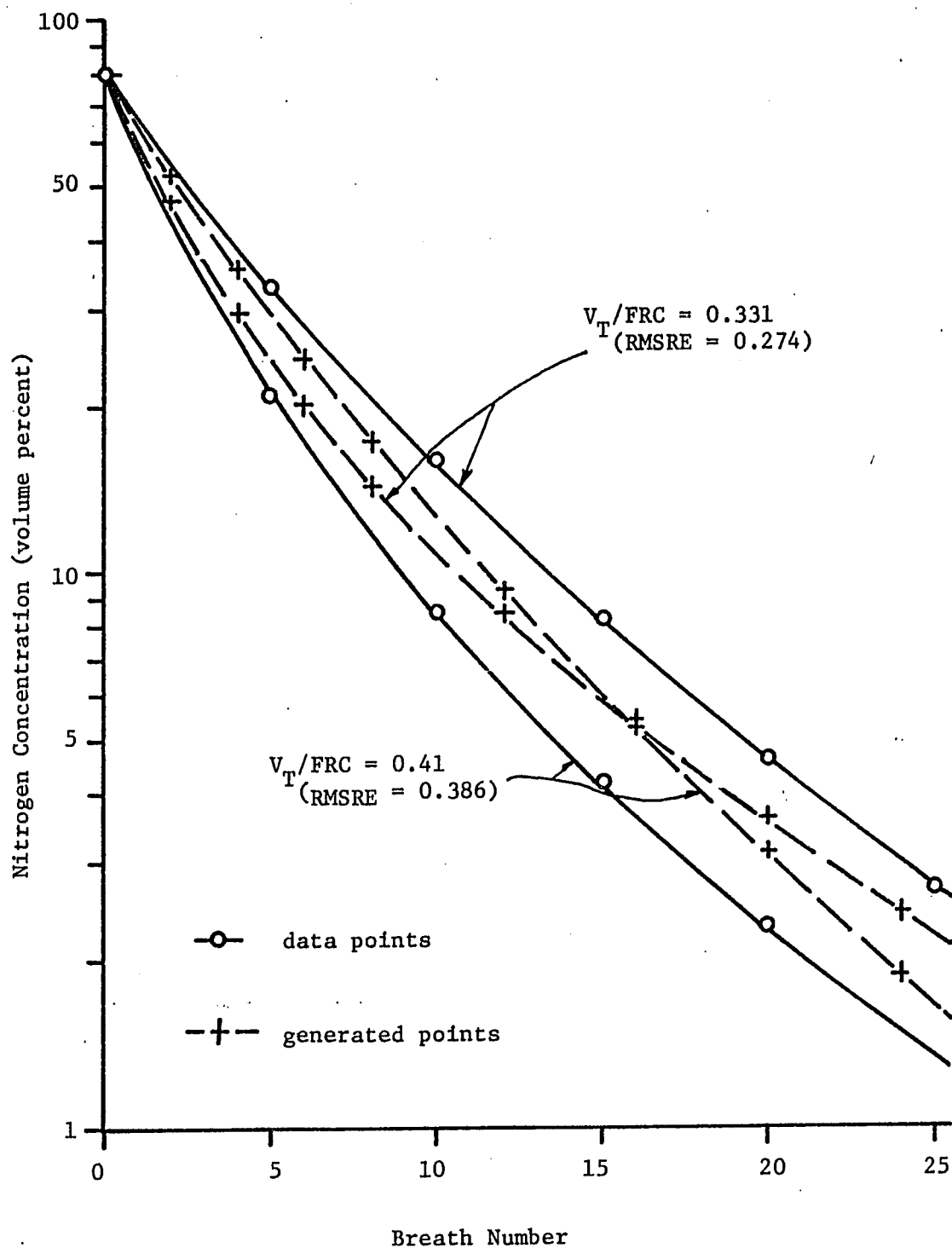(subject MS) Using Parameter Set (V_T/FRC = 0.267 <u>and</u> 0.14)
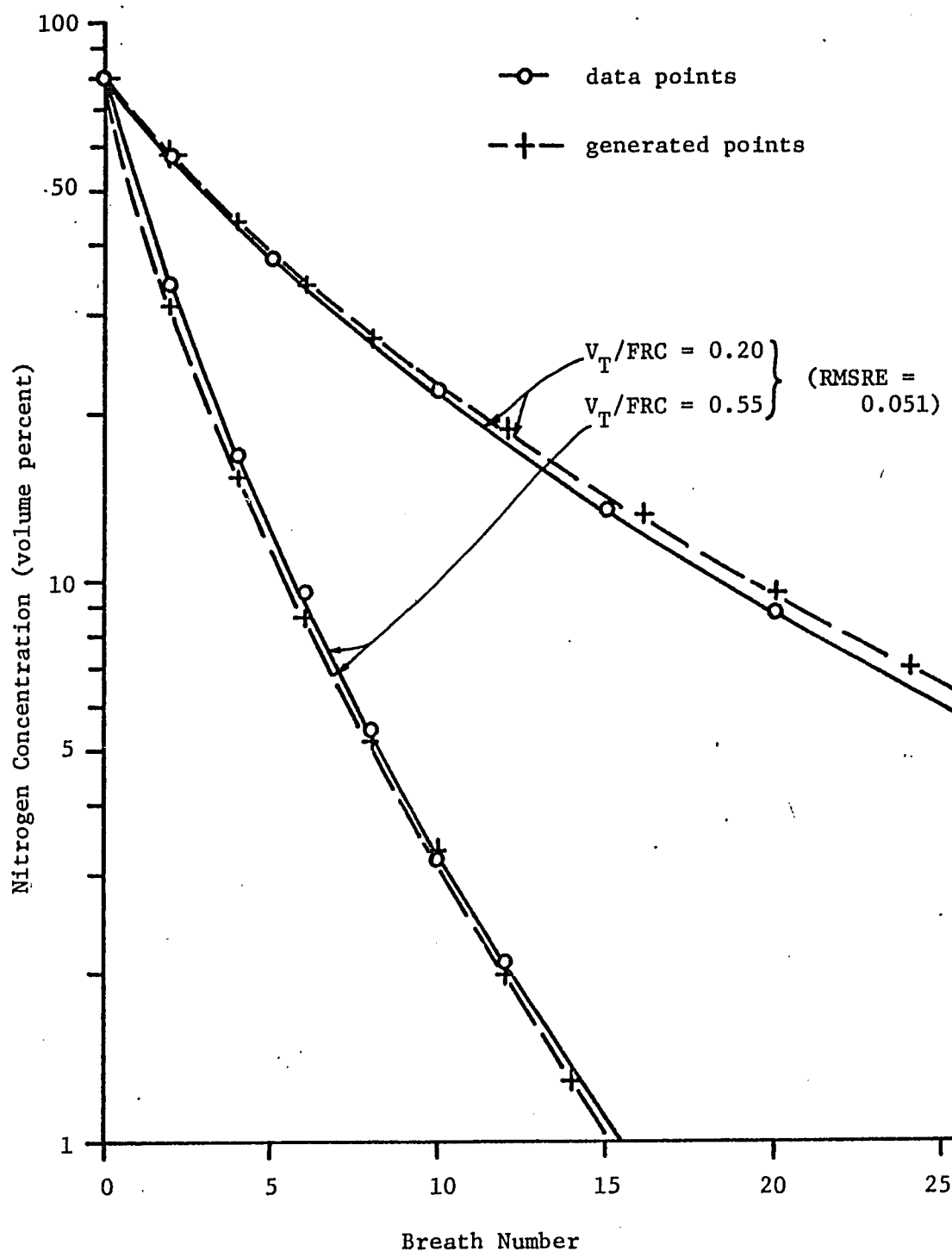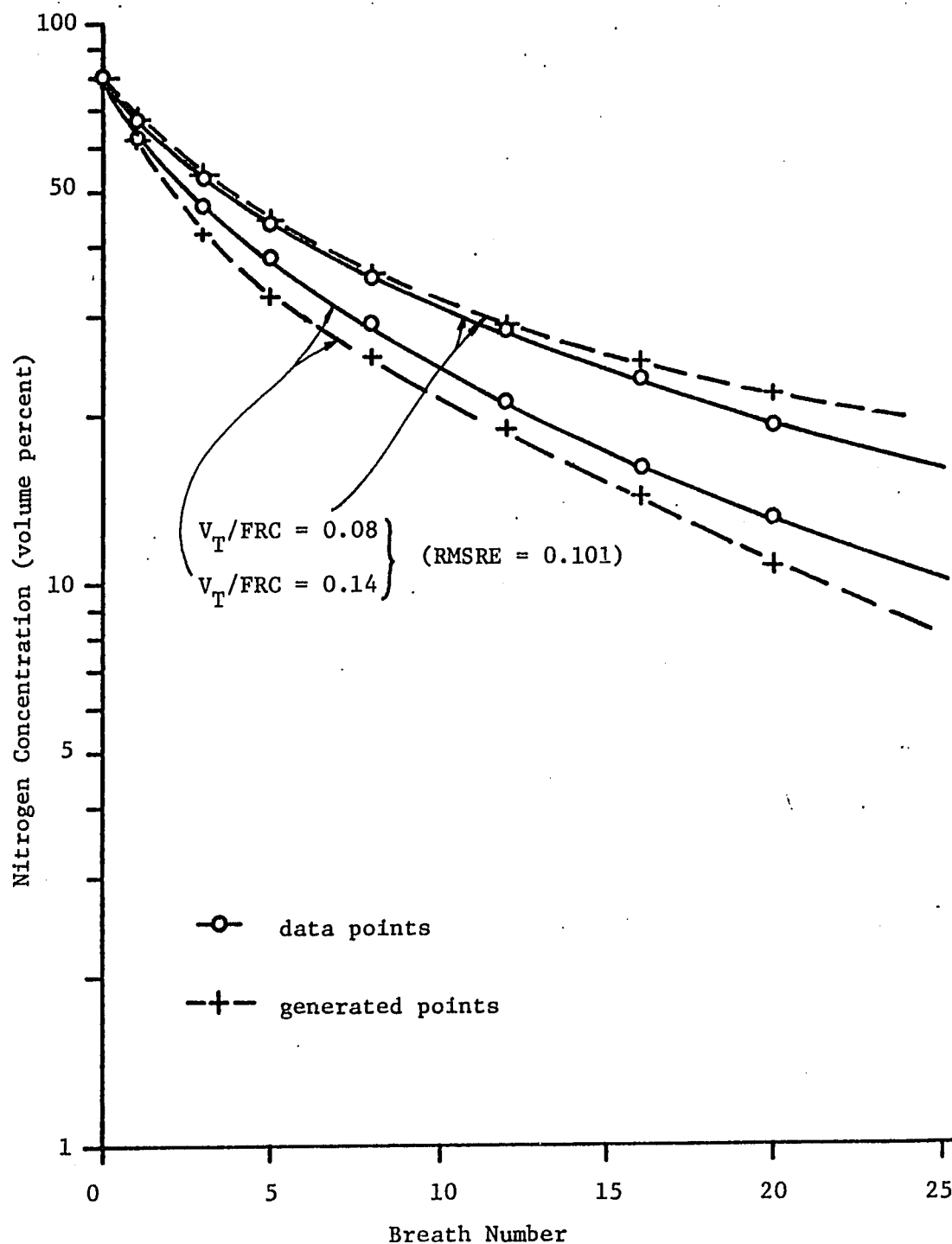and V_T/FRC = 0.267, 0.14.
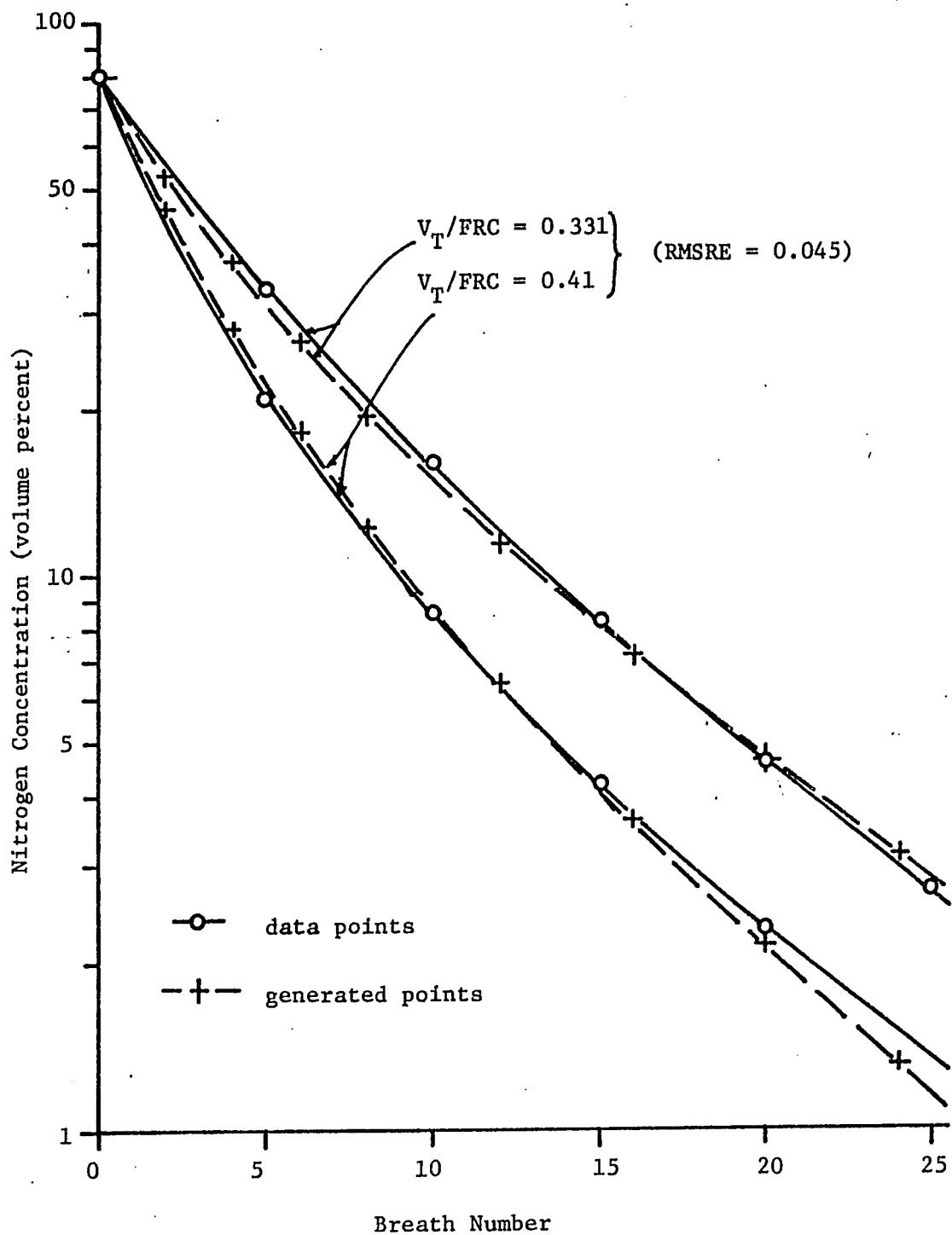
Figure 29. Generated Curves From Common Dead-Space Model (subject KA) Using Parameter Set (V_T/FRC = 0.41 and 0.331) and V_T/FRC = 0.41, 0.331.
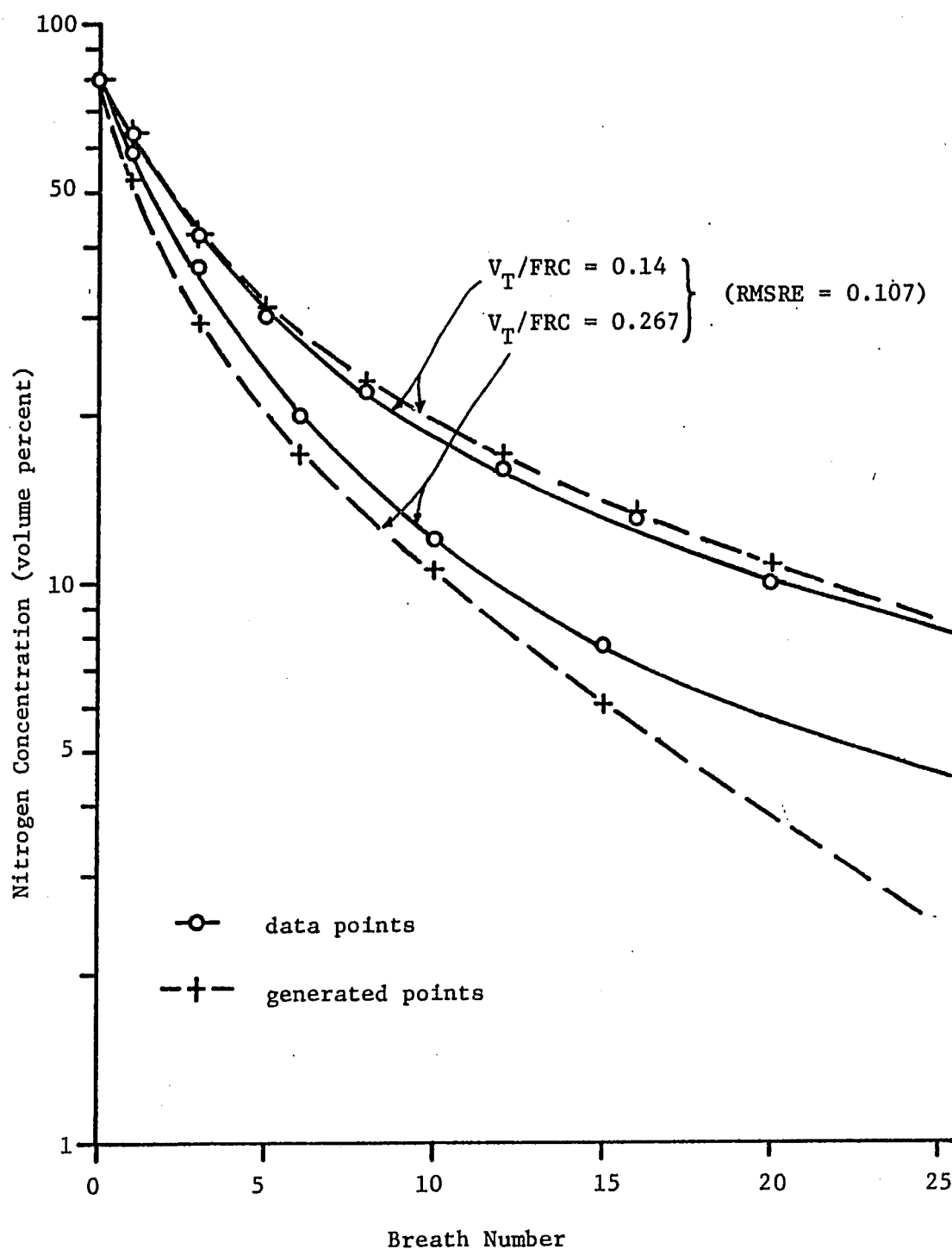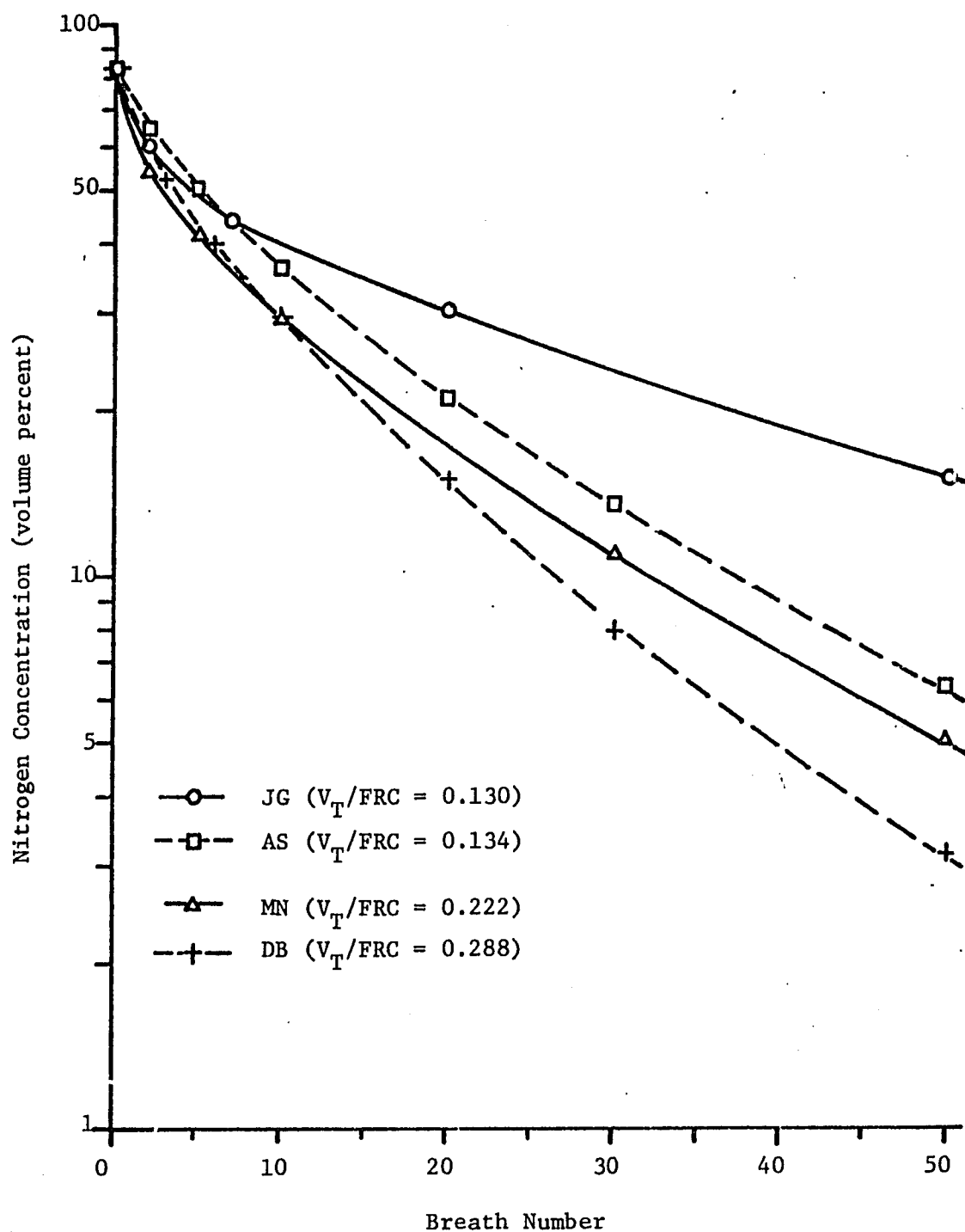
Figure 30. Nitrogen Washout Curves For Four Subjects
(DB, AS, MN, JG).
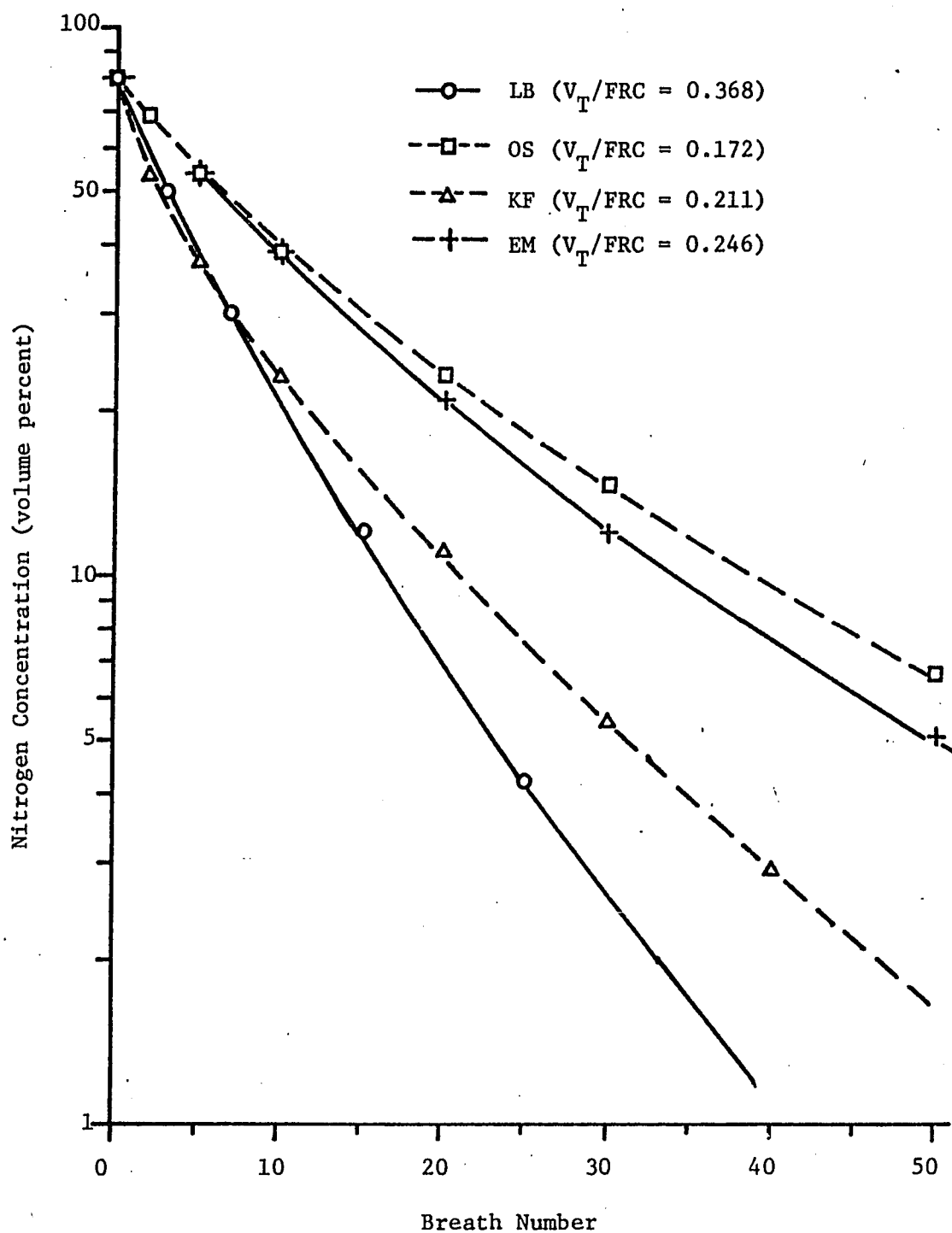
Figure 31. Nitrogen Washout Curves For Four Subjects
(LB, KF, EM, OS).

V. CONCLUSIONS

A compartmental model to simulate open-circuit nitrogen wash-out data was investigated. The governing equations were derived and a closed-form solution for end-expired common dead-space concentration was obtained which consists of the sum of K-exponentials, where K is the number of parallel branches in the model. The concentrations in the alveolar compartments consist of the same K-exponentials, but the coefficients differ depending on the initial conditions and the model parameters. For the specific case of K = 2, which assumes that the washout curve is representable by two exponentials, a single curve will uniquely determine three independent model parameters, say t_1, l_1, and V_D/V_L. This is sufficient to characterize the simpler common dead-space model and the separate dead-space model. However the more general model which requires an additional parameter, α , cannot be uniquely characterized. The number of branches in the model is determined by the number of exponentials that will fit the washout curve well. If the number is K, then (2K-1) independent parameters can be found. The number is also limited by the accuracy of the data points, since the uniqueness of the exponential decomposition is dependent on this factor, as well as the ratios of time constants. The more components there are and the closer the time constants, the more accurate the data points must be specified.

All of the subject data used were fit well by two exponentials with RMSRE values less than 0.05. Two exponentials were used as the minimum number which curve fit the data points to within physiological data accuracy of 10 percent. Parameters sets at several dilution factors for the same subject were noticeably different, which is indicative of the qualitative changes that occur with variations in overall ventilation. Increased overall ventilation is generally accompanied by increased lung volume fraction, as well as a relative increase in the tidal volume of the well-ventilated compartment. Significant ventilation factors are functional residual capacity, FRC, effective dilution factor, $(V_T-V_D)/V_L$, and dilution factor ratio, $(V_{T1}/V_{L1})/(V_{T2}/V_{L2})$. Abnormal changes in each would indicate ventilation irregularities.

The determination of whether the common dead-space model of the separate dead-space model is more representative of the physical system was not made, but simulation of patient data by both models will put bounds on the parameters for the more general model incorporating both kinds of dead space. Common dead-space model values of V_D/V_L and $(V_{T1}/V_{L1})/(V_{T2}/V_{L2})$ were usually larger than those for the separate dead-space model.

The nonlinear least squares Marquadt algorithm is an efficient method of curve-fitting washout data without specification of initial parameters which are close to the optimum set.

APPENDIX A. CLINICAL APPARATUS AND PROCEDURE

The open-circuit nitrogen washout system at Baylor College
of Medicine's Pulmonary Disease Laboratory is shown schematically in
Figure [32]. Portions of the system are also used for single-breath
tests.

The patient who is seated is instructed to breathe normally
through the mouthpiece. Directly behind the mouthpiece is the Ohio 700
nitrogen analyzer sample head which is a miniaturized gas spectrometer.
Here sample gas is continuously withdrawn with a vacuum pump and passed
through the sample head. An Electro Med 2 liter/sec pneumotach head
(bi-directional impact pitot tubes) registers continuous flow rate in
the form of a pressure differential which is converted to an electrical
signal at the pressure transducer. The four-way valve connects the
patient to room air, to the Collins spirometer or to the washout sec-
tion where pure oxygen (greater than 90 percent) is inspired and ex-
pired gases are collected in a Tissot spirometer.

The Collins spirometer is used to measure vital capacity and
to monitor tidal breathing so that the patient can be turned into the
washout section at the end of an expiration, which is done manually by
turning the four-way valve. One-way flapper valves direct the flow of
oxygen from a rubber reservoir bag and also direct the flow of expired
gases to the Tissot spirometer, which is counter-weighted to minimize
back pressure on expiration. All gas flow is through nominal 2-inch

fan motor

counter weight

Tissot spiro-
meter

directional flow "T" valve

three-way valve

reservoir
bag

pressure transducer

four-way valve

one-way
flapper
valves

three-way valve

Collins
spirometer

N_2 sample
head

pneumotach

mouth-
piece

to vacuum
pump

drum recorder
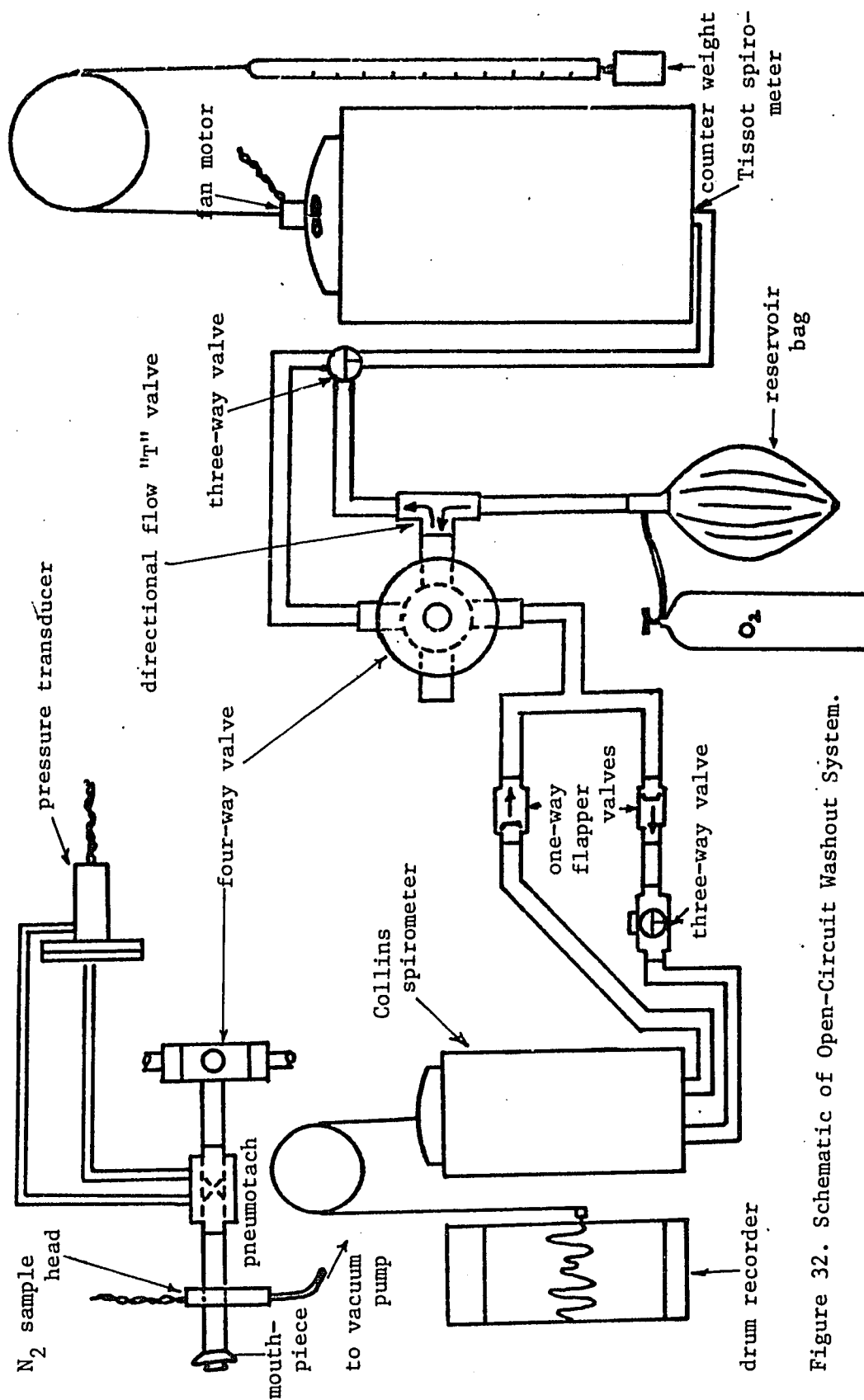
Figure 32. Schematic of Open-Circuit Washout System.

diameter tubing.

At the end of the usual seven minutes, the patient is connected to room air again. The Tissot spirometer contents are mixed with a small electric fan and the concentration is recorded by emptying the contents past the sample head.

Nitrogen concentration is recorded as a function of time on a Houston Instrument Model 97 X-Y recorder for clinical use. For the purposes of this study, flow or volume in addition to nitrogen concentration was recorded on a two-channel Brush recorder.

The electrical signals from the sample head and pressure transducer were fed into amplifiers, linearizers, and then to appropriate data display units. The flow signal from the Electro Med Model 785 Pneumotachograph Converter was directed to an adjacent Model 786 Electronic Integrator for volume output.

List of Equipment

X-Y Recorder   Houston Instrument Inc., Model HR-97
  (with time base)
Collins Spirometer
  (13.5 liter capacity)
Tissot Spirometer
Nitrogen Sample Head   Electro Med Model 701-B
Nitrogen Data Display Electro Med Model 784

Nitrogen Analyzer	Electro Med Model 700	
	(Actual N_2 Concentration)	Accuracy(% of Actual N_2 Concentration)
	2 - 5%	± 5%
	5 - 10%	± 2%
	10 - 85%	± 1%

Pneumotach Head	Electro Med Model 785-2
Pneumotach Converter	Electro Med Model 785
	(Accuracy: 1% full scale;
	linearity: 1% full scale;
	frequency response: within 3 db
	to 50 Hz)
Pressure Transducer	Electro Med Model 782
Pulmonary Integrator	Electro Med Model 900
	(Accuracy: 1% full scale;
	linearity: 1% full scale;
	zeroing stability: 1% full scale
	for 5 minutes)
Two-Channel Recorder	Brush Instruments

Experimental Procedure

All electrical equipment was turned on at least one-half
hour prior to testing. Recording instruments were zeroed and calibrated.
The Tissot spirometer was washed with oxygen and the Collins spirometer

section was washed with room air.

With the four-way valve open to room air, the subject was seated and instructed to place his lips tightly around the mouthpiece. A nose clip was placed over his nose and he was asked to breathe normally. The four-way valve was switched to the Collins spirometer where an expiratory vital capacity measurement was taken and tidal volume recordings were made on the drum recorder.

The X-Y and Brush recorders were turned on, and at the end of an expiration the subject was connected to the nitrogen washout section. The patient was periodically reminded to keep his lips tight and breathing relaxed. The nitrogen recordings were monitored to check for any air leaks which would register as a sudden increase in concentration. The normal washout period is seven minutes, however in cases of severe retarding of nitrogen decay, the period was extended to fifteen minutes. At the end of six minutes, X-Y recorder sensitivity was increased for greater readability. Brush recorder sensitivities were changed usually around nitrogen concentrations of 10 vol. percent, while the time scale was expanded periodically to check the zero position in the volume recording. At the end of the washout test, the patient was asked to expire fully to obtain an alveolar sample.

Once the Tissot spirometer contents were isolated, the electric fan was turned on for about five minutes and a volume reading taken after that. Concentration was obtained by running the contents past the nitrogen sample head and recorded.

The entire procedure was repeated after a period of fifteen minutes to allow for the patient's lungs to again equilibrate with the

room air.

Nitrogen concentration, flow and volume instruments were recalibrated after the two runs.

APPENDIX B. MARQUADT ALGORITHM

The following derivation describes the Marquadt algorithm [23,37], which formed the basis of the parameter estimation scheme used in this study. The algorithm is a gradient method which requires computation or input of the first partial derivatives of the nonlinear function.

In general, given a nonlinear function to be fitted to a set of data points, the measure of best fit is usually taken to be the minimum of the sum of the squared error terms at each of the data points. Denoting the function as $f(n_i, \alpha) = f_i(\alpha)$ and the corresponding i^{th} data point as y_i, than an error term may be defined as:

$$e_i = y_i - f_i(\alpha) \tag{B.1}$$

For the case of k data points, an error vector may be similarly defined:

$$e = y - f(\alpha) \tag{B.2}$$

where $e, f(\alpha), y$ are k-dimension vectors and α is the vector whose elements correspond to the parameters which define the function f.

The total error or sum of the squared error terms is a vector norm of the form:

$$E = \|e\| = e^T e = \sum_{i=1}^{k} e_i^2 \tag{B.3}$$

The least-squares method attempts to minimize E by variations in the parameter vector $\underset{\sim}{\alpha}$. For certain nonlinear functions of $\underset{\sim}{\alpha}$ suitable transformations are available which render the problem linear in the parameters, after which the familiar methods of linear least squares may be applied. However for a sum of exponentials, such a transformation is not available, therefore an approximate linearization becomes necessary provided initial values of the parameter set are sufficiently close to the set which minimizes the norm E. This first order approximation now is linear in the parameter increments and the linear least-squares method can be used to solve for these increments. If desired, the process may be repeated to convergence.

The vector function $\underset{\sim}{f}(\underset{\sim}{\alpha} + \Delta\underset{\sim}{\alpha})$ may be expanded in a Taylor series about $\underset{\sim}{f}(\underset{\sim}{\alpha})$:

$$\underset{\sim}{f}(\underset{\sim}{\alpha} + \Delta\underset{\sim}{\alpha}) = \underset{\sim}{f}(\underset{\sim}{\alpha}) + \frac{\partial \underset{\sim}{f}(\underset{\sim}{\alpha})}{\partial \underset{\sim}{\alpha}}(\Delta\underset{\sim}{\alpha}) + (\Delta\underset{\sim}{\alpha})^T \frac{\partial^2 \underset{\sim}{f}(\underset{\sim}{\alpha})}{\partial \underset{\sim}{\alpha}^2}(\Delta\underset{\sim}{\alpha}) + \cdots$$

$$(B.4)$$

For $\Delta\underset{\sim}{\alpha}$ small enough, the second and higher order terms can be neglected, and the approximation is made that:

$$\underset{\sim}{f}(\underset{\sim}{\alpha} + \Delta\underset{\sim}{\alpha}) \sim \underset{\sim}{\hat{f}}(\underset{\sim}{\alpha}, \Delta\underset{\sim}{\alpha}) \qquad\qquad (B.5)$$

where $\qquad \underset{\sim}{\hat{f}}(\underset{\sim}{\alpha}, \Delta\underset{\sim}{\alpha}) \equiv \underset{\sim}{f}(\underset{\sim}{\alpha}) + \frac{\partial \underset{\sim}{f}(\underset{\sim}{\alpha})}{\partial \underset{\sim}{\alpha}} \Delta\underset{\sim}{\alpha}$

is linear in $\Delta\underset{\sim}{\alpha}$.

An error and total error vector for the linear approximation can be defined as:

$$\hat{\underset{\sim}{e}} = \underset{\sim}{y} - \hat{\underset{\sim}{f}}(\underset{\sim}{x}, \Delta\underset{\sim}{x})$$ (B.6)

and
$$\hat{E} = \hat{\underset{\sim}{e}}^T\hat{\underset{\sim}{e}} = (\underset{\sim}{y} - \hat{\underset{\sim}{f}})^T(\underset{\sim}{y} - \hat{\underset{\sim}{f}})$$

$$= \underset{\sim}{y}^T\underset{\sim}{y} - 2\hat{\underset{\sim}{f}}^T\underset{\sim}{y} + \hat{\underset{\sim}{f}}^T\hat{\underset{\sim}{f}}$$ (B.7)

In order to find $\Delta\underset{\sim}{x}$ that will minimize E, a necessary condition is that the partial derivative of E with respect to $\Delta\underset{\sim}{x}$ be equal to zero:

$$\frac{\partial\hat{E}}{\partial\Delta\underset{\sim}{x}} = -2\left(\frac{\partial\hat{\underset{\sim}{f}}}{\partial\Delta\underset{\sim}{x}}\right)^T\underset{\sim}{y} + 2\left(\frac{\partial\hat{\underset{\sim}{f}}}{\partial\Delta\underset{\sim}{x}}\right)^T\hat{\underset{\sim}{f}} = \underset{\sim}{0}$$ (B.8)

Substituting the expression for $\hat{\underset{\sim}{f}}(\underset{\sim}{x}, \Delta\underset{\sim}{x})$:

$$\frac{\partial\hat{\underset{\sim}{f}}}{\partial\Delta\underset{\sim}{x}} = \frac{\partial}{\partial\Delta\underset{\sim}{x}}\left(\underset{\sim}{f}(\underset{\sim}{x}) + \frac{\partial\underset{\sim}{f}(\underset{\sim}{x})}{\partial\underset{\sim}{x}}\Delta\underset{\sim}{x}\right) = \frac{\partial\underset{\sim}{f}(\underset{\sim}{x})}{\partial\underset{\sim}{x}}$$ (B.9)

Making the substitution of equation (B.9) in (B.8):

$$\left(\frac{\partial\underset{\sim}{f}(\underset{\sim}{x})}{\partial\underset{\sim}{x}}\right)^T\underset{\sim}{y} = \left(\frac{\partial\underset{\sim}{f}(\underset{\sim}{x})}{\partial\underset{\sim}{x}}\right)^T\left(\underset{\sim}{f}(\underset{\sim}{x}) + \frac{\partial\underset{\sim}{f}(\underset{\sim}{x})}{\partial\underset{\sim}{x}}\Delta\underset{\sim}{x}\right)$$

or
$$\left(\frac{\partial\underset{\sim}{f}(\underset{\sim}{x})}{\partial\underset{\sim}{x}}\right)^T\left(\frac{\partial\underset{\sim}{f}(\underset{\sim}{x})}{\partial\underset{\sim}{x}}\right)\Delta\underset{\sim}{x} = \left(\frac{\partial\underset{\sim}{f}(\underset{\sim}{x})}{\partial\underset{\sim}{x}}\right)^T(\underset{\sim}{y} - \underset{\sim}{f}(\underset{\sim}{x}))$$
(B.10)

Denoting $\underset{\sim}{J}$ as the transform fo the Jacobian matrix:

$$\underset{\sim}{J} = \left(\frac{\partial\underset{\sim}{f}(\underset{\sim}{x})}{\partial\underset{\sim}{x}}\right)^T$$

then equation (B.10) can be expressed:

$$\underset{\sim}{J}\underset{\sim}{J}^T\Delta\underset{\sim}{x} = \underset{\sim}{J}\underset{\sim}{e}$$ (B.11)

Equation (B.11) can be solved for $\Delta\underset{\sim}{\alpha}$ which will minimize the approximate total error E, since the functional form of $\underset{\sim}{f}(\underset{\sim}{\alpha})$ is presumably known, as well as the initial parameter set $\underset{\sim}{\alpha}$.

The minimal value of $\hat{E}$ will be exactly the minimal value of E if the original function is linear in the vector $\underset{\sim}{\alpha}$. Since the previous derivation for $\Delta\underset{\sim}{\alpha}$ is based on the assumption that $\hat{\underset{\sim}{f}}(\underset{\sim}{\alpha},\Delta\underset{\sim}{\alpha}) \sim f(\underset{\sim}{\alpha}+\Delta\underset{\sim}{\alpha})$, convergence to the solution of the nonlinear system is assured only when this condition is met. In cases where it is not, an increase in the total error E may result even when the approximate error $\hat{E}$ is minimized.

To assure convergence at least to the minimum of E, Levenberg [18] suggested placing a constraint on $\Delta\underset{\sim}{\alpha}$ in the form of a Lagrange multiplier (Levenberg adjustment) in equation (B.11):

$$(\underset{\sim}{J}\underset{\sim}{J}^T + \lambda \underset{\sim}{I}) \Delta\underset{\sim}{\alpha} = \underset{\sim}{J}\underset{\sim}{e} \qquad (B.12)$$

where λ = Levenberg adjustment

   $\underset{\sim}{I}$ = identity matrix of dimension k.

For λ = 0, equation (B.12) reduces to the Gauss-Newton algorithm which assumes local linearity in order to converge to the minimum E. This method fails when the first order approximation does not adequately describe the function at the initial $\underset{\sim}{\alpha}$, in which case the iteration scheme will lead to a random increase and decrease in total error. Convergence is rapid however, when initial $\underset{\sim}{\alpha}$ is close to the optimum $\underset{\sim}{\alpha}$.

For increasing λ, equation (B.12) approaches the method

of steepest descent in which the parameter set increment, $\Delta \alpha$, is made proportional to the negative gradient of the total error:

$$\Delta \alpha = \frac{1}{\lambda} J e = -\frac{1}{2\lambda} \nabla_\alpha E \qquad (B.13)$$

where $\nabla_\alpha E = \frac{\partial E}{\partial \alpha} = \frac{\partial}{\partial \alpha}(e^T e) = -2 J e$

The method of steepest descent will converge to a global minimum very slowly if the error hypersurface is irregular or perhaps not at all if there are local minima or stationary points. Systematic convergence is assured however, since λ can always be made large enough for the total error E to decrease.

The Marquadt algorithm is a maximum neighborhood method which seeks to take the largest step-size which will decrease E. For any iteration step, a trial and error procedure is followed in which λ is initially weighted towards the Gauss-Newton method and then weighted progressively more towards the method of steepest descent if the total error term fails to decrease for the next step.

APPENDIX C.   CLOSED-FORM SOLUTION FOR THE MODEL

Equations (2.9) are the describing equations for the model.
Introducing the notation change:

$$a_1 = \frac{V_{L1} + V_{DS1}}{V_{L1} + V_{T1}} \quad ; \quad b_1 = \frac{t_1 V_{DC}}{V_{L1} + V_{T1}}$$

$$a_2 = \frac{V_{L2} + V_{DS2}}{V_{L2} + V_{T2}} \quad ; \quad b_2 = \frac{t_2 V_{DC}}{V_{L2} + V_{T2}} \tag{C.1}$$

The set of linear difference equations becomes:

$$f_{A1}^{(n+1)} = a_1 f_{A1}^{(n)} + b_1 f_{DC}^{(n)} \tag{C.2a}$$

$$f_{A2}^{(n+1)} = a_2 f_{A2}^{(n)} + b_2 f_{DC}^{(n)} \tag{C.2b}$$

$$f_{DC}^{(n)} = t_1 f_{A1}^{(n)} + t_2 f_{A2}^{(n)} \tag{C.2c}$$

Introducing the linear operator E, the above equations can be written
in matrix form:

$$
\begin{bmatrix}
(E-a_1) & 0 & -b_1 \\
0 & (E-a_2) & -b_2 \\
t_1 & t_2 & -1
\end{bmatrix}
\begin{Bmatrix}
f_{A1}^{(n)} \\
f_{A2}^{(n)} \\
f_{DC}^{(n)}
\end{Bmatrix}
=
\begin{Bmatrix}
0 \\
0 \\
0
\end{Bmatrix}
\tag{C.3}
$$

where $\quad E^m f^{(n)} = f^{(n+m)}$ $\hfill$ (C.4)

$$E^0 f^{(n)} = f^{(n+0)} = f^{(n)}$$

In a manner analogous to Cramer's rule to solve a set of p algebraic equations in p unknowns, the set of three difference equations can be reduced to a single difference equation in one of the dependent variables, noting that the order of operation must be preserved:

$$\begin{vmatrix} (E-a_1) & 0 & -b_1 \\ 0 & (E-a_2) & -b_2 \\ t_1 & t_2 & -1 \end{vmatrix} f_{DC}^{(n)} = \begin{vmatrix} (E-a_1) & 0 & 0 \\ 0 & (E-a_2) & 0 \\ t_1 & t_2 & 0 \end{vmatrix} = 0$$

(C.5)

Evaluating the operational determinant:

$$\left\{ (E-a_1)\left[-(E-a_2) + b_2 t_2 \right] + t_1 \left[b_1 (E-a_2) \right] \right\} f_{DC}^{(n)} = 0$$

$$\left[E^2 - (t_1 b_1 + t_2 b_2 + a_1 + a_2)E + (t_1 b_1 a_2 + t_2 b_2 a_1 + a_1 a_2) \right] f_{DC}^{(n)} = 0$$

(C.6)

which is a second-order linear difference equation with constant coefficients.

Introducing the notation:

$$a = (t_1 b_1 + t_2 b_2 + a_1 + a_2)$$

$$b = (t_1 b_1 a_2 + t_2 b_2 a_1 + a_1 a_2) \hfill \text{(C.7)}$$

Equation (C.6) becomes:

$$(E^2 - aE + b) f_{DC}^{(n)} = 0 \qquad (C.8)$$

Proceeding in analogy with linear constant coefficient differential equations, a solution of the following form may be assumed:

$$f_{DC}^{(n)} = M^n \qquad (C.9)$$

Substitution into equation (C.8) yields:

$$(M^2 - aM + b) M^n = 0 \qquad (C.10)$$

For a non-trivial solution, $(M^2 - aM + b)$ must be equal to zero, leading to the characteristic equation for the difference equation:

$$M^2 - aM + b = 0 \qquad (C.11)$$

If the roots, M_1 and M_2, are distinct, Casorati's determinant is non-zero:

$$C[M_1^n, M_2^n] = \begin{vmatrix} M_1^n & M_2^n \\ M_1^{n+1} & M_2^{n+1} \end{vmatrix} = M_1^n M_2^n (M_2 - M_1) \neq 0 \qquad (C.12)$$

and the complete solution is of the form:

$$f_{DC}^{(n)} = C_1 M_1^n + C_2 M_2^n \qquad (C.13)$$

where C_1 and C_2 are arbitrary constants to be determined by initial conditions once M_1 and M_2 are found.

If the roots are equal, Casorati's determinant vanishes, so another independent solution must be found. One such solution is:

$$f_{DC}^{(n)} = n M_1^n \tag{C.14}$$

and Casorati's determinant becomes:

$$C\left[M_1^n, n M_1^n\right] = \begin{vmatrix} M_1^n & n M_1^n \\ \\ M_1^{n+1} & (n+1) M_1^{n+1} \end{vmatrix} = M_1^{n+2} \neq 0 \tag{C.15}$$

The complete solution for this case is:

$$f_{DC}^{(n)} = C_1 M_1^n + C_2 n M_1^n \tag{C.16}$$

The other two dependent variables, $f_{A1}^{(n)}$ and $f_{A2}^{(n)}$, can be similarly solved for. The characteristic equations are the same as for $f_{DC}^{(n)}$, and therefore the forms of the solution are the same except for the arbitrary constants, which can be expressed as functions of C_1 and C_2 by substituting the general solution into any two of the three describing equations. The number of independent arbitrary constants in the system of equations is two, the degree of the operator E in the operational determinant.

Assuming distinct roots of the characteristic equation, the forms of solution may be expressed as:

$$f_{A1}^{(n)} = A_1 M_1^n + A_2 M_2^n \tag{C.17}$$

$$f_{A2}^{(n)} = B_1 M_1^n + B_2 M_2^n \tag{C.18}$$

Substituting equations (C.16) and (C.17) into equation (C.2a), and equating the coefficients of M_1^n and M_2^n to zero:

$$\left(A_1 M_1^{n+1} + A_2 M_2^{n+1}\right) - a_1 \left(A_1 M_1^n + A_2 M_2^n\right) - b_1 \left(C_1 M_1^n + C_2 M_2^n\right) = 0$$

$$\left[A_1 (M_1 - a_1) - b_1 C_1\right] M_1^n + \left[A_2 (M_2 - a_1) - b_1 C_2\right] M_2^n = 0$$

or $\qquad A_1 = \dfrac{b_1 C_1}{(M_1 - a_1)} \qquad ; \qquad A_2 = \dfrac{b_1 C_2}{(M_2 - a_1)}$ $\qquad$ (C.19)

Similarly for equation (C.2b) with equations (C.16) and (C.18):

$$\left(B_1 M_1^{n+1} + B_2 M_2^{n+1}\right) - a_2 \left(B_1 M_1^n + B_2 M_2^n\right) - b_2 \left(C_1 M_1^n + C_2 M_2^n\right) = 0$$

$$\left[B_1 (M_1 - a_2) - b_2 C_1\right] M_1^n + \left[B_2 (M_2 - a_2) - b_2 C_2\right] M_2^n = 0$$

$$B_1 = \frac{b_2 C_1}{(M_1 - a_2)} \qquad ; \qquad B_2 = \frac{b_2 C_2}{(M_2 - a_2)} \qquad \text{(C.20)}$$

From assumption (7), in which the nitrogen concentration was assumed to be equal in both alveolar compartments at the start of a washout test (n = 0), C_1 and C_2 can be solved for. Denoting this initial concentration as $f_A^{(0)}$:

$$A_1 + A_2 = f_A^{(0)} \tag{C.21a}$$

$$B_1 + B_2 = f_A^{(0)} \tag{C.21b}$$

or from equations (C.19) and (C.20):

$$\begin{bmatrix} \dfrac{b_1}{(M_1 - a_1)} & \dfrac{b_1}{(M_2 - a_1)} \\[2ex] \dfrac{b_2}{(M_1 - a_2)} & \dfrac{b_2}{(M_2 - a_2)} \end{bmatrix} \begin{Bmatrix} C_1 \\[1ex] C_2 \end{Bmatrix} = \begin{Bmatrix} f_A^{(0)} \\[1ex] f_A^{(0)} \end{Bmatrix} \tag{C.22}$$

The solutions C_1 and C_2 are unique provided the coefficient matrix is nonsingular, and is given by:

$$\begin{Bmatrix} C_1 \\[1ex] C_2 \end{Bmatrix} = \begin{bmatrix} \dfrac{b_1}{(M_1 - a_1)} & \dfrac{b_1}{(M_2 - a_1)} \\[2ex] \dfrac{b_2}{(M_1 - a_2)} & \dfrac{b_2}{(M_2 - a_2)} \end{bmatrix}^{-1} \begin{Bmatrix} f_A^{(0)} \\[1ex] f_A^{(0)} \end{Bmatrix} \tag{C.23}$$

The determinant of the coefficient matrix is nonsingular in general since:

$$\begin{vmatrix} \dfrac{b_1}{(M_1-a_1)} & \dfrac{b_1}{(M_2-a_1)} \\[2ex] \dfrac{b_2}{(M_1-a_2)} & \dfrac{b_2}{(M_2-a_2)} \end{vmatrix} = b_1 b_2 \left[\dfrac{(a_1-a_2)(M_2-M_1)}{(M_1-a_1)(M_2-a_2)(M_1-a_2)(M_2-a_1)} \right]$$

$$(C.24)$$

and from the assumption that the roots of the characteristic equation are distinct, and in general the effective dilution factors, a_1 and a_2, are not equal, except for the singular case $(M_1-M_2 = t_1 b_1 + t_2 b_2)$[1]. It can be seen that initial conditions in any two compartments, either the common dead space and one of the alveolar compartments, or both of the alveolar compartments are sufficient to define the course of the washout for a given parameter set.

In a similar manner for the case of K-parallel alveolar compartments connected to a common dead-space compartment, the set of (K+1) linear difference equations are:

$$f_{Ai}^{(n+1)} = a_i f_{Ai}^{(n)} + b_i f_{Dc}^{(n)}$$

$$(C.25)$$

for i = 1,2,...,K

---

[1] From equation (C.11), $M_1-M_2 = (a^2-4b)^{1/2}$

$$= \left[(t_1 b_1 + t_2 b_2 + a_1 + a_2)^2 - 4(t_1 b_1 a_2 + t_2 b_2 a_1 + a_1 a_2) \right]^{1/2}$$

For $a_1 = a_2 = a$:

$$M_1 - M_2 = t_1 b_1 + t_2 b_2$$

$$f_{Dc}^{(n)} = \sum_{i=1}^{K} t_i f_{Ai}^{(n)} \tag{C.26}$$

where
$$a_i = \frac{V_{Li} + V_{osi}}{V_{Li} + V_{Ti}}$$

$$b_i = \frac{t_i V_{Dc}}{V_{Li} + V_{Ti}}$$

Introducing the E operator, reduction of the set to a single difference equation in one of the dependent variables leads to a Kth-degree polynomial in E. Assuming a solution of the form $f^{(n)} = M^n$, substitution in the above leads to the same K^{th}-degree polynomial in M, which is the characteristic equation for the system. For K-distinct roots, the complete solution is:

$$f^{(n)} = \sum_{i=1}^{K} c_i M_i^n \tag{C.27}$$

The number of independent arbitrary constants is K, and so K initial conditions must be specified in order to obtain the particular solution. All other constants can be solved for by substituting the complete solutions for (K+1) dependent variables into K-linear difference equations, and equating the coefficients to zero. Non-vanishing of Casorati's determinant assures linear independence of the solutions.

It can then be seen that the number of exponentials comprising the solution is determined by the number of parallel branches in the model. The end-expired concentration for the common dead space and all alveolar compartments are of the same form. They consist of the sum of the same exponentials, except that the coefficients differ.

APPENDIX D. COMPARISON BETWEEN A DISCRETELY-VENTILATED

MODEL AND A CONTINUOUSLY-VENTILATED MODEL

Looking at the case of a single compartment of volume, FRC, ventilated with a tidal volume of V_T at a rate of r breaths per minute, the differences in assuming discrete ventilation and an equivalent continuous ventilation on the course of nitrogen washout is studied.

The models are assumed well-mixed and the concentrations at discrete intervals will be compared. The flow rate for the continuous model is assumed to b equal to the tidal volume times the respiratory rate. The governing equation for the discretely-ventilated model assuming an initial concentration of unity is:

$$F_d^{(n)} = \left(\frac{FRC}{V_T + FRC}\right)^n = \left(1 + \frac{V_T}{FRC}\right)^{-n} \tag{D.1}$$

For the case of continuous ventilation, a nitrogen balance yields:

$$\frac{d(FRC \cdot F_c)}{dt} = \dot{V}_{in} F_{in} - \dot{V}_{out} F_{out} \tag{D.2}$$

Assuming:

FRC = constant

F_{in} = 0

V_{in} = V_{out} = $V_T r$

Then:
$$\frac{dF_c}{dt} = -\frac{V_T r}{FRC}$$
(D.3)

or
$$\ln F_c = -\frac{V_T r}{FRC}t + \ln F_0$$

Since $F_0 = 1$:
$$F_c = e^{-\frac{V_T}{FRC}n} = \left(e^{\frac{V_T}{FRC}}\right)^{-n}$$
(D.4)

Expanding the exponential in a series form:

$$e^{V_T/FRC} = 1 + \frac{V_T}{FRC} + \frac{1}{2!}\left(\frac{V_T}{FRC}\right)^2 + \cdots$$
(D.5)

To first order terms, both models give identical results. The significance of the second order and high terms increase with the factor, V_T/FRC. For nominal values of 500 ml for V_T and 2000 ml for FRC, the remainder accounts for a 3 percent difference between the arguments.

Denoting $\phi = V_T/FRC$ and the difference in concentrations from both models as ϵ :

$$\epsilon(n) = (1+\phi)^{-n} - \left(e^{\phi}\right)^{-n}$$
(D.6)

The maximum difference occurs at:

$$\frac{d\,\epsilon(n)}{dn} = -\frac{\ln(1+\phi)}{(1+\phi)^n} + \frac{\phi}{e^{n\phi}} = 0$$

or

$$n_{max} = \frac{\ln\left[\frac{\phi}{\ln(1+\phi)}\right]}{\ln\left[\frac{e^{\phi}}{1+\phi}\right]}$$
(D.7)

For various values of ϕ :

$\phi = 0.1$: $\epsilon_{max} = 0.0177$ at n = 10.2

relative error = 0.0467

$\phi = 0.25$: $\epsilon_{max} = 0.0418$ at n = 4.2

relative error = 0.1076

$\phi = 1.0$: $\epsilon_{max} = 0.1341$ at n = 1.19

relative error = 0.307

Figure [33] shows the decay of both functions for two values of ϕ plotted on linear scales, and Figure [34] shows the same functions plotted on semilogarithmic graph paper.
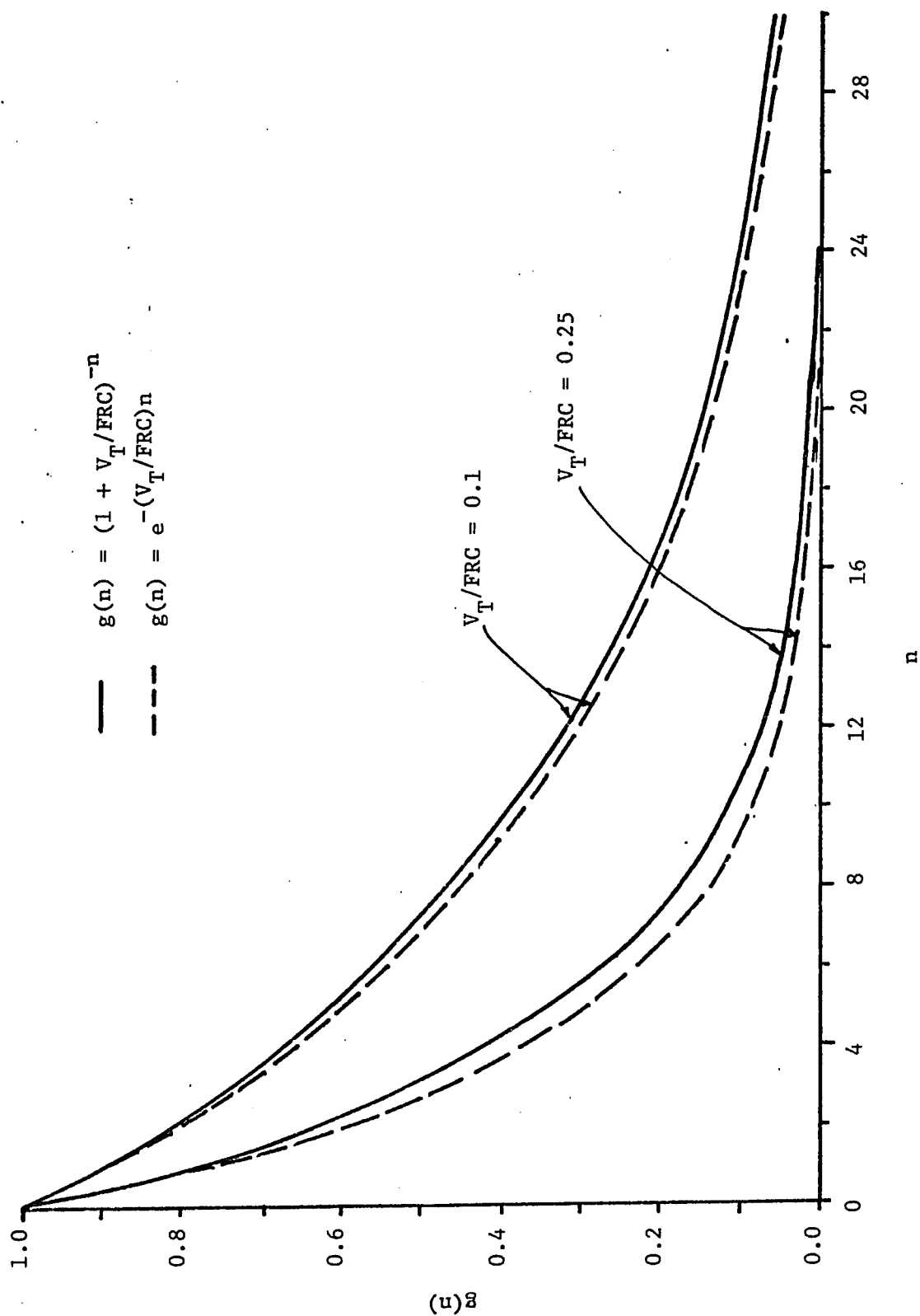
Figure 33. Plots of Two Functions ($g(n) = (1 + V_T/FRC)^{-n}$ and $g(n) = e^{-(V_T/FRC)n}$) for V_T/FRC = 0.1, 0.25.
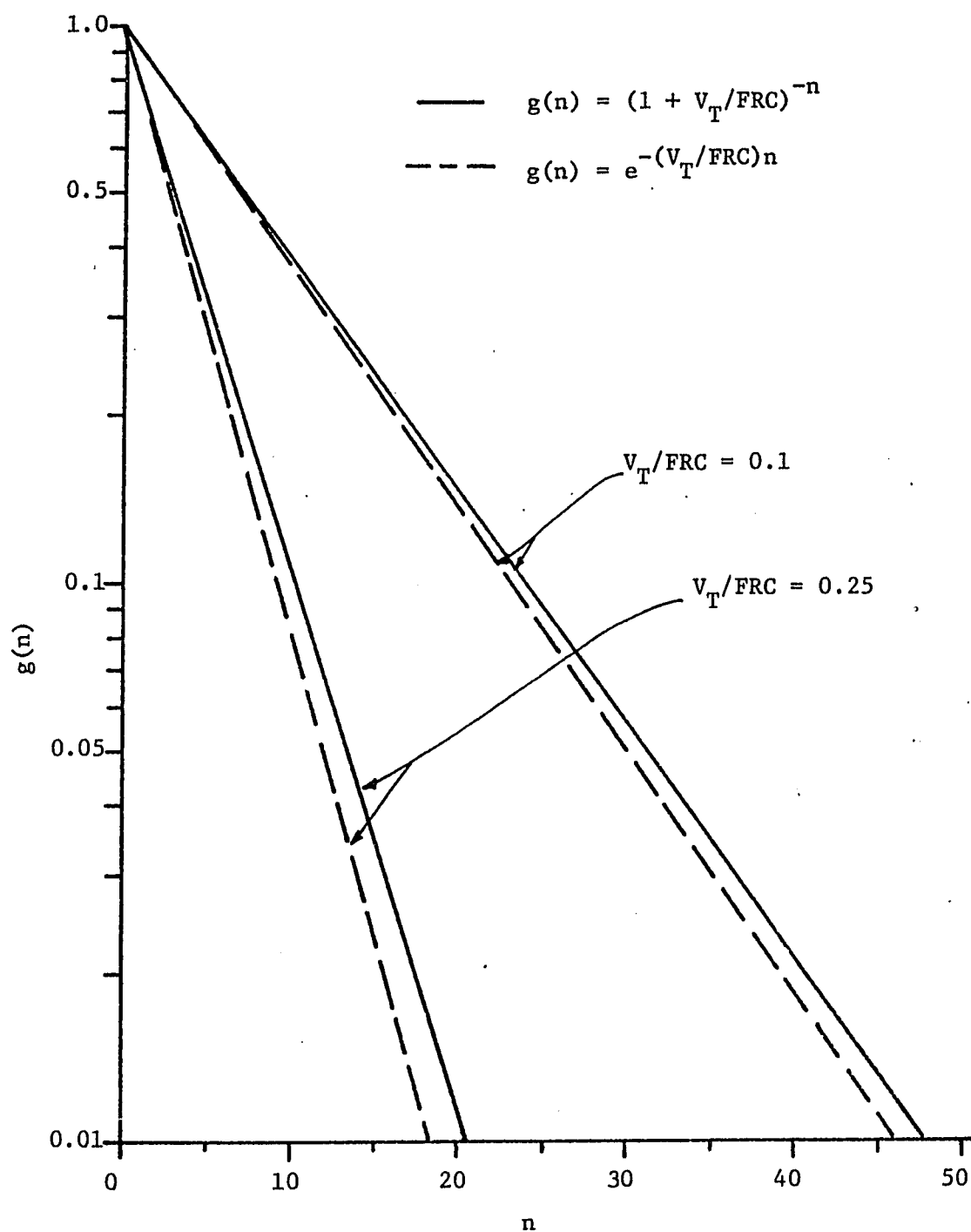
Figure 34. Plots of Two Functions $(g(n) = (1 + V_T/FRC)^{-n}$ and $g(n) = e^{-(V_T/FRC)n})$ For $V_T/FRC = 0.1$, 0.25.

REFERENCES

1. Bouhuys, A., R. Jonsson, and G. Lundin, "Influence of Added Dead
        Space on Pulmonary Ventilation," Acta Physiol. Scand. 39:
        105-120, 1957.

2. Bouhuys, A., R. Jonsson, and G. Lundin, "Nonuniformity of Pulmo-
        nary Ventilation in Chronic Diffuse Obstructive Emphysema,"
        Acta Med. Scand. 162: 29-46, 1958.

3. Bouhuys, A., S. Lichtneckert, C. Lundgren, and G. Lundin, "Volun-
        tary Changes in Breathing Patterns and N_2 Clearance from
        Lungs," J. Appl. Physiol., 16: 1039-1042, 1961.

4. Briscoe, W. A., "The Current Status of Pulmonary Function Tests,"
        Arch Environ. Health, 16: 531, 1968.

5. Briscoe, W. A. and A. Cournand, "Uneven Ventilation of Normal and
        Diseased Lungs Studied by an Open-Circuit Method," J. Appl.
        Physiol. 14: 284-290, 1959.

6. Ordinary Differential and Difference Equations, Chorlton, F.,
        D. Van Nostrand Company, Ltd., London, 1965.

7. The Lung: Clinical Physiology and Pulmonary Function Tests; Com-
        roe, J. H., R. E. Forster, A. B. Dubois, W. A. Briscoe, and
        E. Carlsen, Yearbook Medical Publishers Inc., Chicago,
        1962.

8. Lung Function: Assessment and Application in Medicine; Cotes, J. E.,
        F. A. Davis Company, Philadelphia, 1968.

9. Cournand, A., E. D. Baldwin, R. C. Darling and D. W. Richards.
        "Studies on the Intrapulmonary Mixture of Gases. IV. The
        Significance of Pulmonary Emptying Rate and the Simplified
        Open-Circuit Measurement of Residual Air" J. Clin. Invest.,
        20: 681-689, 1941.

10. Cutillo, A., E. Omboni, and S. Delgrossi, "Effects of Respiratory
        Frequency on Distribution of Inspired Gas in Normal Sub-
        jects and in Patients with Chronic Obstructive Lung Di-
        sease," Amer. Rev. Resp. Dis., 105: 756-767, 1972.

11. Darling, R. C., A. Cournand, and D. W. Richards, Jr., "Studies on
        the Intrapulmonary Mixture of Gases. III. An Open Circuit
        Method for Measuring Residual Air," J. Clin, Invest., 19:
        599-618, 1940.

12. Mathematical Methods in Physics and Engineering, Dettman, J. W.,
        McGraw-Hill Book Company, New York, 1969.

13. *Measurement Systems: Application and Design*, Doebelin, E. O., McGraw-Hill Book Company, New York, 1966.

14. Fowler, W. S., E. R. Cornish, Jr., and S. S. Kety, "Lung Function. Studies. VIII. Analysis of Alveolar Ventilation by Pulmonary N_2 Clearance Curves," J. Clin. Invest., 31: 40-50, 1952.

15. Gomez, D. M., "Mathematical Treatment of the Distribution of Tidal Volume Throughout the Lung," Proc. Nat. Acad. Sci. U. S., 49: 312-319, 1963.

16. Gomez, D. M., "A Physico-Mathematical Study of Lung Functions in Normal Subjects and in Patients with Obstructive Pulmonary Diseases," Med. Thorac., 22: 275-294, 1965.

17. *Handbook of Physiology*, Sec. 3, Vol. 1, Respiration, Fenn, W. O. and H. Rahn, American Physiological Society, Washington, D. C., 1964.

18. Levenberg, K., "A Method for the Solution of Certain Nonlinear Problems in Least Squares," Quarterly of Applied Mathematics, 2: 164-168, 1944.

19. *Finite Difference Equations*, Levy, H. and F. Lessman, The Mac-Millan Company, New York, 1961.

20. Lillington, G. A., W. S. Fowler, R. D. Miller, and H. F. Helmholz, Jr., "Nitrogen Clearance Rates of Right and Left Lungs in Different Positions," J. Clin. Invest., 38: 2026-2034, 1959.

21. Lundin, G., "Alveolar Ventilation (in normal subjects) Analyzed Breath-by-Breath as Nitrogen Elimination During Oxygen Breathing," Scan. J. Clin. Lab. Invest. 7: Suppl. 20: 39-51, 1955.

22. McIntire, L. V., Physicochemical Hydrodynamics class notes, Rice University, 1973.

23. Marquadt, D. W., "An Algorithm for Least-Squares Estimation of Nonlinear Parameters," J. Soc. Indust. Appl. Math., 11: 431-444, 1963.

24. *Methods in Medical Research*, Vol. 2 (II. Intrapulmonary Gas Mixing), Comroe, Jr., J. H. (Editor-in-chief), The Year Book Publishers Company, Chicago, 1950.

25. Militano, T. C., Ph. D. Thesis, Case Western Reserve University, Cleveland, Ohio, 1970.

26. Mulligan, J. T. and A. Bouhuys, "Mathematical Models of Non-uniform Intrapulmonary Gas Distribution," Bull. Math. Biophys. 27: 473-476, 1965.

27. Nakamura, T., T. Takishima, T. Okubo, T. Sasaki, and H. Takahashi, "Distribution Function of the Clearance Time Constant in Lungs," J. Appl. Physiol., 21: 227-232, 1966.

28. Nye, R. E., "Theoretical Limits to Measurement of Uneven Ventilation," J. Appl. Physiol., 16: 1115-1123, 1961.

29. Okubo, T. and C. Lenfant, "Distribution Function of Lung Volume Ventilation Determined by Lung N_2 Washout," J. Appl. Physiol., 24: 658-667, 1968.

30. Pappenheimer, J. R., "Standardization of Definitions and Symbols in Respiratory Physiology," Fed. Proc., 9: 602-605, 1950.

31. Piiper, J. and P. Scheid, "Respiration: Alveolar Gas Exchange," Annual Review of Physiology, 33: 131-154, 1971.

32. Riggs, D. S. and A. Goldstein, "Equation of Inert Gas Exchange which Treats Ventilation as Cyclic," J. Appl. Physiol., 16: 531-537, 1961.

33. Robertson, J. S., W. E. Siri, and H. B. Jones, "Lung Ventilation Patterns Determined by Analysis of Nitrogen Elimination Rates: Use of the Mass Spectrometer as a Continuous Gas Analyzer," J. Clin. Invest., 29: 577-590, 1950.

34. Rossing, R. G., "Evaluation of a Computer Solution of Exponential Decay of Washout Curves," J. Appl. Physiol., 21: 1907-1910, 1966.

35. Physiology and Biophysics, Ruch, T. C. and H. D. Patton, W. B. Saunders Company, Philadelphia and London, 1965.

36. Saidel, G. M., T. C. Militano, and E. H. Chester, "Pulmonary Gas Transport Characterization by a Dynamic Model," Resp. Physiol., 12: 305-328, 1971.

37. Thomasson, W. M., Master's Thesis, Rice University, Houston, Texas, 1973.

38. Van Liew, H. D., "Semilogarithmic Plots of Data which Reflect a Continuum of Exponential Processes," Science, 138: 682-683, 1962.

39. Weber, J. and A. Bouhuys, "Theoretical Considerations on Lung Clearance," Acta Physiol. Pharmacol., 8: 121-136, 1959.

40. Wise, M. E. and J. G. Defares, "A Model for Unequal Ventilation of the Lungs Assuming a Common Dead Space and Two Separate Dead Spaces," Bull. Math. Biophys., 21: 343-362, 1959.

41. Wylie, Jr., C. R., Advanced Engineering Mathematics, McGraw-Hill Book Company, New York, 1966.